Stony Brook University

The specific interactions between dendritic cells and *Porphyromonas gingivalis*

A Dissertation Presented

by

Amir Emanuel Zeituni

to

The Graduate School

in Partial Fulfillment of the

Requirements
for the Degree of

Doctor of Philosophy

in

Molecular Genetics and Microbiology

Stony Brook University

December 2010

Stony Brook University
The Graduate School
Amir Emanuel Zeituni

We, the dissertation committee for the above candidate for the Doctor of Philosophy degree, hereby recommend acceptance of this dissertation.

Dr. Christopher W. Cutler- Dissertation advisor
Associate Dean for Research, Professor- Department of Periodontics and Implantology

Dr. David G. Thanassi- Chairperson of Defense
Professor- Department of Molecular Genetics and Microbiology

Dr. Michael Hayman
Professor- Department of Molecular Genetics and Microbiology

Dr. Adrianus (Ando) W. M. van der Velden
Assistant Professor- Molecular Genetics and Microbiology

Dr. Caroline Attardo Genco
Professor- Department of Medicine, Section of Infectious Diseases
Department of Microbiology, Boston University School of Medicine

This dissertation is accepted by the Graduate School.

Lawrence Martin
Dean of the Graduate School

The specific interactions between dendritic cells and *Porphyromonas gingivalis*

by

Amir Emanuel Zeituni

Doctor of Philosophy

in

Molecular Genetics and Microbiology

2010

The broad objective of this dissertation is to elucidate the specific interactions between *Porphyromonas gingivalis* (*P. gingivalis*) and dendritic cells (DCs). *P. gingivalis* is a black pigmented, anaerobic, Gram-negative bacterium that is associated with most cases of chronic periodontitis. *P. gingivalis* expresses a myriad of virulence factors, most notably, fimbrial adhesins that enable it to bind to and invade host epithelial cells, endothelial cells, macrophages and DCs. While much is known about the 41 kDa major fimbria adhesins of *P. gingivalis,* the minor fimbriae have received little attention. The results presented here suggest that the minor fimbriae may serve as an immunosuppressive factor, by targeting the C-type lectin receptor DC-SIGN. DC-SIGN (CD209) is involved in uptake of certain pathogens by DC, in the formation of DC-T cell conjugates, and is increasingly expressed in chronic periodontitis (CP) lesions. Targeting DC-SIGN for entry into DCs has proved an effective immuno-evasive strategy for certain pathogens. DC-SIGN ligation down-modulates maturation of DCs, dampens DC secretion of pro-inflammatory and Th_1-cytokines necessary for induction of protective immunity and, possibly, compromises intracellular killing mechanisms. The aim for this research was to investigate the role of the minor fimbriae of *P. gingivalis* in invasion of DC's and in activation of immunosuppressive innate signaling pathways. I determined that the minor fimbriae targets DC-SIGN on DCs. Furthermore, I discovered that the minor fimbriae are glycosylated with DC-SIGN targeting sugars (fucose, mannose, galactose, and N-acetylglucosamine). Detection of glycosylation was determined using endoglycosidases and then confirmed via gas chromatography-mass spectrometry (GC-MS). Finally, it was determined that minor fimbriae targeting of DC-SIGN has an immunosuppressive effect on DCs as well as on T cells co-cultured with pulsed DCs.

Table of Contents

List of Figures

List of Tables

Acknowledgments:

I would like to express my gratitude to my dissertation advisor Dr. Christopher W. Cutler. I greatly appreciate this opportunity to work with you. I am grateful for your patience and your support in all of my endeavors. Also, I will forever be thankful for your guidance and encouragement in my writing publications, grants and presentations. I appreciate the opportunity to make my own mistakes and supportive environment you provided in the lab. I feel that you have truly been a mentor in the truest sense of the word. I count you as both a friend and teacher. I feel that you have greatly influenced me in my scientific career, and I thank you deeply from the bottom of my heart for the opportunity. Thank you for your unwavering support, I believe that it has enabled me to be a more confident independent scientist. Also, I would like to thank the Cutler lab members past and present: Dr. Sivaraman Prakasam, Dr. Julio Carrion, and Liz Scisci for our scientific discussions and for making work such an enjoyable experience.

I would like to thank Dr. David G. Thanassi for being my Dissertation chair. Thank you for taking the time to look over my proposals, grants and papers. I believe that your input, criticisms, critiques and fresh perspective facilitated in the grant getting funded and the papers being published so easily. Thank you for opening up your lab to me and for your enthusiasm in my project. I would also like to thank William McCaig from the Thanassi lab for running the TEM on the purified minor fimbriae.

I would like to thank the remainder of the committee as well. First, I would like to thank Dr. Caroline A. Genco for agreeing to be the outside committee member. Your insight, expertise, experience and guidance have made this journey truly enjoyable. Secondly I want to thank you for opening up your lab in Boston and teaching me how to

purify the fimbriae of *P. gingivalis*. I would also like to thank Dr. Michael Hayman and Dr. Ando W. M. van der Velden for their guidance and suggestions during the proposal and all subsequent committee meetings. Dr. Hayman's experience with endoglycosidases was invaluable for this dissertation.

I would like to thank the Chair of the Molecular Genetics and Microbiology department, Dr. Jorge Benach. Thank you for providing me with the opportunity to conduct my research at such a world class institution. I would also like to thank you for allowing me to use the HPLC in your lab for my protein purification, and for our candid discussions about my future. More importantly though, I would like to thank you for the support and enthusiasm that you give to all the students in the department. I would like to thank Dr. Tim LaRocca for his insight and aid in troubleshooting the HPLC and for your friendship these past few years. Also, I would like to thank Todd Rueb for his assistance with flow cytometry, Dr. Toni Koller for running the proteomics center and for operating the mass spectrometer, and Dr. Ann Savitt for generating the monoclonal antibody against the minor fimbriae.

I would also like to thank all of the friends I have made here at Stony Brook University. Thank you all for providing vents from the rigors of research. I would especially like to thank my fiancée Dr. Erin Mathieson for her love, courage, and strength. I would also like to thank my parents Myriam and Nuriel Zeituni and my sister Michal Zeituni for their constant encouragement and support. Without these four people I do not believe I would have made it. Thank you all!

Chapter One:

Introduction:

Porphyromonas gingivalis and Periodontitis

Chronic periodontitis (CP) is the most common clinical oral disease, affecting 40-60% of the US population (1). It is a chronic inflammatory disease that is characterized by the induction of a non-protective immune response. The inflammatory response leads to soft and hard tissue destruction of the tooth supporting structures (2, 3). The patho-physiological manifestations of this disease are gum inflammation, increased crevicular fluid flow and a massive influx of polymorphonuclear leukocytes (PMN) into the gingiva which contribute to connective tissue destruction and alveolar bone loss (3, 4). These bouts of periodontal destruction occur in short bursts and are followed by longer periods of calm or inactivity (4). The gradual modification of the oral cavity creates ecological niches (i.e. periodontal pockets) that promote the growth of the most pathogenic plaque dwellers, anaerobes; which in turn increases the frequency in which these short bouts of periodontal tissue destruction occur (4). More recent studies have shown that the CP lesion is characterized by an influx of myeloid DCs into the lamina propria and the formation the of DC-CD4+ T cell conjugates (5).

While most human plaque harbors a biofilm consisting of roughly 500 bacterial species, *P. gingivalis* stands apart as one of several causative agents of CP (6). *P. gingivalis* utilizes a myriad of various virulence factors that contribute to chronic periodontitis. Among these are the capsule, fimbriae, proteases for opsonins C3 and IgG, gingipains, bacterial lipopolysaccharides (LPS), toxins and hemagglutinins (7, 8).

***Porphyromonas gingivalis* and the gingipains:**

P. gingivalis has three promiscuous proteinases, termed gingipains, that cleave natural or synthetic substrates after arginine (RgpA, RgpB) or lysine (Kgp) residues (3, 9-13). These gingipains are associated with the bacterium and get secreted into the extracellular matrix or biofilm in a more soluble form. The gingipains are responsible for 85% of all general proteolytic activity of *P. gingivalis* and 100% of its "trypsin-like activity (14)."

The *rgpA* gene encodes a "polyprotein consisting of a profragment, a catalytic domain and a hemagglutinin/ adhesion domain" (14), resulting in 3 possible forms of the RgpA. RgpA can exist as just the catalytic domain. RgpA can also be modified to fit on the cell envelope of the bacteria; but the most prevalent form of RgpA is when it is associated with the hemagglutinin/ adhesion domain. This enzyme can either be secreted or associated with the cell membrane, but it is preferentially found on the cell envelope fraction of *P. gingivalis* (14). In comparison to the *rgpA* gene the *rgpB* gene lacks the entire hemagglutinin/ adhesion domains, but does encode its own profragment and catalytic domain. Like RgpA, RgpB exists as either a membrane bound enzyme or as a soluble product (14). Once again, the *kgp* gene encodes "a polyprotein with a typical leader sequence, a profragment, catalytic domain, and a C-terminal extension harboring hemagglutinin/ adhesion domains" (14). The gingipains' hemagglutinin activity is not the only adhesive role of these gingipains; they are also implicated in binding to connective tissue components like fibronectin and fibrinogen followed by the subsequent degradation of these proteins (14). The gingipains have also been associated with

degradation of host extracellular matrix components such as laminin, fibronectin, and collagen type III, IV and V (14).

The gingipains are also active in degrading cytokines that are either associated with the bacterium or present in the biofilm. So how does *P. gingivalis* make use of these gingipains to mediate progression of infection? Table 1 is a review of the various cytokine substrates of the gingipains already described in the literature. As seen in Table 1, most of the cytokines that are digested by the gingipains are pro-inflammatory cytokines. One must also consider that *P. gingivalis* is able to degrade the complement peptides C3 and C5 with its RgpA and RgpB gingipains (15, 16). This degradation produces a functional C5a and short lived C3a chemotactic factors. The gingipains also target the C5aR receptors from the PMN surface for degradation (15). Overall this suggests that the organism may benefit from recruitment of activated PMN's to the site of infection.

P. gingivalis is incapable of completely degrading host proteins by itself, as it lacks the proper proteases (14). It is now believed that it receives its amino acid and nitrogen requirements from the fragmentation and degradation of host proteins that are degraded by activated PMN broad specificity proteinases (3, 7). Harbrechet *et al*. 1993, showed that phorbol 12-myristate 13-acetate (PMA) stimulated PMN's indiscriminately destroyed rabbit hepatocytes if they were co-cultured together; however minimal to no tissue damage was observed if the PMN's were not stimulated (17). The *P. gingivalis* virulence factors, particularly the gingipains protect it from being opsonized by complement and antibodies. Also, *P. gingivalis* is uniquely equipped with gingipains that are capable of destroying the chemotactic gradient away from the organism. Van Dyke *et*

al. 1982 first described the ability of *P. gingivalis* supernatants or sonic extracts in Boyden chamber assays', to inhibit PMN migration (18). This suggests that the bacterium has evolved to exploit actively recruited PMN's, which digest the gingival tissues and create a new ecological niche for it.

Moreover, further perturbation of the normal immune response through promotion of a non-protective Th_2 response may be mediated by the gingipains. They appear to show some selectivity to the interleukins (IL) they are able to degrade in the presence of serum. For example Yun *et al.*, 2003, showed that in the presence of serum, degradation of IL-4 is inhibited, while without serum, IL-4 is degraded readily. When they compared gingipain activity in the presence/absence of serum for IFN-γ and IL-12 p70, IL-12 p40 and p35, they determined that serum does not play an inhibitory role (12, 19). Also, they were able to show that CD69 (activation marker) gets up regulated on B cells that are co-cultured with gingipains, and that RgpA induces an up regulation of IL-4R (10). These findings together suggest that through some yet to be elucidated mechanism the gingipains are promoting B cell proliferation.

Current data suggest that *P. gingivalis* major fimbriae induce a primarily pro-inflammatory response (20). This pro-inflammatory response, however, is not detrimental to the microbe as one might expect. Quite the contrary, it benefits the pathogen by enhancing tissue degradation, providing nutrients, and a new ecological niche. The pro-inflammatory cytokine response recruits PMN's to the site of *P. gingivalis infection*. However, the microbe appears to degrade the chemotactic signals in its vicinity (with the use of its gingipains); thereby enhancing destructive effect of the

PMN's in the surrounding tissues. It may also regulate PMN recruitment using its gingipains to favor a Th_2 response.

Porphyromonas gingivalis and its Fimbriae

The fimbriae of *P. gingivalis* play a crucial role in adhesion and invasion of host cells. *P. gingivalis* has two predominant fimbriae termed the major and minor fimbriae. The major fimbriae are composed of a 41 kDa protein termed fimbrillin, encoded by the *fimA* gene (21). Much less is known about the minor fimbriae. The minor fimbriae are comprised of a 67 kDa (22) protein that is encoded by the *mfa1* gene. The major and minor fimbriae are antigenically distinct and they also differ based on amino acid composition and size (22, 23).

Low temperatures (34°C) have been determined to be essential for maximal transcription of the *fimA* gene (24, 25), and additionally, the presence of both gingipains (RgpA and Kgp) are necessary for maximal transcription of *fimA (26).* Recently, Wu *et al.* (2007) discovered that the major and minor fimbriae are regulated by a two component regulatory system termed FimS/FimR (27). It was also determined that while FimR binds directly to *mfa1*, it will only bind to the first gene of the *fimA* gene cluster, *pg2130* (27, 28). Moreover, this two component regulatory system responds to environmental cues like heme and temperature (27). As can be seen in Figure 1, *fimA* is upstream of other fimbriae genes (*fimC, fimD* and *fimE*) in ATCC 33277 and 381. Conversely, *mfa1* is upstream of putative and hypothetical genes. Other surface proteins *ragA* and *ragB* are downstream of the *mfa1* gene (Figure 1).

The formation and secretion of the major fimbriae is a complex reaction consisting of numerous steps. It is done in a completely novel manner and the genome of *P. gingivalis* has no sequence homology for any of the established pili/fimbriae secretion pathways. *P. gingivalis* uses a Sec protein secretion system that is essential for transfer of prefimbrillin proteins from the cytoplasm to the periplasm. Prefimbrillin proteins get transferred from the cytoplasm to the periplasm using an N-terminal signal peptidase II (lipoprotein specific signal peptidase) (29, 30). As prefimbrillin crosses the inner membrane it gets its N-terminal signal peptide cleaved by the signal peptidase II (29, 30). Prefimbrillin is then transported to the outer face of the outer membrane, by some unknown process, where it is processed into its mature form by Arg-gingipains (Rgp) which cleave prefimbrillin at Arg^{46}-Ala^{47} to yield the mature form, which subsequently assembles into fimbriae structures (30-32). Therefore in the absence of Rgp, such as in a gingipain-null mutant, prefimbrillin proteins are accumulated on the cell surface and little or no fimbriation occurs on the bacterial surface (30). Furthermore, ectopic expression of the fimbria in other organisms like *E. coli* results in the fimbriae being found in inclusion bodies. Also, if the N-terminal signal peptide is removed and the fimbria are expressed in *E. coli* then the fimbriae are secreted into the supernatant but never assemble on the bacteria surface.

Deciphering the cellular receptors for the fimbriae is an active area of research. Yilmaz *et al*. (2002) have shown that the cellular targets of the major fimbriae are the β-1 integrins (CD29) (33, 34). Others have shown a role for β-2 integrins (CD18) (35-37). Other groups have also suggested a role for toll like receptors 2 and 4, as well as complement receptor 3 and CD14 as receptors for the major fimbriae and may be

involved in signaling (38, 39). Recently Davey *et al*. (2008) showed that both the major and minor fimbriae specifically bind to chimeric TLR2 and CD14 proteins in endothelial cells as well as in a cell free ELISA (40); however, the specific endocytic receptors on DCs that bind and internalizes the minor fimbriae of *P. gingivalis* have not been established.

Many mucosal pathogens exhibit glycosylation motifs on their flagella, pili, and fimbriae (41). Glycosylation reportedly plays a role in maintaining the protein structure, in protection against proteolytic degradation, immune evasion, host cell adhesion and surface recognition (41). There is evidence suggesting a role for glycosylation of the fimbriae in *P. gingivalis*. Knockouts of *gftA* (a *wcaE* glycotransferase homolog of *E. coli*) in *P. gingivalis* fail to make mature fimbriae (42). There is evidence that the gingipains are glycosylated (43) and that this activity is regulated by the *vimF*, *vimA* and *vimE* glycotransferase genes (44, 45). Knocking out these genes causes a failure to glycosylate these gingipains, leading to their inactivation (43-45). Recently it was discovered that the RagA protein (a surface protein encoded downstream of the minor fimbriae) is glycosylated (46). The gingipains, RagA and RagB as well as the major and minor fimbriae are outer membrane proteins. They all encode for a signal peptide that is cleaved before they exit the periplasm (29, 47, 48). Intriguingly, after analysis of the minor fimbria protein sequence, we discovered that there are two putative N-glycosylation motifs (see Figure 4). Given that all of the elements for glycosylation are present in *P. gingivalis*, and that there exist two conserved Asn-Xaa-Ser/Thr N-glycosylation motifs in the minor fimbriae (41, 49), we proposed that the minor fimbriae are glycosylated. We demonstrated that the minor fimbriae exhibit both N- and O- linked

glycosylation, and that the minor fimbriae are glycosylated with DC-SIGN targeting sugars, accounting for their ability to bind to the C-type lectin DC-SIGN (50).

Dendritic Cells (DCs) and How Bacteria Exploit Them to Modulate the Immune Response

Immature DCs (iDC) reside almost exclusively in tissues where they capture and process antigens (51). While processing the antigens they undergo maturation, during which they migrate towards T-cell areas such as lymph nodes. While migrating/maturing, DCs lose their ability to uptake and process antigen and they acquire the ability to present antigens to T-cells (52). As maturing DCs migrate out of the tissues and towards the lymph nodes, monocytes from the blood enter the tissues and can differentiate into DCs (53). This process ensures that there is always a steady state level of DCs present in the tissues which can be dynamically increased under inflammatory conditions (53). Specifically, the influx of myeloid DCs has been observed in periodontitis (54, 55) and recently, into the respiratory tract of asthmatic patients (56). Fully matured DC's express the signaling molecule CD40, intercellular adhesion molecule CD54 (ICAM-1), B7 family co-stimulatory molecules CD80 (B7-1), CD86 (B7-2), the DC final maturation marker CD83, and HLA-DR (MHCII) (52, 54, 57, 58).

DCs act as the main communicators between the innate and adaptive immune responses. Consistent with this, myeloid DCs have been shown to bias the T-helper cell effector response towards Th_1, Th_2, Th_{17} or T_{reg} CD4+ T cell response. The production of IL-12 and type I IFN by Th_1 effector cells (51, 59, 60) promote other pro-inflammatory cells such as macrophages, neutrophils, and CD8+ cytotoxic T cells to kill microbes.

Conversely, Th_2 cells, which produce IL-4, IL-5 and IL-13 (61), activate pro-allergic responses and humoral immune responses (60). Jotwani *et al.* (2003) showed that monocyte derived DCs (MoDCs) pulsed with *E. coli* LPS induced Th_1 responses, while those pulsed with *P. gingivalis* LPS induced Th_2 responses (57). Other researchers have noted similar findings with the pathogen associated molecular patterns (PAMPS) of other species, as reviewed by Kodowaki 2007 (60). Thus, different microbes interact with innate immune cells such as DCs and can determine the type of adaptive immune response that is elicited. This in turn can modify the ability of the host to clear the infection, versus allowing the pathogen to colonize a niche.

The DC maturation process is initiated by microbial and inflammatory stimuli and involves phosphorylation of mitogen-activated protein kinases (MAPKs), specifically, ERK, JNK, and p38 MAPK. These three MAPK signaling pathways have distinct roles in the DC maturation process (summarized in Figure 2) (52, 58, 62, 63). JNK and p38 MAPK cascades are strongly activated by stress stimuli and inflammatory cytokines, and are closely linked with Th_1 DC differentiation (64). These signaling cascades are coordinated to positively and negatively regulate phenotypic maturation of MoDCs. Phosphorylation of both/either p38 MAPK and/or JNK results in secretion of pro-inflammatory cytokines (IL-12 p70, TNF-α, etc.) as well as up-regulation of CD80, CD86, CD83 and CD54 (52, 64). Conversely, ERK acts as a direct inhibitor of p38 MAPK. ERK has been implicated in dampening CD86, HLA-DR and CD83, as well as in inhibiting production of pro-inflammatory cytokines by MoDC's (52, 64). Also, constitutive levels of ERK act to bias the immune response towards the Th_2 pathway (52, 64). Thus, as Steinman put it: "Different maturation programs essentially allow DC to

control the distinct qualities of subsequent lymphocyte responses." (65) Recent findings of Medzhitov indicate that TLR-mediated activation of NFkB is required for optimum phagolysosome fusion and intracellular killing (66-68). Not surprisingly, induction of endotoxin tolerance, which downregulates TLRs, dampens killing of *P. gingivalis* by macrophages (69). Ligation of DC-SIGN also apparently negatively regulates TLR signaling, but its effects on killing of *P. gingivalis* by DCs are unclear (70).

DC-SIGN: A Unique C-type Lectin Receptor

DCs are capable of internalizing pathogens by phagocytosis, sampling fluid via macropinocytosis, and utilizing their C-type (Ca^{2+} dependent) lectin receptors, such as mannose receptor (MR, CD206), DEC 205, Fcγ and Fcε, to mediate adsorptive endocytosis (51). Of particular interest to this study is the C-type lectin receptor DC-specific intracellular adhesion molecule grabbing nonintegrin (DC-SIGN). DC-SIGN is a type II membrane protein in which the extracellular domain consists of a stalk that promotes tetramerization (71). DC-SIGN contains a C-terminal carbohydrate recognizing domain (CRD) that belongs to the C-type lectin superfamily (71). Early studies by Feinberg et al. (2001) showed that the DC-SIGN CRD preferentially binds to the high-mannose N-linked oligosaccharides GlcNAc (N-acetylglucosamine) and Manα1-3[Manα1-6] Man (mannose). Furthermore, Appelmelk et al. (2003) showed that DC-SIGN also binds to fucose-containing Lewis blood antigens (72). Guo *et al.* (2004) utilized an extensive glycan array and showed that DC-SIGN will bind high mannose-containing glycans or glycans that contain terminal fucose residues (73). Guo *et al.* further suggest that "… this receptor has evolved to recognize specific classes of glycans

that are expressed on mammalian glycoproteins…(73)". Previous studies showed that DC-SIGN is used by microorganisms such as *N. gonorrhoeae* (74), *M. tuberculosis* (72, 75, 76), *M. leprae*, HIV (77) and *H. pylori* (72) to target DCs for entry and immune suppression. Interestingly these pathogens all can cause lifelong infections.

There is strong evidence suggesting that DC-SIGN forms clusters on the surface of DC's and Raji DC-SIGN cells. Raji DC-SIGN cells, used in this dissertation, are a B-cell line that has been genetically engineered to constitutively express DC-SIGN) (73, 78, 79). DC-SIGN clusters on DCs are located at the leading edges of the DC surface (79, 80). DC-SIGN clusters then travel rearward from the edges of the MoDC along the plasma membrane and do not internalize until they reach the main body of the cell (79). Neumann *et al.* (2008) also demonstrated that DC-SIGN clusters get rapidly internalized by iDCs and targeted predominantly to the medial and perinuclear zone regions (79). In iDCs the DC-SIGN targeted vesicles have a mean pH of 5.47 and are located predominantly at perinuclear zones (80). In mature DCs the mean pH is 6.45 and DC-SIGN is targeted closer to the cell surface (80). Moreover, DC-SIGN expression on mature DCs is modestly down regulated (80). Engering *et al.* (2002) have also determined that optimal binding to DC-SIGN is done at neutral and basic pH and that at acid pH [5] DC-SIGN losses 20% of its binding abilities (80). To date DC-SIGN vesicles have not been shown to associate with any lysosomal compartments (78-80). Numerous groups have proposed that pathogen recognition by DC-SIGN can bias the adaptive response towards a Th_2 response (72, 76, 81). We hypothesize that while the major fimbriae are involved in attachment to β-integrins on DCs, this facilitates close interactions of the minor fimbriae with DC-SIGN. This allows *P. gingivalis* to exploit

the immuno-modulating potential of DC-SIGN to dampen the immune response, thus allowing *P. gingivalis* to persist as a chronic pathogen. Our published data supports an immuno-modulating role for the minor fimbriae in reducing the response of DCs to the major fimbriae (20).

FimA gene cluster

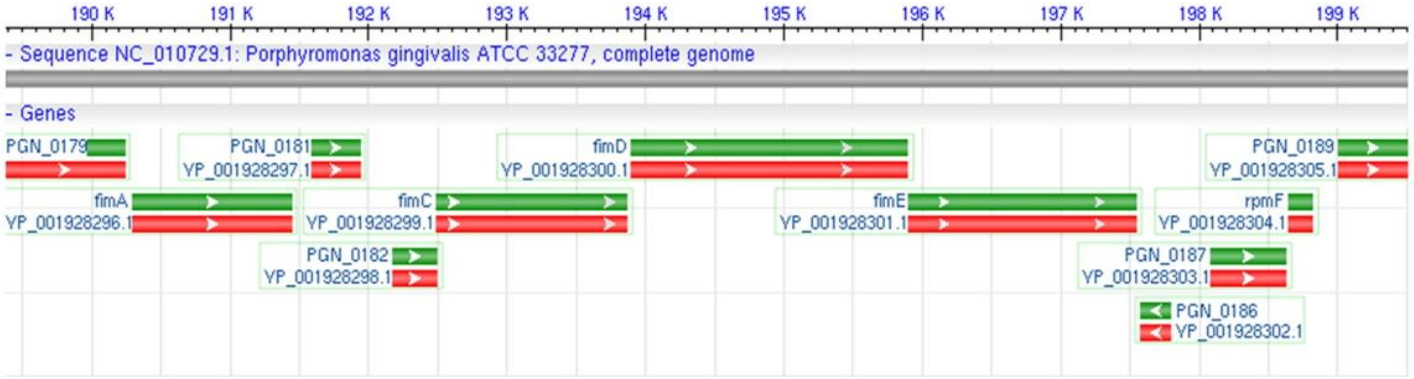

Mfa-1 gene cluster

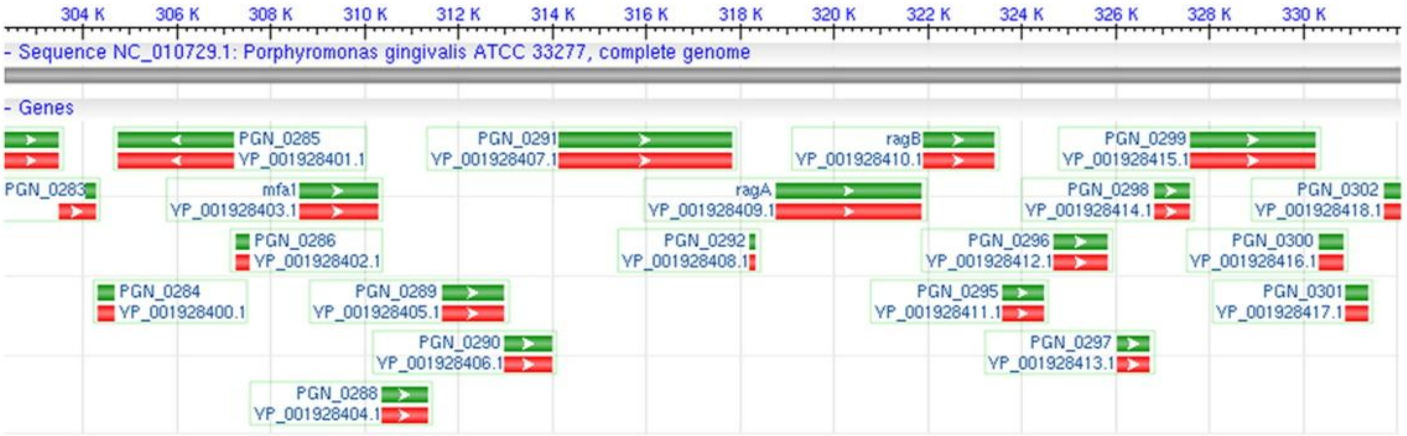

Figure 1. The *FimA* and *Mfa1* gene clusters.

(*Top*) The *fimA* gene cluster of Pg381 and ATCC 33277. Gene *FimA* is upstream of other major fimbriae genes *fimCDE*.

(*Bottom*) The *mfa1* gene is upstream of hypothetical and putative proteins of unknown function. A few genes downstream of *mfa1* another glycosylated surface protein RagA is present.

Effects of MAPK on DC's

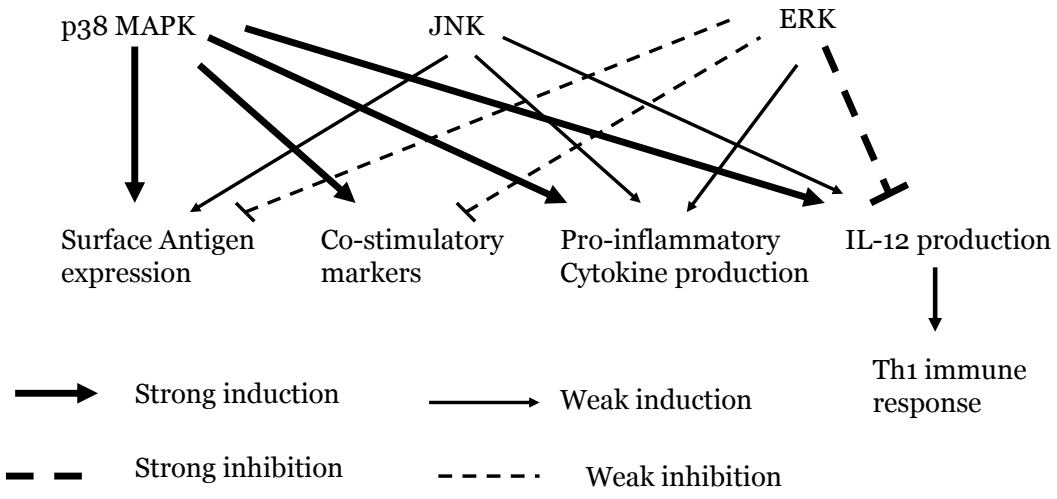

Adapted from Nakahara *et al* 2006

Figure 2. Schematic representation of the effects of different MAPK signaling cascades.

p38 MAPK and to a lesser extent JNK act as promoters for a Th1 immune response. p38 MAPK is a strong upregulator of HLA-DR expression, CD80, 83, 86 expression and pro-inflammatory cytokine secretion (including IL-12). JNK is a much weaker inducer of HLA-DR, CD80, 83 and 86. JNK is also capable of promoting pro-inflammatory cytokine secretion but is incapable of promoting IL-12 secretion. ERK acts as an inhibitor of p38 MAPK activity. It acts to abrogate IL-12 cytokine secretion and can attenuate HLA-DR expression and CD 80, 83 and 86 expression.

Table 1: Degradation of cytokines by *P. gingivalis* in serum:

Cytokine degraded	Enzyme responsible	Reference:
IFN-γ, TNF-α, IL-6, IL-8, IL-12, IL-4, IL-5,	RgpA or RgpB	(3, 6, 12, 19, 82, 83)
IFN-γ, TNF-α, RANTES, IL-12, IL-4, IL-5,	Kgp	(3, 6, 12, 19, 83)
VCAM-1, VEGF, IL-17, IL-1β, IL-1ra, CD14, C5, C3	LIVE *P. gingivalis*: Not clear which if any gingipains	(6, 13, 16, 84-86)

Chapter Two:

Experimental Methods:

Bacterial strain, growth conditions, bacterial labeling and uptake experiments.

WT Pg381, which expresses both minor and major fimbriae (Pg $^{min+/maj+}$), isogenic minor fimbriae-deficient mutant MFI, which expresses only the major fimbriae (Pg $^{min-/maj+}$), isogenic, major fimbriae-deficient mutant DPG3, which expresses only the minor fimbriae (Pg $^{min+/maj-}$), and the double fimbriae mutant MFB (Pg $^{min-/maj-}$) were obtained from C. A. Genco and maintained anaerobically (10% H_2, 10% CO_2, 80% N_2) in a Forma Scientific Anaerobic System glove box model 1025/1029 at 37°C (40, 87) in Difco Anaerobe Broth MIC. Erythromycin (5 µg/ml) and tetracycline (2 µg/ml) were added according to the selection requirements of the strains. Bacteria were pelleted, washed once in phosphate buffered saline (PBS) and for FACS based analyses, stained with CFSE (Molecular Probes, Eugene Oregon, USA), as described (88). Briefly, bacteria in PBS were stained with CFSE at a final concentration of 5µM for 30 min at 37°C and protected from light. The bacterial suspension was washed five times in PBS and *P. gingivalis* were resuspended to an O.D. at 660nm of 0.11, previously determined to be equal to 5 x 10^7 CFU (89). MoDCs and Raji cells were pulsed with *P. gingivalis* strains at 5:1 or 25:1 multiplicity of infection (MOI) for from 1.5 to 18 hr. Low MOI's were used to mimic a natural infection as well as to avoid overwhelming the host response. The percentage viable MoDC or Raji (typically >90% after 18 hrs) were monitored by trypan blue exclusion and did not differ between the strains (not shown). MoDCs and

Raji cells were fixed and stained for FACS analysis of %Pg-CFSE$^+$ cells as described in figure legends.

Raji and Raji DC-SIGN$^+$ cells, antibodies.

Raji cell lines (78) were obtained courtesy of D. R. Littman (Skirball Institute of Biomolecular Medicine, NYU), maintained in 10% heat inactivated FBS (GIBCO), RPMI 1640 with L-Glutamine and $NaHCO_3$ (SIGMA) in a 5% CO_2 incubator at 37°C. Staining to verify surface receptor expression was performed using monoclonal antibodies (BD-Biosciences): FITC anti-CD14 (cat # 555397); anti-CD209 (cat # 551264); anti-E-Cadherin (cat # 612130); anti-CD19 (cat #557697); IgG1 isotype (cat # 349041); anti-CD80 (cat# 557226); IgG2a isotype (cat # 349051); PE anti-CD29 (cat# 555443); anti-CD209 (cat# 551265); anti-CD18 (cat# 555924); anti-CD206 (cat# 555954); anti-HLA-DR (cat# 555812); anti-CD86 (cat# 555657); anti-CD11a (cat# 555379); IgG1 isotype (cat #349043); APC anti-CD205 (cat# 558156); anti-CD11b (cat# 550019); IgG1 isotype cat# 557732; (eBiosciences) PE anti-human TLR4 (cat# 12-9917-73); FITC anti-human TLR4 (cat# 53-9917-73); FITC anti-human TLR2 (cat# 11-9922-73); (Immunotech) FITC CD83 (cat# PN IM2410); (Immunotech) PE anti-CD207 (cat# IM3577); (Invitrogen) PE anti-CD11c (cat# 349863a); (Dako) FITC anti-CD1a (cat# F7141).

Raji cell Adhesion Assay.

CFSE- or Syto-stained bacteria were added at an MOI of 5:1 to either Raji or Raji DC-SIGN (78, 90). Binding was conducted on ice to prevent loss of surface DC-SIGN,

which cycles rapidly on Raji cells at 37°C (78, 79, 90). Cells were pulsed with CFSE stained bacteria for from 1-18 hr either at 37°C, on ice (87) or in the presence of cytochalasin D (0.5 μM the minimal concentration needed to arrest cytoskeletal rearrangements in Raji cells). Cells were washed to remove unbound bacteria, fixed in 1% formalin and analyzed by FACS. Association was quantified via FACS as previously described (76, 91, 92). In brief, 10,000 Raji cells were gated on forward and side scatter characteristics based on size and to exclude debris and unbound bacteria and then %CFSE positive cells in FITC channel quantitated.

Carbohydrate/ antibody/ gp120 blocking assay.

Carbohydrates were purchased from SIGMA: D-Mannose (cat# M-6020); L-Fucose (cat# F2252-5G); D-Fucose (cat# F-8150); Mannan from *Saccharomyces cerevisiae* (cat# M7504-5g) were all diluted into 2% heat inactivated FBS (GIBCO) PBS and filter sterilized. 5-100 μg of carbohydrates were added to block DC-SIGN receptor. The following reagent was obtained through the NIH AIDS Research and Reference Reagent Program, Division of AIDS, NIAID, NIH: HIV-1 gp120 CM envelope protein (Cat #2968). 1.5-9 μg of gp120 was added to block DC-SIGN receptor. Blocking antibodies to human DC-SIGN were purchased from R&D systems (cat# MAB161) (clone 120507); IgG2B Isotype control antibodies (cat#MAB004) (clone 20116); Anti-human integrin beta2 (CD18) mAb from Chemicon (cat#CBL158); Anti-human integrin beta1 mAb from Chemicon (cat#MAB1987Z); Anti-human CD11c mAb from BD Pharmingen™ (cat#555390 clone B-ly6); IgG1 isotype control from Chemicon (cat#CBL600) were added at a final concentration of 10 μg/ml. Raji and Raji DC-SIGN

cells were pre-incubated with blocking antibodies or carbohydrates for at least 30 min on ice. CFSE stained bacteria were then co-cultured for 1 hr on ice and binding was measured via FACS as described in adhesion assay. MoDC's were pre-incubated with carbohydrates, HIV-1 gp120 CM envelope protein, or antibodies for at least 30 min at 37°C before being co-cultured with CFSE stained bacteria. Co-cultures proceeded for 3 hr at 37°C and association was measured via FACS as described in the Raji adhesion assay.

DC cultures, multi- parameter flow cytometry analysis.

MoDCs were generated as we have previously described (20). Briefly, monocytes were isolated from mononuclear fractions of peripheral blood of healthy donors and seeded in the presence of GM-CSF (100 ng/mL) and IL-4 (25 ng/mL) at a concentration of 1–2 X 10^5 cells/mL for 6–8 days, after which flow cytometry was performed to confirm the immature DC phenotype (CD14- CD83- CD1a+DC-SIGN+). Cell surface markers of DCs were evaluated by four-color immunofluorescence staining with the following mAbs: CD1a- FITC (Biosource), CD80-PE (Becton Dickinson), CD83-PE (Immunotech), CD86- PE (Pharmingen), HLA-DR-PerCP (Becton Dickinson), CD14- APC (Caltag). After 30 minutes at 4^oC and washing with staining buffer (PBS, ph7.2, 2 mM EDTA, 2%FBS), cells were fixed in 1% paraformaldehyde. Analysis was performed with FACScalibur^{TM} (Becton Dickinson). Marker expression was analyzed as the percentage of positive cells in the relevant population defined by forward scatter and side scatter characteristics. Expression levels were evaluated by assessing mean fluorescence intensity (*MFI*) indices calculated by relating *MFI* noted with Pg-CFSE or

the relevant mAb to that with the isotype control mAb for samples labeled in parallel and acquired using the same setting.

Cytokines from MoDCs.

Culture supernatants were collected from MoDC's pulsed with *P. gingivalis strains* for 3 and 18 hr. Culture supernatants were analyzed by flow cytometry using a cytometric bead array (CBA kit; BD Biosciences, San Diego, Calif.) following manufacturers' instructions. A standard curve was achieved for each cytokine; the CBA software calculates levels in picograms per milliliter.

T cell priming.

For T cell priming experiments, the responder cells were autologous CD4+ naïve T cells purified from mononuclear fraction of human buffy coats by positive selection, using anti-CD4 MAb and goat anti-mouse immunoglobulin G-coated microbeads (Miltenyi Biotech GmbH, Gladbach, Germany) as described previously (20, 57) . Briefly, isolation of CD4+ cells was achieved using Minimacs separation columns (Miltenyi Biotech GmbH) as described by the manufacturer. In all experiments the isolated cells were 80 to 90% CD4+, as determined by staining with fluorescein isothiocyanate-conjugated anti-CD4 MAb followed by flow cytometry analysis (results not shown). MoDCs were washed extensively after an 18-hr pulsing with *P. gingivalis* strains and cultured at graded doses (1,000, 500, and 50 DCs, all per 200 μl) in complete RPMI medium with 10% heat-treated fetal calf serum with autologous T cells (50,000 cells/ 200 μl). Proliferation was determined after 5 days by loss of CFSE staining.

Bacterial growth conditions and minor fimbriae purification.

Isogenic, major fimbriae-deficient mutant DPG3 which expresses only the minor fimbriae (Pg $^{min+/maj-}$) was maintained anaerobically (10% H2, 10% CO2, 80% N2) in a Forma Scientific Anaerobic System glove box model 1025/1029 at 37°C in Difco Anaerobe Broth MIC. Erythromycin (5 µg/ml) was added according to the selection requirements of the strain (20, 40, 87, 93). Fimbriae were purified as described by Davey *et al.* (40). Briefly, bacterial pellets of *P. gingivalis* DPG3 were shattered by ultrasonication for 5 min pulsing at 50% power on ice. The cellular debris was removed by centrifugation and the remaining supernatant combined with saturated ammonium sulfate (40%) to precipitate out the fimbriae. After centrifugation the resulting pellets were dialyzed in 20 mM Tris buffer (pH 7.8). The dialysate was further purified by multiple runs on a Diethyl amino Ethanol (DEAE) Sepharose column CL-6B (Amersham Biosciences) equilibrated with 20 mM Tris buffer (pH 7.6-8.0) and eluted with a linear gradient of 0-1.0 M NaCl. Fractions were analyzed by 12% SDS-PAGE and silver staining (BIO-RAD) to ensure purity and quantified by Bradford assay. Fimbriae preparations underwent further screening to confirm lack of LPS contamination via silver staining (93). Samples were then analyzed by MS/MS mass spectrometry to verify identity and to ensure no other protein contaminants were present.

Tandem Mass Spectrometry

To confirm the identity of the minor fimbriae, purified proteins were separated by a SDS-PAGE gel and analyzed by the proteomics center at Stony Brook University. Gel bands were cut out, destained, reduced, alkylated and digested with trypsin (Promega

Gold, Mass Spectrometry Grade) as described by Shevchenko *et al*. (1996) with minor modifications (94). The resulting concentrated peptide extract was diluted into a solution of 2% Acetonitrile (ACN), 0.1% formic acid (FA) (Buffer A) for analysis. For solution digest, 10 µl of purified protein was diluted in 40 µl of 50 mM ammonium bicarbonate. The proteins were reduced with 2 mM DTT and alkylated with 4 mM iodoacetamide for 30 min each. 0.25 µg of trypsin was added and digests were incubated for overnight at 37° C. Protease reactions were stopped with 100% formic acid (final 5%). 10 µl of the peptide mixture was analyzed by automated microcapillary liquid chromatography-tandem mass spectrometry. Fused-silica capillaries (100 µm i.d.) were pulled using a P-2000 CO2 laser puller (Sutter Instruments, Novato, CA) to a 5 µm i.d. tip and packed with 10 cm of 5 µm Magic C18 material (Agilent, Santa Clara, CA) using a pressure bomb. This column was then placed in-line with a Dionex 3000 HPLC equipped with an autosampler. The column was equilibrated in buffer A, and the peptide mixture was loaded onto the column using the autosampler. The HPLC separation at a flow rate of 300 nl/ min was provided by a gradient between Buffer A and Buffer B (98% acetonitrile, 0.1% formic acid). The HPLC gradient was held constant at 100% buffer A for 5 min after peptide loading followed by a 30-min gradient from 5% buffer B to 40% buffer B. Then, the gradient was switched from 40% to 80% buffer B over 5 min and held constant for 3 min. Finally, the gradient was changed from 80% buffer B to 100% buffer A over 1 min, and then held constant at 100% buffer A for 15 more minutes. The application of a 1.8 kV distal voltage electrosprayed the eluted peptides directly into a Thermo LTQ ion trap mass spectrometer equipped with a custom nanoLC electrospray ionization source. Full masses (MS) spectra were recorded on the peptides over a 400-2000 m/z range,

followed by five tandem mass (MS/MS) events sequentially generated in a data-dependent manner on the first, second, third, fourth and fifth most intense ions selected from the full MS spectrum (at 35% collision energy). Mass spectrometer scan functions and HPLC solvent gradients were controlled by the Xcalibur data system (ThermoFinnigan, San Jose, CA). MS/MS spectra were extracted from the RAW file with ReAdW.exe (http://sourceforge.net/projects/sashimi). The resulting mzXML file with all the data for all MS/MS spectra was read by the subsequent analysis software. The MS/MS data was searched with Inspect (95) against a *Porphyromonas gingivalis* database containing 4251 proteins, in addition to an *Escherichia coli* database plus common contaminants, with modifications: +16 on Methionine, +57 on Cysteine, +1 on Asparagine and Glutamine. Only peptides with at least a p value of 0.01 were analyzed further.

Detection of glycosylation.

To detect the presence of glycosylation, purified native minor fimbriae were analyzed by SDS-PAGE and carbohydrates stained using the ProQ Emerald Glycoprotein Stain Kit (Molecular Probes) following manufacturer's instructions. Further verification of glycosylation on the minor fimbriae included treatment with "Native Protein De-glycosylation Kit (NDEGLY)" (SIGMA) following manufacturer's instructions. This kit is specific for N-glycosylation and utilizes three different Endoglycosidase (Endo) F enzymes. According to the manufacturers' instructions Endo F1 cleaves all asparagine-linked hybrid or high mannose oligosaccharides but not complex oligosaccharides. Endo F2 cleaves biantennary complex and to lesser extent high mannose oligosaccharides.

Fucosylation has little effect on Endo F2 cleavage of biantennary structures. Endo F2 will not cleave hybrid structures. Endo F3 cleaves biantennary and triantennary complex oligosaccharides. However, non-fucosylated biantennary and triantennary structures are hydrolyzed at a slow rate by Endo F3 Core fucosylated biantennary structures are efficient substrates for Endo F3 oligosaccharides. Core fucosylation of biantennary structures increases activity up to 400-fold. Endo F3 has no activity on oligomannose and hybrid molecules. The untreated and treated minor fimbriae were separated under native non-reducing conditions and reducing conditions with boiling on SDS-PAGE and probed with ProQ to detect loss of glycosylation. Further glycosylation analysis was performed using the "Enzymatic Protein Deglycosylation kit (E-DEGLY)" (SIGMA) following manufacturers' instructions. This kit utilizes PNGase F (cleaves N-glycosylation), α-2(3,6,8,9) neuraminidase (removes sialic acids), O-glycosidase (endo-α-N-acetylgalactosaminidase removes core structure with no modifications to serine or threonine residues), β-1,4 galactosidase, β-N-acetylglucosaminidase. Samples were then run on 12% SDS-PAGE and stained for ProQ. Additionally, we pre-incubated the minor fimbriae with α-L-fucosidase (from bovine kidney SIGMA) following manufacturers' instructions prior to treatment with E-DEGLY.

Monosaccharide analysis by Gas Liquid Chromatography-Mass Spectrometry (GC-MS).

To identify the carbohydrate motifs, 2 mg of purified minor fimbriae was sent to a commercial laboratory (M-SCAN, Inc, West Chester, PA) for analysis by gas chromatography-mass spectrometry (GC-MS). An aliquot of purified minor fimbriae (60

µl) was spiked with 10 µg Arabitol (Ara) as an Internal Standard (IS) and lyophilized. The dried sample was hydrolyzed, re-N-acetylated, derivatised and analyzed by GC-MS. A standard mixture, containing 10 µg each of Fucose (Fuc), Xylose (Xyl), Mannose (Man), Galactose (Gal), Glucose (Glc), N-Acetylgalactosamine (GalNAc) and N-Acetylglucosamine (GlcNAc) plus Arabitol (Ara) and a tube/reagent blank containing 10 µg Arabitol (Ara) were also hydrolyzed, re-N-acetylated, derivatised and analyzed by GC-MS (as described below) alongside the carbohydrate sample. An aliquot (1 µl) of each derivatised carbohydrate sample dissolved in hexane (2 ml) was analyzed by GC-MS using a Perkin Elmer Turbomass quadrupole mass spectrometer with integrated gas chromatograph under the following conditions:

Samples were injected onto a DB5 column at 95°C using helium as a carrier gas. The program was run as follows: 1 minute at 90°C, then 25°C/minute to 140°C, then 5°C/minute to 220°C, then 10°C/min to 300°C, finally held at 300°C for 5 minutes. Mass Spectometry ionization voltage was 70eV, the acquisition mode was set to scanning, and mass range was 50-500 Daltons. Monitored ions were 173 for N-Acetylhexosamines, 204 for hexoses, deoxyhexoses and pentoses, 217 for arabitol. On comparison of the data with that obtained from the standard mixtures containing known amounts of the expected monosaccharides, the sugars hydrolyzed from the sample were identified and the quantity of each monosaccharide present was estimated.

Transmission Electron Microscopy of native minor fimbriae.

For transmission electron microscopy (TEM), 0.8 µg/µl solution of purified native Mfa1 protein in 20 mM Tris HCl pH 7.8 was adsorbed onto polyvinyl formal-carbon-

coated grids (Ernest F. Fullam, Latham, NY) for 2 minutes, washed twice with PBS, twice with water and then negatively stained with 0.5% phosphotungstic acid (Ted Pella, Inc., Redding, CA) for 30 seconds. All grids were viewed in a transmission electron microscope (FEI TECNAI 12 BioTwin G02) at 80-kV accelerating voltage, and images were obtained by using an AMT XR-60 charge-coupled device digital camera system. Direct magnification was at 98,000 X.

Derivation of monoclonal antibody to minor fimbriae.

MAb 89.15 against the minor fimbriae was derived by the Cell Culture/Hybridoma Facility at Stony Brook University. Briefly, three female 6-8 week old BALB/c mice (Charles River) were immunized intraperitoneally with three 50 µg doses of recombinant minor fimbriae (Mfa-1) in Sigma adjuvant (Sigma-Aldrich Co., St. Louis, MO) at two-week intervals, following which sera was drawn and tested by enzyme-linked immunosorbent assay (ELISA) for the presence of antigen-specific antibodies. The mouse selected for splenectomy had a titer of >1:1000 to the protein. Prior to fusion, the mouse was boosted intraperitoneally with 1 µg of Mfa-1 in PBS (Gibco-Invitrogen, Carlsbad, CA). Four days following the booster, the mouse was sacrificed, the spleen cells isolated aseptically and fused with mouse myeloma cell line Sp2/0 (ATCC), as described (96). Clones were screened by ELISA against native minor fimbriae. Clones were then further screened using a whole bacteria ELISA against MFI, which expresses only the major fimbriae (Pg $^{min-/maj+}$), and DPG3, which expresses only the minor fimbriae (Pg $^{min+/maj-}$). Clone 89 was determined to be positive both by native minor fimbria ELISA and whole bacteria ELISA and thus was selected for sub cloning by

limiting dilution. Sub clone 89.15 was selected by ELISA for further study. MAb 89.15 was determined to be of the IgG_1 isotype having a κ light chain, by use of the IsoStrip Mouse Monoclonal Antibody Isotyping Kit (Roche Applied Science, Indianapolis, IN). Antibodies from this sub clone will be referred to as AEZαMfa1.

ELISA

Purified recombinant Mfa-1 protein was applied to Maxisorp U-bottomed 96-well plates (Nunc cat # 449824) at 1 µg/mL in coating buffer, blocked and probed with hybridoma supernatants as described (96). For whole cell ELISA, formalin fixed DPG3 or MFI were applied to Maxisorp U-bottom 96-well plates (Nunc) at a final concentration of 2×10^8 bacteria/ mL in coating buffer, blocked and probed with hybridoma supernatants.

TEM Immunogold Labeling.

For immunogold-EM, Mfa1 protein in 20mM Tris (5µg/ml) was adsorbed onto polyvinyl formal-carbon-coated grids (Ted Pella, Inc., Redding, Ca) for 2 minutes, washed twice with PBS and then blocked in PBS containing 1% Bovine Serum Albumin (BSA) (Fisher Scientific, Pittsburg, PA) for 30 minutes. Grids were then placed on a 1% BSA solution containing AEZαMfa1 antibody (0.025mg/ml) or an isotype control antibody (0.02mg/ml) for 1 hr, washed three times with PBS, then placed on 1% BSA solution containing anti-mouse IgG antibody conjugated to 18 nm diameter colloidal gold particles (Sigma-Aldrich) for 1 hr. Grids were washed three times with PBS, twice with water and then negatively stained with 0.5% phosphotungstic acid (Ted Pella, Inc.,

Redding, CA). All grids were viewed in a transmission electron microscope (FEI TECNAI 12 BioTwin G02) at 80-kV accelerating voltage, and images were obtained by using an AMT XR-60 charge-coupled device digital camera system.

Western Blotting

Protein concentrations were determined by Bradford assay. Samples were boiled in Laemmli sample buffer (Bio-Rad) at 100°C for 10 min. Proteins were run on a 12% SDS-PAGE gel and transferred to PVDF membranes (Bio-Rad). Membranes were blocked with 5% nonfat milk Tris-based saline (TBS), 0.1% Tween 20. In case of MAPK signaling, membranes were blocked with 3% BSA TBS 0.1% Tween 20. Membranes were subsequently incubated with appropriate antibodies for immunoblotting and detected with appropriate anti- rabbit or mouse HRP conjugated antibodies. Detection was performed using Kodak film and SuperSignal West Pico Chemiluminescent substrate (Thermo Scientific). AEZαMfa1 was used to detect minor fimbriae. Phospho-p38 MAPK, phospho-JNK, phospho-ERK, p38 MAPK, ERK and JNK antibodies were from (Cell Signaling Technologies).

Immunofluorescent detection of *P. gingivalis*/ dendritic cells in the tissue specimen.

Gingival tissue specimens were embedded in OCT medium (Sakura Finetek, Torrance, CA) and frozen at -70º C. Gingival tissue were properly oriented in OCT medium by insertion of a tooth landmark (3-mm strip of filter paper) alongside the tissue specimen, flash-frozen and then stored at -80°C. Seven-micron-thick cryostat sections were cut and fixed in cold acetone for 10 min. At the time of staining, slides were

brought to room temp and conditioned in PBS (pH7.4) for 10-15 minutes. Blocking was done with addition 400µl of 2% BSA overnight in a humid box (slide box) at room temperature. To reduce the auto-fluorescence the slides were placed under the light of the microscope and allowed bleach for 15 minutes. 400µl of polyclonal rabbit anti- *P. gingivalis* (Lampire) antibody (1:200 diluted with 2%BSA/PBS) were added to the slides and incubated at 37º C for 1.5 hr in a humid box. The slides were washed in PBS and incubated with the secondary goat anti-rabbit IgG Texas Red® (T-2767, Invitrogen) 4 µg/ml) for 1 hr at room temperature. It is followed by washing three times in PBS for minimum of 5 minutes each. As negative control, slides were processed with pre-immune rabbit-serum.

Limulus Amebocyte Lysate Assay.

Lack of endotoxin was verified by using the Limulus Amebocyte Lysate (LAL) Pyrogent 03 Plus (Lonza cat #N294-03) gel clot assay following manufacturers' instructions. Briefly an *E. coli* LPS standard, as well as 100 µg/ml, 50 µg/ml and 25 µg/ml replicates of purified minor fimbriae were incubated with Limulus Amebocyte Lysate for 1 hr at 37°C. After 1 hr the glass test tubes were inverted. A positive test was characterized by formation of a firm gel momentarily when the tube is inverted. A negative test is the absence of a solid clot. The sensitivity of this test is 0.03 EU/ml. Endotoxin Unit (EU) is defined by the manufacturer the endotoxin activity of 0.2 ng of "Reference Endotoxin Standard."

Chapter Three:

The Minor Fimbriae Targets DC-SIGN: Immunological Consequences.

Abstract:

The oral mucosal pathogen *Porphyromonas gingivalis* expresses at least two adhesins: the 67 kDa mfa-1 (minor) fimbriae and the 41 kDa fimA (major) fimbriae. In periodontal disease, *P. gingivalis* associates *in situ* with dermal dendritic cells (DCs), many of which express DC-SIGN (CD209). The cellular receptors present on DCs that are involved in the uptake of minor/major fimbriated *P. gingivalis*, along with the effector immune response induced, are presently unclear. In this study, stably transfected human DC-SIGN$^{+/-}$ Raji cell lines and monocyte-derived DCs (MoDCs) were pulsed with whole, live wild-type Pg381, isogenic major- (DPG-3), minor- (MFI) or double-fimbriae (MFB) deficient mutant *P. gingivalis* strains. The influence of blocking antibodies, carbohydrates, full-length glycosylated HIV-1 gp120 envelope protein and cytochalasin D on uptake of strains and on the immune responses was determined *in vitro*. We show that binding of minor fimbriated *P. gingivalis* strains to Raji cells and MoDCs is dependent on DC-SIGN, while the double-fimbriae mutant strain does not bind. Binding to DC-SIGN on MoDCs is followed by internalization of *P. gingivalis* into DC-SIGN rich intracellular compartments and MoDCs secrete low levels of inflammatory cytokines and remain relatively immature. Blocking DC-SIGN with HIV-1 gp120 prevents uptake of minor fimbriated strains and deregulates expression of inflammatory cytokines. Moreover, MoDCs promote a Th_2 or Th_1 effector response, depending on whether they

are pulsed with minor or major fimbriated *P. gingivalis* strains, respectively, suggesting distinct immunomodulatory roles for the two adhesins of *P. gingivalis.*

Introduction:

The C-type lectin DC-specific ICAM-3 grabbing non-integrin (DC-SIGN) is a pattern recognition receptor (PRR) and adhesion molecule expressed by dendritic cells (DCs) and by certain types of macrophages (80). It is used to endocytose microbial antigens in the periphery, to bind to ICAM-2 on endothelial cells (97) and to mediate immune clustering with ICAM-3+ T cells in the lymph nodes (62, 80, 98). It is also expressed on blood DCs (99) and in pathological conditions such as rheumatoid arthritis (100) and in rupture prone atherosclerotic plaques (101, 102). Recent studies indicate that DC-SIGN+ DCs increase in the oral mucosal disease chronic periodontitis (CP) (54, 57, 103). DC-SIGN is one of a family of calcium-dependent C-type lectins that bind to carbohydrate motifs and to Lewis blood group antigens (71, 72). Although lacking Toll-IL-1r activation domains, DC-SIGN has emerged as a key player in the induction of immune responses against numerous pathogens, via modulation of TLR-induced immune activation (104). This occurs by activation of ERK (105), and Raf-1 kinase-dependent acetylation of transcription factor NF-κB (70, 106). *Mycobacterium tuberculosis* (107) *Mycobacterium leprae* (76), and *Helicobacter pylori* (81) target DC-SIGN to gain entry into DCs, disrupt full DC maturation and inhibit Th1 effector cell polarization. *Neisseria meningitidis and Lactobacillus spp.,* on the other hand, target DC-SIGN to modulate the immune response towards Th1 (108) or Treg (109), respectively.

The immunopathogenesis of chronic periodontitis (CP) has been linked to negative regulation of TLRs (69, 110, 111) and to the presence of Th2 effector T cell populations (reviewed in (112), but the specific role of oral mucosal pathogens in induction of Th2 effector responses are just beginning to be identified (9). The oral mucosa in CP contains organized lymphoid aggregates, called oral lymphoid foci, or OLF (113). OLF contain immune conjugates consisting of dermal DCs and CD4+ T cells, as well as B cells (114). Of particular interest is the presence of an intense infiltrate of DC-SIGN+ DCs in the lamina propria of CP, combined with evidence that DCs in the lesions appear to mobilize towards the capillaries (114). This has fueled speculation that, as with gut lamina propria DCs (115), specific microbiota in the oral mucosa target lamina propria DCs that can direct the T cell effector responses (116, 117).

P. gingivalis is one of several intracellular pathogens implicated in CP (reviewed in (118)). Most pathogens, *P. gingivalis* included (119) express different pathogen-associated molecular patterns (PAMPs) that can trigger distinct classes of PRRs on a single cell simultaneously (104). Of particular relevance are the two adhesins of *P. gingivalis*, termed the Mfa-1 (minor) and FimA (major) fimbriae. Adhesion of pathogens to host tissues and subsequent invasion are important early events in mucosal pathogenesis (120). The minor and major fimbriae of *P. gingivalis* have been shown in the rat model to play roles in the pathogenesis of periodontal disease (120). The two fimbriae are distinct antigenically, by amino acid composition, and by size (22, 23). The major fimbriae is composed of a 41 kDa protein, encoded by the *fimA* gene (21). Much is known of the PRRs targeted by the major fimbriae (33-37) and of the intracellular signaling pathways that are activated (38, 39). In contrast, little is known of the cellular

receptors targeted by the 67 kDa minor fimbriae, encoded by the *mfa1* gene. Expression of both fimbriae is regulated under different environmental conditions (24, 25, 27) Understanding the immunobiological properties of these two fimbriae could help in understanding how this oral mucosal pathogen evades the immune response and induces periodontal disease, described as a Th_2 type disease (24).

The purposes of the present study were: (i) to determine the role of DC-SIGN in binding and uptake of isogenic minor and major fimbriae-deficient mutants of *P. gingivalis* using stably transfected Raji (B-) cell lines and monocyte-derived dendritic cells (MoDCs), and; (ii) to determine how minor/major fimbriae influence DC maturation, cytokine secretion and the T cell effector responses induced by MoDCs. Our results show that the minor fimbriae of *P. gingivalis* are required for binding to the endocytic receptor DC-SIGN, leading to internalization in DC-SIGN rich compartments. This uncouples cytokine secretion from maturation of DCs and elicits a Th2-biased effector T cell response. Overall these results may help explain how this oral pathogen evades and suppresses the immune response.

Results:

DC-SIGN-mediated binding of *P. gingivalis* to Raji cells dependent on minor fimbriae.

P. gingivalis has been previously shown to associate *in situ* with DCs in human oral mucosa from chronic periodontitis patients (121) and to be taken up by MoDCs *in vitro* (122) but the cellular receptors used for binding to MoDCs and uptake are unclear.

DC-SIGN is of particular interest as DC-SIGN+ DCs increase in inflamed oral mucosa in chronic periodontitis (54, 114). To determine the ability of wt Pg381 to bind to DC-SIGN, stably transfected DC-SIGN positive (Raji-DCS) and negative Raji cells (Raji) were obtained and the phenotype verified by flow cytometry (Fig. 3A). Our results indicate that Raji-DCS and Raji are positive and negative, respectively, for DC-SIGN, as previously reported (78). The expression level of other relevant cell surface receptors are also shown in Fig 3A. To determine binding of *wt* Pg381 (Pg $^{min+/maj+}$) to Raji-DCS and Raji, bacteria were Syto- or CFSE-labeled and binding analyzed qualitatively by image-enhanced fluorescence microscopy at low magnification (Fig. 3B, panels 1-4) and at higher magnification (Fig. 3B, panels 5, 6). Our results indicate that DC-SIGN is required for optimum binding of *wt* Pg381 to Raji cell lines. This disparity in binding to Raji-DCS vs. Raji was quantitated by flow cytometry, with binding analyzed at 1.5 hr, 3 hr and 6 hr. Optimum binding was achieved at 1.5 hr. Shown in Fig. 3C is the percentage of Raji-DCs and Raji that were associated with *wt* Pg381 at 1.5 hr. The results indicate a significantly decreased binding of *wt* Pg381 to Raji vs. Raji-DCS (↓43%, $p<0.05$, Student t-test) (Fig. 3C, Fig 3D). This decrease in binding to Raji was greater (↓71%) with strain DPG-3. In contrast, there was no difference in binding of MFI or MFB to Raji vs. Raji-DCS. Binding of MFI to Raji likely depends on CD29, expressed equally by Raji-DCS and Raji (Fig 3A) and previously shown to bind major fimbriae (33). MFB failed to associate with either Raji-DCS or Raji (Fig 3D). To further verify the role for DC-SIGN in binding of minor vs. major fimbriated *P. gingivalis* strains to Raji-DCS, we blocked DC-SIGN with L-fucose, mannose and mannans (Fig. 4). D-fucose, a stereoisomer of L-fucose, does not block DC-SIGN (123) was used as a negative control for sugar blocking.

Preliminary studies established optimum dose (50 μg/ml) of sugars for blocking of DC-SIGN on Raji DCS by FACS analysis (not shown). We show that binding of *wt* Pg381 and DPG-3 to Raji-DCS was blocked by L-fucose, D-mannose and mannans, but not control D-fucose (Fig. 4). Strain MFI was not blocked by any of the sugars; nor did the sugars result in significant blocking of any of the strains to Raji cells (not shown). Blocking of MFB with sugars was not performed as this strain did not bind to either Raji cell line.

DC-SIGN-mediated uptake of *P. gingivalis* by MoDCs is mediated by minor, not major fimbriae.

Phenotypic analysis of day 6 MoDCs by flow cytometry indicates that MoDCs express surface DC-SIGN, as well as CD29, CD11b, CD11c, CD18 and DEC-205 (Fig. 5A). Human MoDCs were pulsed with the four CFSE-labeled strains. The results of flow cytometry analysis (Fig. 5B) indicate that association of three of the *P. gingivalis* strains with MoDCs occurred within 3 hr, in the following order: MFI > *wt* Pg381 > DPG-3. MFB did not bind to MoDCs over background of 3%. Antibody blocking studies were thus performed with all strains except MFB. Shown in Fig. 6A are results with *wt* Pg381. Antibody blocking studies revealed that anti-DC-SIGN, but not anti-CD11c, anti-CD18 or anti-CD29 resulted in a significant reduction in association of *wt* Pg381 with MoDCs. Endocytosis of FITC-dextran (124) was unaffected by anti-DC-SIGN antibody (not shown), indicating that phagocytosis was still intact. Use of cytochalasin D, which inhibits actin polymerization required for internalization, but not binding, demonstrates that *P. gingivalis* is being internalized by MoDCs. DC-SIGN-

blocking sugars mannose and mannan diminished uptake of *wt* Pg381 (Fig. 6A) (72). As mannose is a minor component sugar of the LPS of *P. gingivalis* (125, 126) we tested the ability of *P. gingivalis* LPS to block uptake of *wt* Pg381, but there was no effect (data not shown). To further confirm the role of DC-SIGN on MoDCs in binding to *P. gingivalis*, we used DC-SIGN-targeting HIV-1 glycosylated envelope protein gp120 as a blocking agent (Fig. 6B). We show that gp120 resulted in a dose-dependent loss of uptake of *wt* Pg381 and DPG-3, but not MFI to MoDCs.

Attachment of *P. gingivalis* to DC-SIGN on MoDCs is followed by uptake into DC-SIGN-rich intracellular compartments.

To visualize extracellular and intracellular association of Syto-labeled *wt* Pg381, MoDCs were probed with FITC-labeled anti-DC-SIGN at 1 hr (Fig. 7A) and 6 hr (Fig 7B, Fig 7C), then analyzed by image enhanced fluorescence microscopy, aided by deconvolution analysis. Early attachment to surface DC-SIGN (Fig 7A, arrows) is followed by intracellular localization of *P. gingivalis* with DC-SIGN in MoDCs (Fig 7B, 7C, arrows). At later time points (18 hrs), large numbers of essentially intact *wt* Pg381 were detected within as yet undefined intracellular compartments (Pg-containing vesicles or PgCV) of MoDCs (Fig 7D).

Inflammatory cytokine production induced by major fimbriae, regulated by DC-SIGN-targeting minor fimbriae.

Microbial DC-SIGN ligands reportedly dampen TLR-dependent production of inflammatory and Th_1-biasing cytokines by MoDCs (81). We therefore analyzed the

production of inflammatory cytokines by MoDCs pulsed with the *P. gingivalis* strains for 3 hr (Fig. 8A) and 18 hr (Fig. 8B). We show that MFI was the most potent inducer of IL-1β, IL-8, IL-6 and TNFα at 3 hr and of IL-1β, IL-10, IL-12p70, IL-8 and TNFα at 18 hr. In contrast, DC-SIGN targeting strain DPG-3 induced no detectable TNFα and significantly lower levels of IL-1β (vs. *wt* Pg381 or MFI) at 3 hr and of IL-1β, IL-12p70, IL-8, IL-6 and TNFα (vs. MFI) at 18 hr. Double mutant MFB induced the lowest levels of nearly all cytokines at 3 hr and 18 hr. To further confirm the influence of DC-SIGN on regulation of inflammatory cytokine production by *P. gingivalis,* DC-SIGN was blocked with HIV-1 gp120 prior to pulsing with all strains except the double mutant. The results for *wt* Pg381 (Fig 8C) indicate that blocking DC-SIGN enhances the induction of inflammatory cytokines IL-1β, IL-12p70, IL-8 and IL-6, but not IL-10. In contrast, in the absence of the activating major fimbriae (i.e. DPG-3), blocking DC-SIGN with gp120 does not increase cytokines IL-12p70, TNFα and IL-6. Interestingly, HIV-1 gp120 blocking of DC-SIGN also deregulated inflammatory cytokine production by MFI, which does not express DC-SIGN ligand. HIV-1 gp120 alone did not induce inflammatory cytokines, but did induce IL-10, as previously reported (127).

DC maturation induced by major fimbriae, regulated by minor fimbriae.

DCs were further analyzed for maturation status at 18 hr (Fig 9A-C). We show that, while HLA-DR induction was nearly equivalent for all strains, strain MFI was the strongest inducer of CD80 and CD83, and MFB was the weakest inducer of all co-stimulatory and maturation markers. Compared to MFI, strain DPG-3 was a relatively weak inducer of CD80, CD83 and CD86, with *wt* Pg381 falling somewhere between

DPG-3 and MFI (i.e. in induction of CD80 and CD86). Blocking DC-SIGN with HIV-1 gp120 inhibited MoDC maturation as was previously published by Shan *et al.* 2007 (127). Furthermore, pre-incubation with HIV-1 gp120 prior to co-culture with *P. gingivalis* strains inhibited the MoDC maturation induced by DC-SIGN targeting strains *wt* Pg381 and DPG-3, unlike the inflammatory cytokine response, which was enhanced by HIV-1 gp120 (Fig 8C). The presence of HIV1 gp120 inhibited DPG-3-induced co-stimulatory molecules CD80, CD86 and CD83 upregulation the strongest, followed by *wt* Pg381. Blocking DC-SIGN did not block upregulation of HLA-DR, CD80 or CD83 induced by non-DC-SIGN targeting strain MFI (Fig 9B, C). These results suggest an uncoupling of DC maturation from the inflammatory cytokine response when DCs phagocytose whole live bacteria that express a DC-SIGN ligand.

Minor fimbriated strain induces a Th2 effector response, major fimbriated strains a Th1-effector response.

Previous studies have shown that DC-SIGN ligands can induce a Th2-based effector response (81, 127). In the present study, MoDCs were pulsed with each of the four *P. gingivalis* strains, then co-cultured with autologous naïve CD4+ T cells for 7 days, after which T cell cytokines and T cell proliferation were analyzed. We show that MoDCs pulsed with DC-SIGN-binding strain DPG-3 induced release of significantly higher IL-4 levels from T cells compared to all other strains and very low levels of IL-12p70 relative to MFI (Fig. 10A). When expressed as Th_1/Th_2 cytokine ratios (IFNγ/IL-4 and IL-12p70/IL-4), DPG-3-pulsed MoDCs induced the lowest levels of all strains except for MFB and yielded a very low Th_1 index (Table 2). In contrast, MFI pulsed MoDCs

induced significantly lower levels of the Th_2 cytokine IL-4, but comparable levels of IFNγ and very high levels of IL-12p70 from T cells. This yielded high ratios of IFNγ/IL-4 and IL-12p70/IL-4 and a relatively high Th_1 index (=8.81) (81). *Wt* Pg381 induced the lowest levels of IL-4 low levels of IL-12p70, and comparable levels of IFN-γ by T cells. The low levels of IL-4 by MFI resulted in the highest Th_1 index (10.63) while DPG-3 induced the lowest levels of IFN-γ and IL-12p70 and had the lowest Th_1 index (=1.15) (Table 2).

To determine if the immuno-proliferative ability of *P. gingivalis* pulsed MoDCs would correlate with the Th_1 index, CFSE-labeled naïve CD4+ T cells were analyzed at various stimulator: effector ratios for 7 days. 1:50 MoDC-T cell ratio yielded the maximum proliferation. Our results (Fig 10B) show that MoDCs pulsed with DPG-3 and MFB induced the weakest T cell proliferative responses, while *wt* Pg381 and MFI induced the strongest T cell proliferative responses. The weak T cell proliferation and cytokine secretion exhibited by the double fimbriae knockout MFB could be attributed to its lack of binding and uptake (Fig 5B). However, we can attribute the impaired proliferation of co-cultured CD4+ T cells to the minor fimbriae of DPG-3 interacting with DC-SIGN. While the MoDCs co-cultured with DPG-3 upregulated more of their maturation markers and co-stimulatory markers when compared to wt Pg381, the cytokines that both the MoDC's and T cells secreted in response to DPG-3 had a distinct Th_2 bias (Fig 8 and 10). This bias could explain the disparity between the higher co-stimulatory molecule expression on the DPG-3 pulsed MoDCs (Fig 9), and the reduced T cell proliferation observed (Fig 10B). Furthermore, we can attribute the robust IL-12p70 cytokine production of MFI to that strain's lack of immunosuppressive DC-SIGN

targeting fimbriae. Linear regression analysis of % T cell proliferation induced by MoDCs pulsed with each strain, showed a significant association ($r^2 = 0.857$, p=.024 [SPSS, ver. 15]) with the Th_1 index.

Discussion:

Overall, these results indicate that both the major and minor fimbriae of *P. gingivalis* are involved in binding of the whole live bacterium to Raji cell lines (Fig 3) and to DCs (Fig 5); however, the minor fimbriae are required for binding to DC-SIGN (Figs 3, 4, 6). This results in *P. gingivalis* being internalized and routed in large numbers into as yet undefined intracellular vesicles of DCs (Fig. 7). DCs that have internalized *P. gingivalis* strains that lack the major fimbriae are poorly matured (Fig. 9), secrete very low levels of inflammatory cytokines (Fig. 8) and induce a Th_2-biased, weak immunoproliferative T cell response (Fig. 10). While these findings were established using isogenic fimbriae-deficient mutants of *P. gingivalis*, expression of the fimbriae have been shown to be regulated by growth conditions, including temperature (24, 128) and hemin levels (25) Apparently, a two-component regulatory system (FimS/FimR) controls the two fimbrial genes at different levels depending on heme and temperature (27). Other systemic mucosal pathogens such as *Yersinia pseudotuberculosis* (129), *Salmonella enterica (130, 131)* also regulate their invasive potential under environmental pressures. This is of particular relevance here since the preferred ecological niche of *P. gingivalis*, a hemin-requiring anaerobe are deep bleeding "crypts" in the human oral mucosa, called

periodontal pockets (117). These pockets are subjacent to OLF and to lamina propria dermal DCs (113) where *P. gingivalis* infects DCs *in situ* (121). *P. gingivalis* initially colonizes surface mucosa and tooth surfaces, where hemin levels and temperature are reduced, forming part of a complex biofilm (117, 132). The major fimbriae appear required for initial attachment to host cells (87, 122, 133-135), while the minor fimbriae appear to play an important role in microcolony formation by facilitating cell–cell interactions and promoting biofilm formation (132, 136, 137). Both fimbriae play essential roles in induction of alveolar bone loss (120) and atherosclerosis (138) in rats, but the specific mechanisms of these (seemingly) disparate processes are unclear. A recent review describes the important role for Th_2 type responses in the inability of the host to successfully resolve periodontal disease (112), suggesting clinical relevance to our findings of Th_2-responses biased by the minor fimbriae of *P. gingivalis*.

Relatively little is known about the steps involved in the formation and secretion of minor fimbriae and of the cellular receptors and signaling pathways it targets. In contrast, the major fimbriae are under intense investigation in this regard (22, 23, 33-35, 37, 117, 139, 140). The major fimbriae activate macrophages through TLR2 and TLR4, as well as complement receptor 3 and CD14 (38, 39). Davey *et al*. (2008) showed that both the major and minor fimbriae specifically bind to chimeric TLR2 and CD14 proteins in a cell free ELISA (40). TLR2 appears to be particularly important in IL-10-mediated mucosal immune homeostasis in response to commensals (141). DC-SIGN-ligation (using purified microbial ligands) has also been shown to induce IL-10, by triggering Raf-1 phosphorylation (70). Combined with activation of TLR4, DC-SIGN ligation results in enhanced and prolonged NFκB activation and stronger IL-10 production (70).

Our cytokine results corroborate cross-talk between DC-SIGN and TLRs. For example, the most profound effect that blocking DC-SIGN had on cytokine secretion was observed with *wt* Pg381 (Fig. 8C), which expresses ligands for DC-SIGN (minor fimbriae) and TLR2/4 (major fimbriae). With Pg381 we saw an enhancement (deregulation) of IL-1β, IL-12p70, IL-8 and IL-6. In contrast, blocking DC-SIGN did not enhance IL-1β, IL-12p70, or IL-6 in response to strain MFI, which lacks DC-SIGN ligand minor fimbriae. Moreover, in the absence of major fimbriae (DPG-3), blocking DC-SIGN decreased IL-12p70 and IL-6. TNFα, a good indicator of NFkβ activation was consistently dampened by gp120 (Fig. 8C), regardless of bacterial strain used. Although DC maturation and cytokine secretion are both generally attributed to ligation of TLRs leading to NFκβ activation (68), phagocytosis/endocytosis in itself triggers a family of intracellular signaling pathways (reviewed in (52, 142, 143). Consistent with this concept, we show that blocking DC-SIGN reduces phagocytosis of *P. gingivalis* by MoDCs (Fig. 6), and reduces upregulation of costimulatory molecules (Fig. 9B, 9C) but not certain cytokines (Fig. 8). Overall, these results suggest an uncoupling between the DC cytokine response and maturation by DC-SIGN ligands that warrants further analysis with purified native fimbriae.

In this context, Chapter 4 will examine the possibility of the minor fimbriae being glycosylated. In brief purified the minor fimbriae by HPLC and analyzed the protein sequence by MALDI-TOF. We discovered that there are two conserved Asn-Xaa-Ser/Thr N-glycosylation motifs on the minor fimbriae sequence (49). Putative glycosylation of the 67 kDa minor fimbriae was further verified by Pro-Q Emerald glycoprotein staining, a periodate- and fluorescence-based reaction (Section 4). The

purified minor fimbriae were analyzed by monosaccharide compositional analysis and LC-MS/MS. There are reports of a role for glycosylation of the fimbriae in *P. gingivalis*. Knockouts of *gftA* (a *wcaE* glycotransferase homolog of *E. coli*) in *P. gingivalis* fail to make mature fimbriae (42). The gingipains of *P. gingivalis* are apparently glycosylated (43) and this glycosylation is regulated by the *vimF, vimA* and *vimE* glycotransferase genes (44, 45). Knocking out these genes causes a failure to glycosylate these gingipains, leading to their inactivation (43-45). Kadowaki *et al.* (1998) have identified that Arg gingipain activity is essential for the processing and translocation of mature fimbriae (32). Recently, it was discovered that the RagA proteins of *P. gingivalis* are glycosylated (46). The commonalties among these outer membrane proteins is that they encode for an N-terminal, long signal peptide that gets cleaved once they enter the inner membrane (29, 47, 48). Many mucosal pathogens exhibit glycosylation motifs on their flagella, pili, and fimbriae for binding to host cells (41). Glycosylation also reportedly plays a role in maintaining the protein structure, in protection of proteolytic degradation and in immune evasion (41, 49). Additionally, it was recently determined that the glycosylation of soluble peanut allergen was sufficient for targeting DC-SIGN in MoDCs and that its recognition by DC-SIGN skewed the T cell response to a Th_2 phenotype (144). Finally, it is believed that the carbohydrate moieties of HIV-1 gp120 confer the immunosuppressive effects on MoDCs (127). Glycosylation on the minor fimbriae might enable *P. gingivalis* to prompt its immunosuppressive phenotype in a similar manner.

In conclusion, our results show distinct immunomodulatory roles for two adhesins expressed by the mucosal pathogen *P. gingivalis*. We show the major fimbriae are immunostimulatory and the minor fimbriae are immunosuppressive. Although co-

expressed in wild type strains under laboratory conditions, the two fimbriae are regulated by environmental conditions of direct relevance to their preferred niche. Overall these results may help explain how this oral mucosal pathogen evades and/or suppresses the mucosal immune response, i.e. by uncoupling DC maturation from the cytokine response, leading to anergy.

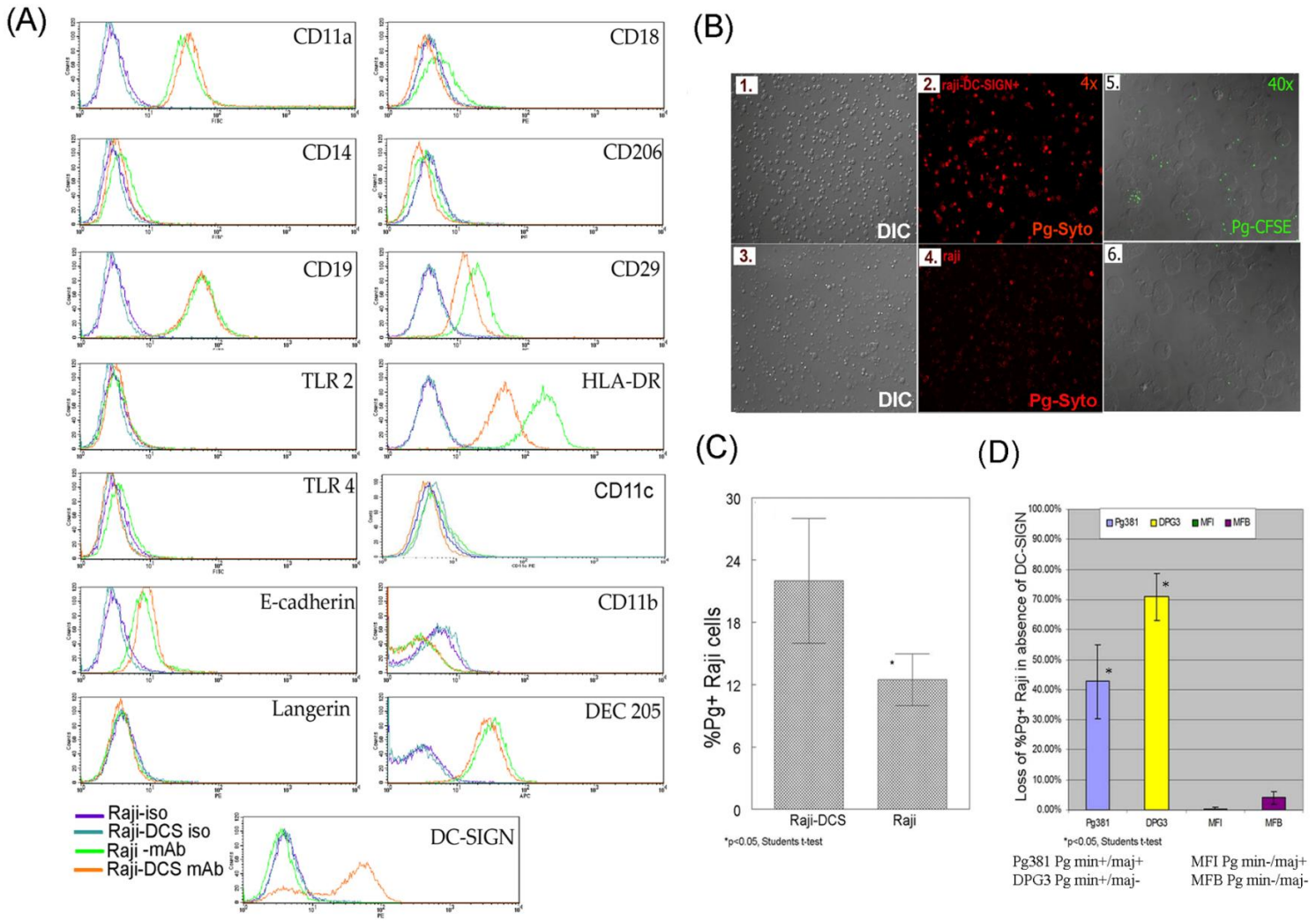
(A)
CD11a
CD18
CD14
CD206
CD19
CD29
TLR 2
HLA-DR
TLR 4
CD11c
E-cadherin
CD11b
Langerin
DEC 205
DC-SIGN
Raji-iso
Raji-DCS iso
Raji -mAb
Raji-DCS mAb
(B)
1.
2. raji-DC-SIGN+ 4x
5. 40x
DIC
Pg-Syto
Pg-CFSE
3.
4. raji
6.
DIC
Pg-Syto
(C)
%Pg+ Raji cells
30
24
18
12
6
0
Raji-DCS
Raji
*p<0.05, Students t-test
(D)
Loss of %Pg+ Raji in absence of DC-SIGN
100.00%
90.00%
80.00%
70.00%
60.00%
50.00%
40.00%
30.00%
20.00%
10.00%
0.00%
Pg381
DPG3
MFI
MFB
*p<0.05, Students t-test
Pg381 Pg min+/maj+
DPG3 Pg min+/maj-
MFI Pg min-/maj+
MFB Pg min-/maj-

FIG 3. *P. gingivalis* binding to Raji cells dependent on DC-SIGN expression and on minor fimbriae. (A) Phenotype of stably transfected DC-SIGN positive (Raji-DCS) and negative (Raji) Raji B- cell lines. Shift to the right of histograms indicates increased mean fluorescence intensity (*MFI*) of Raji-DCS (red tracing) relative to Raji (green tracing) or relative to isotype control antibodies (ISO) (blue and purple tracings). (B) Binding of *Syto*-labeled (B1-4) or CFSE-labeled (B5, 6) *P. gingivalis* to Raji-DCS and Raji was visualized by epifluorescence microscopy at a final magnification of 40x (B2, B4) and 400x (B5, B6). Cells were also examined by phase contrast (differential interference contrast [DIC]) microscopy (B1, B3). (C) FACS analysis of % Raji-DCS, Raji positive for CFSE-labeled Pg381 (Pg $^{min+/maj+}$) at 1.5 hrs. Data are representative of a minimum of three experiments. The means $\pm$ S.E.M, in triplicate, were analyzed by Students T-test and the significant differences between Raji-DCS and Raji are shown. (C2) Percentage loss of Pg^+ Raji, relative to Raji-DCS, calculated by: % of Pg^+ Raji DCS minus % Pg^+ Raji divided by % Pg^+ Raji-DCS x 100. Strains shown are Pg381 (Pg $^{min+/maj+}$) (light blue), DPG-3 (Pg $^{min+/maj-}$) (yellow), MFI (Pg $^{min-/maj+}$) (green), MFB (Pg $^{min-/maj-}$) (purple). The means $\pm$ S.E.M, in triplicate, were analyzed by Students T-test and the significant differences between Raji-DCS and Raji are shown.

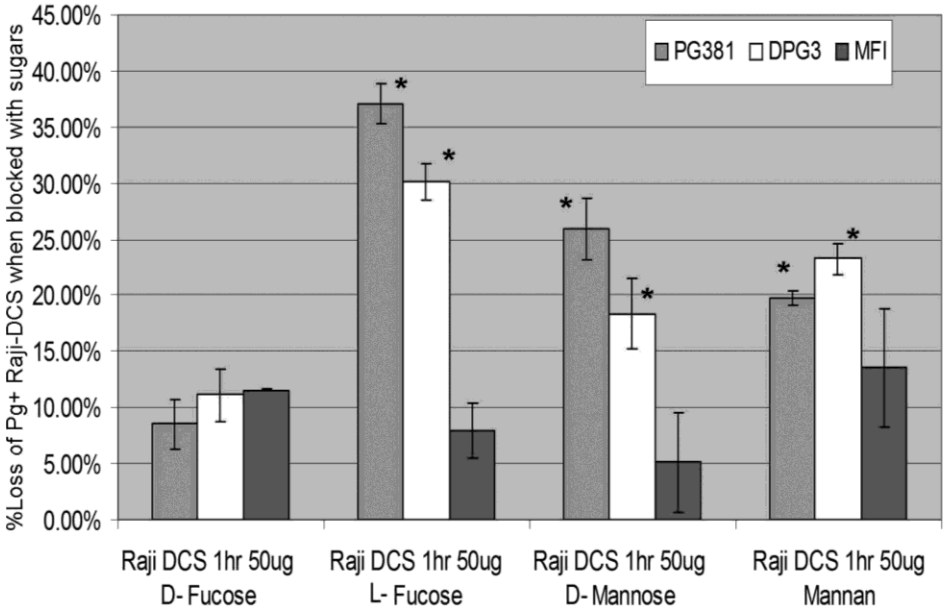

*Significant loss of association relative to control, P<0.05, Students t-test

FIG 4. Specific carbohydrate blocking of DC-SIGN inhibits binding of minor fimbriated *P. gingivalis* strains to Raji cells. Raji-DCS were pre-treated with carbohydrates at doses shown for 30 min; after which Pg381 (Pg $^{min+/maj+}$), DPG-3 (Pg $^{min+/maj-}$), MFI (Pg $^{min-/maj+}$) were added to Raji-DCS and Raji (not shown) for 1 hr and binding analyzed by FACS analysis. % Loss of Pg binding in presence of carbohydrate was calculated by % Pg^{+} Raji DCS minus % Pg^{+} Raji DCS in presence of carbohydrate, divided by % Pg^{+} Raji DCS x 100. Data are representative of a minimum of three experiments. The means $\pm$ S.E.M, in triplicate, were analyzed for significant differences between no blocking (none) and sugar blocking by Students t –test.

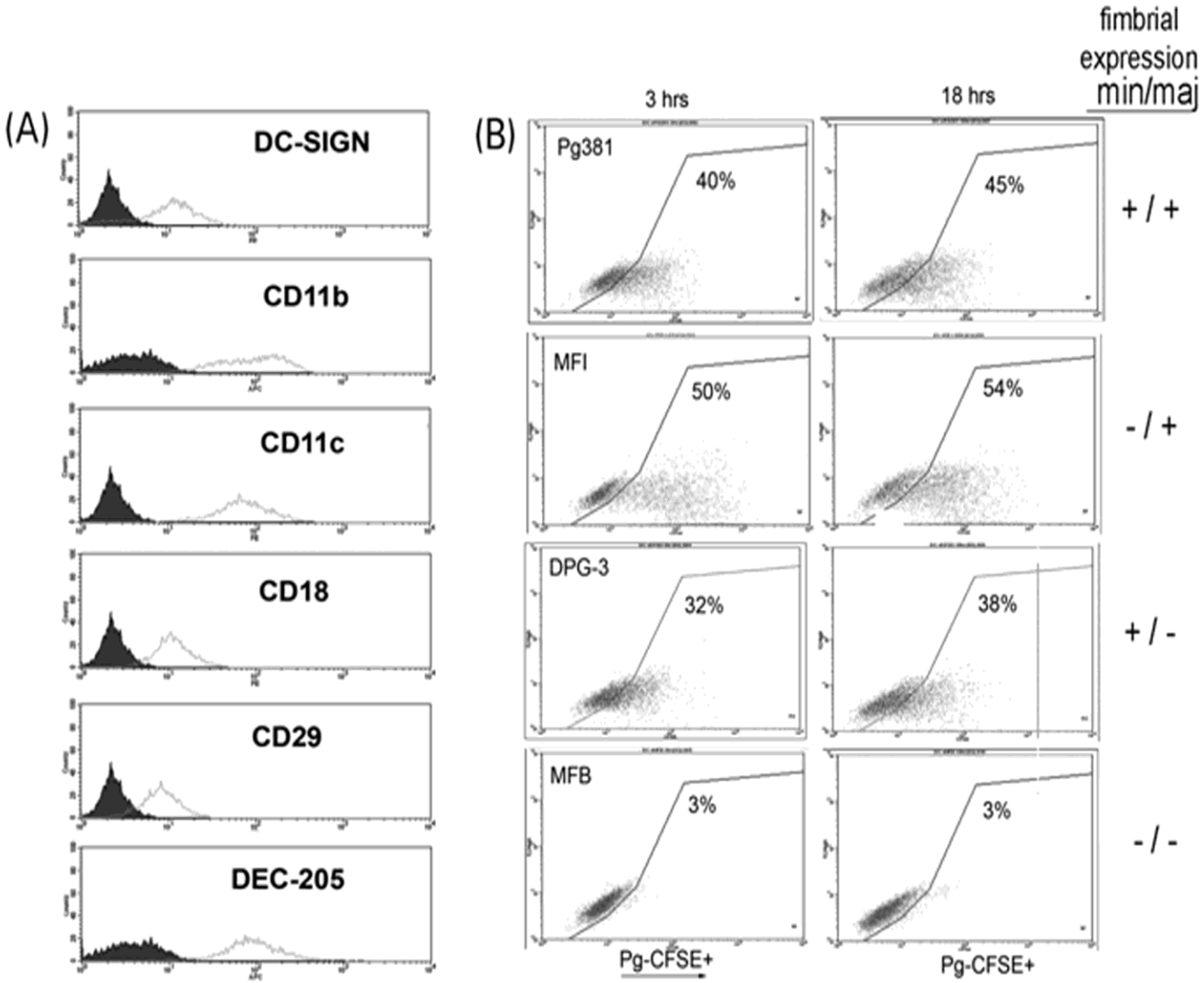
(A)
DC-SIGN
CD11b
CD11c
CD18
CD29
DEC-205
(B)
3 hrs
18 hrs
fimbrial expression min/maj
Pg381
40%
45%
+ / +
MFI
50%
54%
- / +
DPG-3
32%
38%
+ / -
MFB
3%
3%
- / -
Pg-CFSE+
Pg-CFSE+

FIG 5. MoDCs express DC-SIGN; bind fimbriated *P. gingivalis* strains (A) Day 7 immature CD1a+ MoDCs were analyzed for expression of DC-SIGN and other putative endocytic receptors by FACS analysis. MoDCs were labeled with isotype control mAb (filled histogram) or receptor specific mAb (open histogram), showing expression (shift to the right) of DC-SIGN, CD11b, CD11c, CD18, CD29 and DEC-205. (B) FACS scatter graph showing % binding (to the right of line) of CFSE-labeled *P. gingivalis* strains to MoDCs at 3h and 18h.

(A)

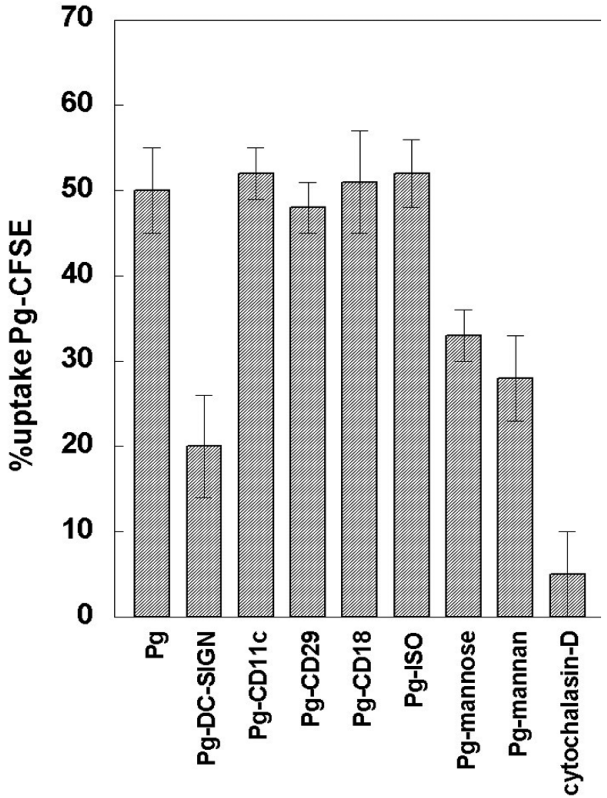
%uptake Pg-CFSE
70
60
50
40
30
20
10
0
Pg
Pg-DC-SIGN
Pg-CD11c
Pg-CD29
Pg-CD18
Pg-ISO
Pg-mannose
Pg-mannan
cytochalasin-D

(B)

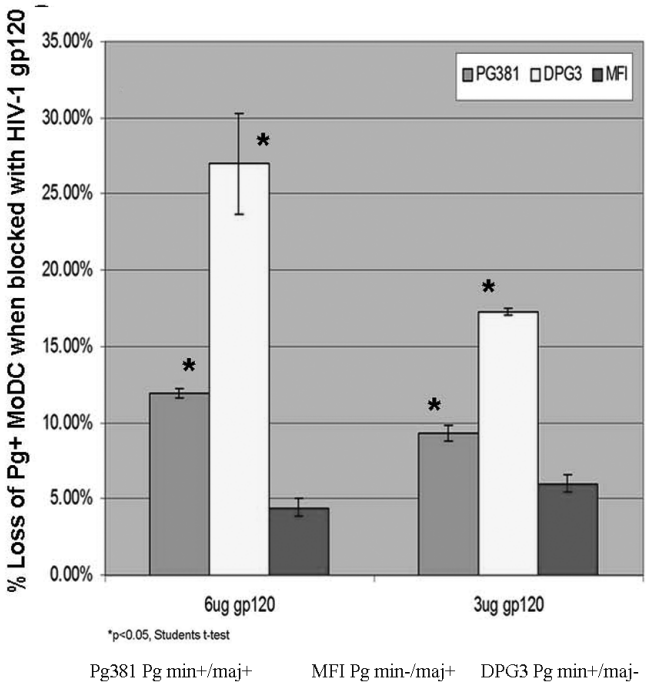
% Loss of Pg+ MoDC when blocked with HIV-1 gp120
35.00%
30.00%
25.00%
20.00%
15.00%
10.00%
5.00%
0.00%
PG381
DPG3
MFI
*
6ug gp120
3ug gp120
*p<0.05, Students t-test
Pg381 Pg min+/maj+
MFI Pg min-/maj+
DPG3 Pg min+/maj-

FIG 6. Blocking DC-SIGN on MoDCs with antibody or carbohydrates inhibits uptake of *P. gingivalis* (A) MoDCs were pretreated for 30 min with mAb to DC-SIGN, CD11c, CD29, CD18, isotype control, 50 μg mannose or 50 μg mannan at 50:1 MOI or (B) 3 and 6 μg HIV gp120 prior to adding CFSE-*P. gingivalis* strain 381 at 5:1 MOI, after which association was assessed, in triplicate, at 3h at 37°C. Shown are the means $\pm$ S.E.M. of % uptake of Pg-CFSE by MoDCs. For (B), % reduction in presence of gp120 was calculated as % Pg^+ MoDC minus % Pg^+ MoDC in presence of gp120 divided by % Pg^+ MoDC x 100.

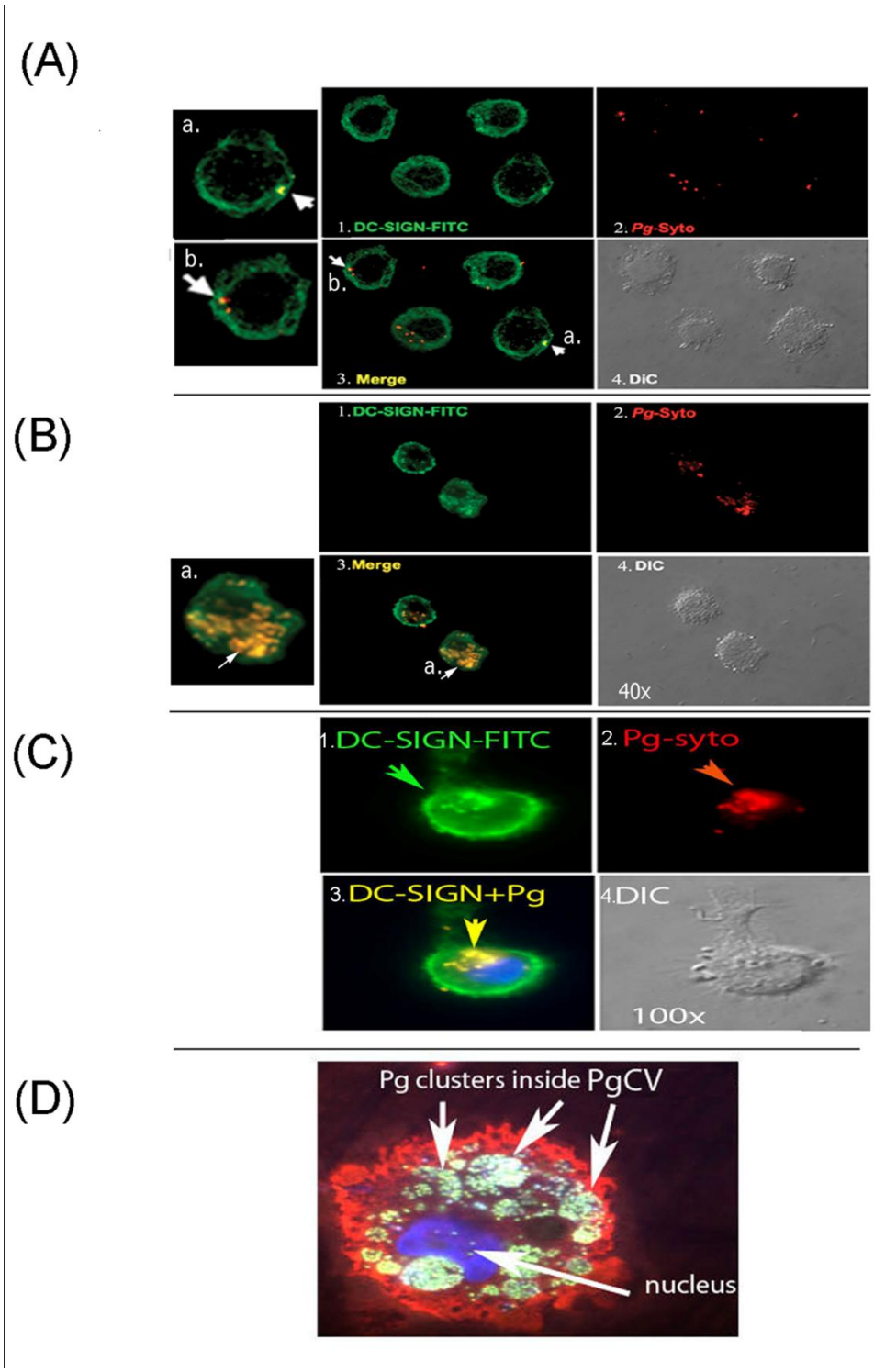
(A)
a.
1. DC-SIGN-FITC
2. Pg-Syto
b.
b.
a.
3. Merge
4. DIC
(B)
1. DC-SIGN-FITC
2. Pg-Syto
a.
3. Merge
a.
4. DIC
40x
(C)
1. DC-SIGN-FITC
2. Pg-syto
3. DC-SIGN+Pg
4. DIC
100x
(D)
Pg clusters inside PgCV
nucleus

FIG 7. *P. gingivalis* colocalizes with membrane DC-SIGN and is taken inside DC-SIGN-rich compartments. Day 7 immature MoDCs were pulsed with Syto-labeled (red fluorescence) *P. gingivalis* 381 at a 50:1 MOI and cells fixed at 1 hr (A) 6 hrs (B, C) or DAPI-labeled *P. gingivalis* 381 at 18 hrs (D). (A-C) MoDCs were probed with mAb to DC-SIGN (clone DCN46, BD-Biosciences), followed by anti-mouse Alexa-Fluor 488 (Molecular Probes) antibodies (green fluorescence). Controls were labeled with isotype control primary mAb (not shown). (B-D) MoDC's were permeabilized prior to probing with DC-SIGN mAb to visualize intracellular DC-SIGN rich vesicles. Slides were analyzed by epifluorescence microscope (Nikon E600), equipped with SPOT CCD camera, integrated with a Pentium IV PC running ImagePro and deconvolution software. Extracellular *P. gingivalis* 381 is shown at 1 hr (A2), binding to DC-SIGN is shown in merged channels (A3 panels a, b) (yellow fluorescence). Intracellular localization of *P. gingivalis* 381 (B2, C2) within DC-SIGN-rich compartments (B3, C3) (yellow fluorescence) (D) At 18 hrs, large numbers of *P. gingivalis* 381 accumulate inside vesicles (Pg containing vesicles or PgCV) of MoDCs. Viability dye propidium iodide (red) is excluded by the outer membrane of MoDCs, attesting to viability of MoDC, and potentially, *P. gingivalis*. DAPI-positive nucleus wrapped around PgCV is also shown.

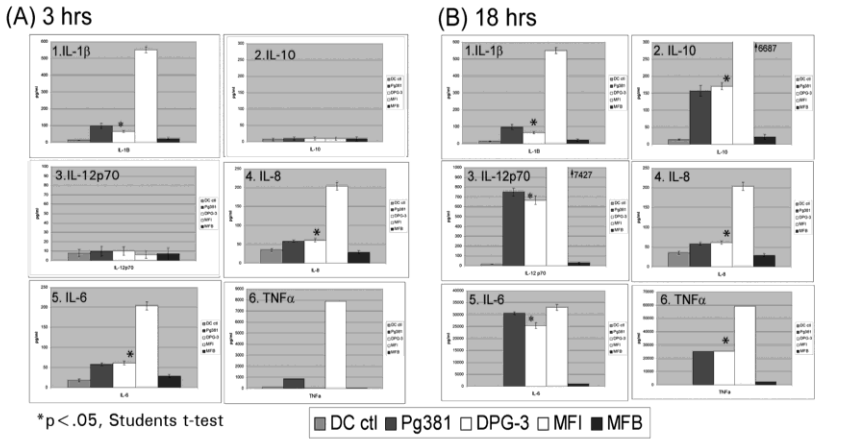
(A) 3 hrs
(B) 18 hrs
1.IL-1β
2.IL-10
3.IL-12p70
4. IL-8
5. IL-6
6. TNFα
*p<.05, Students t-test
DC ctl
Pg381
DPG-3
MFI
MFB

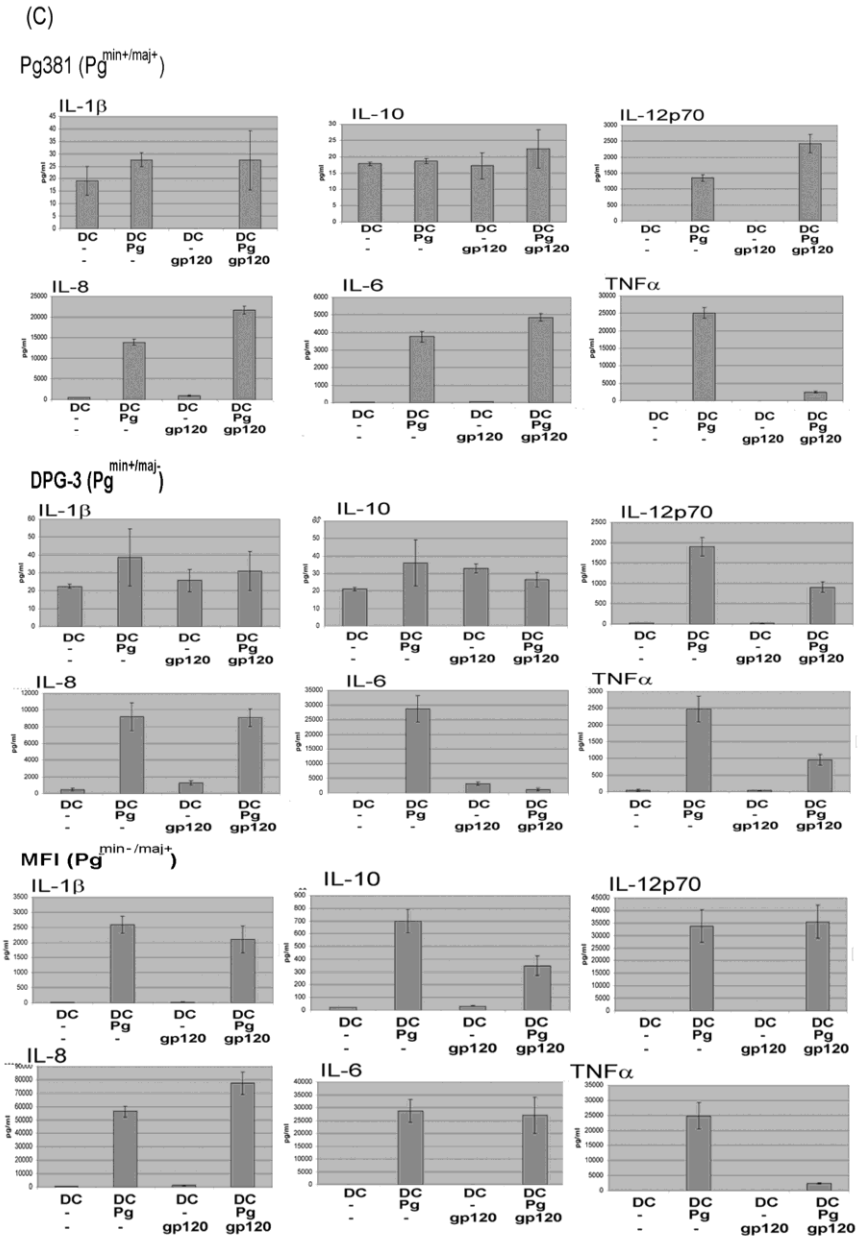
(C)
Pg381 (Pg min+/maj+)
DPG-3 (Pg min+/maj-)
MFI (Pg min-/maj+)
IL-1β
IL-10
IL-12p70
IL-8
IL-6
TNFα
DC
DC Pg
DC gp120
DC Pg gp120

FIG 8. Minor fimbriated strains induce in MoDCs a distinct cytokine response. Supernatants from MoDCs pulsed for: (A) 3h, (B) 18h with *P. gingivalis* 381, DPG-3, MFI, MFB or no bacteria (DC control) or (C) 18hr cytokine response of MoDCs pretreated with 6 μg/ml of HIV-1 gp120 CM and pulsed with Pg381, DPG-3, MFI and no bacteria were analyzed in triplicate by flow cytometry using the cytometric bead array (CBA Kit, BD Biosciences, SanDiego, CA). Based on a standard curve for each cytokine, the software calculates levels in pg/ml. Results shown are mean $\pm$ S.E.M.

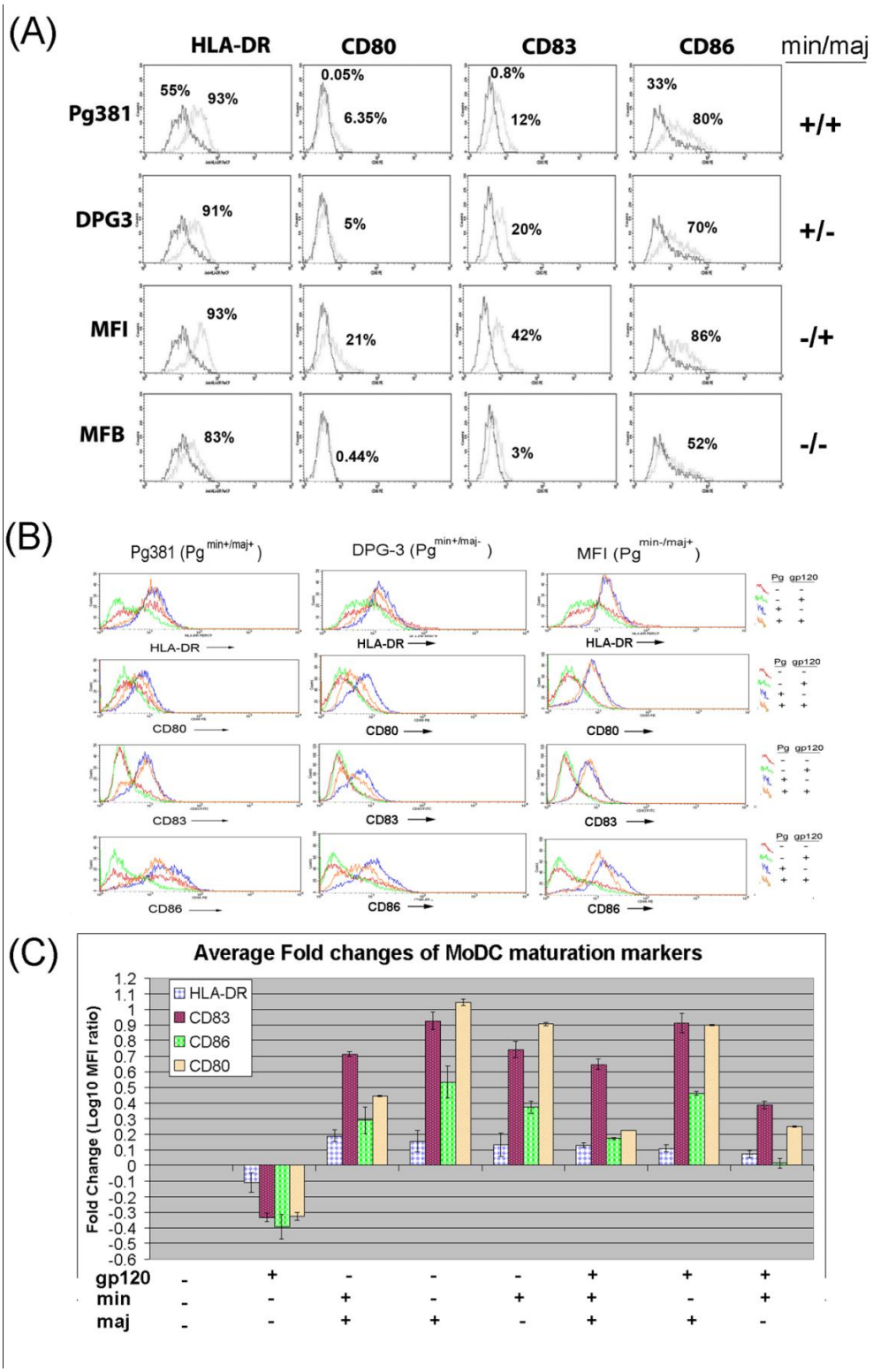
(A)
HLA-DR
CD80
CD83
CD86
min/maj
Pg381
55%
93%
0.05%
6.35%
0.8%
12%
33%
80%
+/+
DPG3
91%
5%
20%
70%
+/-
MFI
93%
21%
42%
86%
-/+
MFB
83%
0.44%
3%
52%
-/-
(B)
Pg381 (Pg min+/maj+)
DPG-3 (Pg min+/maj-)
MFI (Pg min-/maj+)
HLA-DR
CD80
CD83
CD86
Pg gp120
(C)
Average Fold changes of MoDC maturation markers
Fold Change (Log10 MFI ratio)
HLA-DR
CD83
CD86
CD80
gp120
min
maj

FIG 9. Minor fimbriated strains induce in MoDCs a distinct maturation profile. (A) Differences in upregulation of HLA-DR, CD80, CD83 and CD86 on MoDCs by FACS analysis after pulsing with Pg381, DPG-3, MFI , MFB (light tracings) or no bacterial control (dark tracings). (B) Differences in upregulation of HLA-DR, CD80, CD83, and CD86 on MoDCs by pulsing with Pg381, DPG-3, MFI or no bacterial control on MoDCs pre-treated with 6 μg/ml of HIV-1 gp120 CM. Red tracings represent uninfected MoDC control, green tracings are MoDC control pre-treated with HIV-1 gp120 CM, blue lines represent MoDCs that have been pulsed with either Pg381, DPG-3 or MFI, orange lines represent MoDCs that have been pre-treated with HIV-1 gp120 CM and pulsed with either Pg381, DPG-3 or MFI. Results are representative of three separate experiments. (C) The average fold changes in mean fluorescence intensity values (*MFI*) for MoDC cell surface marker expression. The ratios of the *MFI* experimental condition over control were calculated for each cell marker. The *MFI* for the uninfected control conditions were set at 1.0 (log ratio = 0). The means of the $_{10}$logarithms of the ratios for all conditions were calculated. Fold change of HLA-DR is represented in blue bars, CD83 in purple bars, CD86 in green bars, and CD80 in orange bars, are plotted relative to baseline value of uninfected control. Data shown are the means of three separate experiments, $\pm$ S.D., as previously performed (127).

(A)

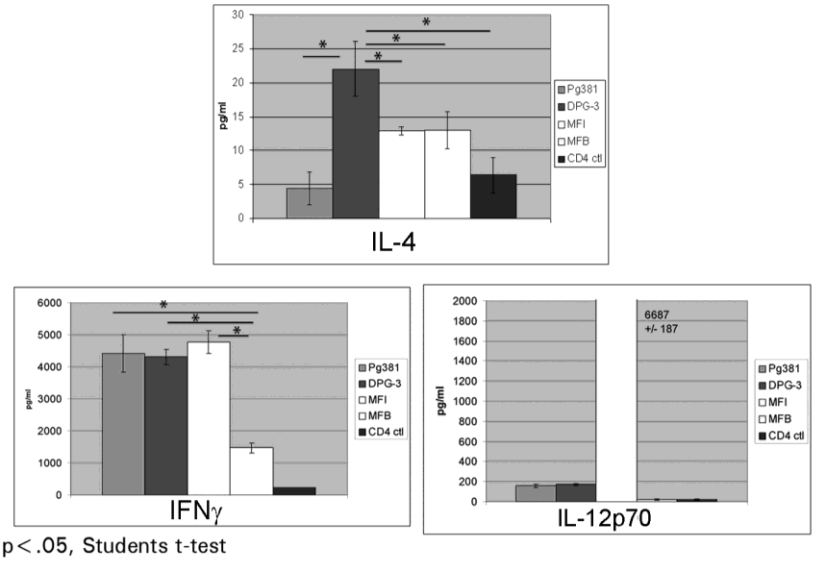

*p < .05, Students t-test

(B)

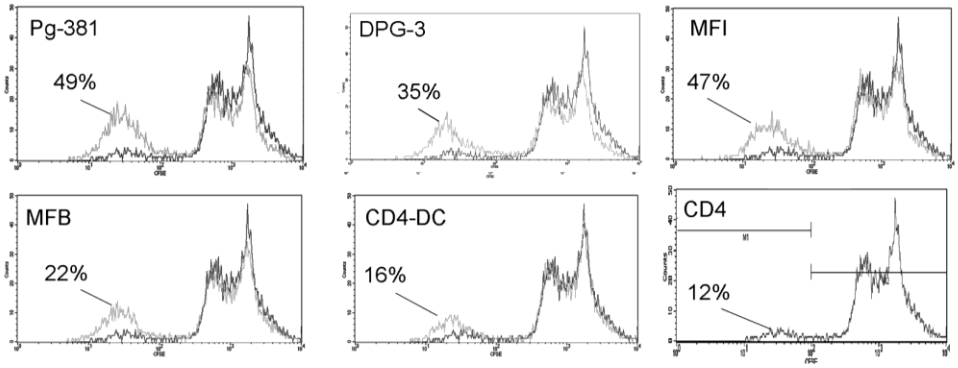

FIG 10. Minor fimbriated mutant induces a Th2 response, major fimbriated mutant a Th1 response (A) Cytokines from naïve autologous CD4+ T cells co-cultured with MoDCs at a 1:50 stimulator: responder ratio were analyzed in triplicate by flow cytometry using the cytometric bead array (CBA Kit, BD Biosciences, SanDiego, CA). Based on a standard curve for each cytokine, the software calculates levels in pg/ml. Results shown are mean ± S.E.M. (B) MoDCs that had been pulsed with Pg381, DPG-3, MFI, MFB or no bacteria (CD4+-DC control) for 18hrs were washed extensively and cultured for 5 days at graded doses (5000 DC / 200μl, 1000 DC / 200 μl and 300 DC / 200 μl in complete RPMI) with naïve autologous CD4+ T cells (50,000 cells/200 μl) pre-labeled with CFSE. %Proliferation was quantitated by loss of CFSE (light tracings), compared to CD4+ control (dark tracings) by FACS analysis. Results are representative of a minimum of three separate experiments.

***P. gingivalis* strain**	**Fimbriae expression**		***Autologous naïve CD4+ T cell response***			
	Minor	Major	IFNγ/IL-4 ratio$^{\zeta}$	IL-12^{p70}/IL-4 ratio$^{\psi}$	Th1 index$^{\varpi}$	*Proliferation**
Pg381	+	+	1027	36.5	10.63	*49%*
DPG-3	+	-	195	1.69	1.96	*35%*
MFI	-	+	367	514	8.81	*47%*
MFB	-	-	112	3.5	1.15	*22%*
CD4-DC control			16	36	0.52	*16%*
CD4 control			35	7.8	0.43	*12%*

*ζ: pg/ml IFNγ ψ: pg/ml IL-12 / pg/ml IL-4 ϖ: IFNγ/IL-4 + IL-12^{p70}/IL-4 / pg/ml IL-4 / 100 *%CFSE negative*

Table 2. Alteration in Th1 index and immunoproliferation dependent on Minor/Major Fimbriae

Levels of IL-4, IFNγ and IL-12p70 from DC-T cell cocultures, as in figure 8 were analyzed for IFNγ/IL-4 ratio and IL-12p70/IL-4 ratio, as shown and Th1 index calculated and tabulated

Chapter Four:

How do the minor fimbriae target DC-SIGN? Is there a role for glycosylation?

Abstract:

We recently reported that the oral mucosal pathogen *Porphyromonas gingivalis*, through its 67 kDa Mfa1 (minor) fimbriae, targets the C-type lectin receptor DC-SIGN for invasion and persistence within human monocyte-derived dendritic cells (DCs). The DCs respond by inducing an immunosuppressive and Th2-biased CD4+ T cell response. We have now purified the native minor fimbriae by ion exchange chromatography and sequenced the fimbriae by tandem mass spectrometry (MS/MS), confirming its identify and revealing two putative N-glycosylation motifs as well as numerous putative O-glycosylation sites. We further show by ProQ staining, that the minor fimbriae are glycosylated and that glycosylation is partially removed by treatment with β-1,4-galactosidase, but not by classic N- and O-linked deglycosidases. Further monosaccharide analysis by gas chromatography-mass spectrometry (GC-MS) confirmed that the minor fimbriae contains the DC-SIGN targeting carbohydrates fucose (1.35 nmol/mg) mannose (2.68 nmol/mg), N-acetylglucosamine (2.27 nmol/mg) and N-acetylgalactosamine (0.652 nmol/mg). Analysis by transmission electron microscopy revealed that the minor fimbriae form fibers approximately 200 nm in length, which could be involved in targeting/ cross-linking DC-SIGN. These findings shed further light

on molecular mechanisms of invasion and immunosuppression by this unique mucosal pathogen.

Introduction:

Porphyromonas gingivalis is one of several mucosal pathogens that have been implicated in chronic periodontitis (CP) a common oral disease that affects 40-60% of the US population (1). *P. gingivalis* utilizes a myriad of virulence factors that contribute to chronic periodontitis. Among these are a polysaccharide capsule, fimbriae, proteases for opsonins C3 and IgG, gingipains (145-148), bacterial lipopolysaccharides (LPS) (57, 59), toxins and hemagglutinins (7, 8).

The fimbriae of *P. gingivalis* play a crucial role in adhesion to and invasion of host cells. We have shown that optimum entry of *P. gingivalis* into human dendritic cells (DCs) requires the presence of two fimbriae, termed the major and minor fimbriae. The major fimbriae are composed of a 41 kDa protein termed fimbrillin, encoded by the *fimA* gene (21). Much less is known about the minor fimbriae, the focus of this paper. The minor fimbriae are comprised of a 67 kDa (22) protein that is encoded by the *mfa1* gene. The major and minor fimbriae are antigenically distinct and they also differ based on amino acid composition and size (22, 23). Very little is understood about the formation and secretion of the minor fimbriae and about possible posttranslational modifications of these fimbriae. Formation and secretion of the major fimbriae is a complex reaction consisting of numerous steps required for transfer of prefimbrillin proteins from the

cytoplasm to the periplasm, cleavage of the N-terminal signal peptide (29, 30), transport of prefimbrillin to the outer face of the outer membrane and assembly into fimbriae structures (30-32).

Deciphering the cellular receptors for the fimbriae is an active area of research. Evidence suggests that the cellular targets of the major fimbriae are the β-1 integrins (CD29) (33, 34). Others have proposed a role for β-2 integrins (CD18) (36, 37, 149) in the cellular response to major fimbriae. In contrast, little is known of the cellular receptors for the minor fimbriae. Lamont *et al.* (2002) have shown that the minor fimbriae of *P. gingivalis* intimately interact with the SspB protein of *S. gordonii* (150). This interaction might aid in *P. gingivalis* colonization of plaque biofilm before it invades gingival tissue (150, 151). We recently showed that the minor fimbriae target DC-SIGN on DCs for entry into DCs, and that this targeting has an immunological consequence of dampening the immune response (20).

DC-SIGN is a type II membrane protein on DCs in which the extracellular domain consists of a stalk that promotes tetramerization (71). DC-SIGN contains a C-terminal carbohydrate recognizing domain (CRD) that belongs to the C-type lectin superfamily (71). Early studies by Feinberg *et al*. (2001) showed that the DC-SIGN CRD preferentially binds to the high-mannose N-linked oligosaccharides GlcNAc (N-acetylglucosamine) and Manα1-3[Manα1-6] Man (mannose) (71). Furthermore, Appelmelk *et al*. (2003) showed that DC-SIGN also binds to fucose-containing Lewis blood antigens (72). Guo *et al*. (2004) utilized an extensive glycan array and showed that DC-SIGN will bind high mannose-containing glycans or glycans that contain terminal fucose residues (73). Previous studies showed that DC-SIGN on DCs is used by

microorganisms such as *N. gonorrhoeae*, *M. tuberculosis*, *M. leprae*, HIV and *H. pylori* for entry to DCs and induction of immunosuppression (72, 75-77, 152). Like *P. gingivalis*, many of these pathogens can induce chronic lifelong infections.

Our previously published work established that the minor fimbriae were necessary for targeting DC-SIGN, resulting in entry of *P. gingivalis* into DCs (20). We were able to abrogate minor fimbriae mediated DC-SIGN ligation using DC-SIGN blocking agents or agonists including fucose, mannose, and mannan (20). Additionally we described that the minor fimbriae were able to induce immunosuppression of DCs via their interaction with DC-SIGN and which was blocked by sugars (20). Further, we demonstrated that minor fimbriated strains of *P. gingivalis* inhibited DC maturation and suppressed pro-inflammatory cytokine secretion (20). Moreover, DCs that were pulsed with minor fimbriated strains of *P. gingivalis* and then co-cultured with autologous T cells, shifted the T cell effecter phenotype to a Th_2 effecter phenotype as evidenced by high IL-4 production (20).

Our results described above suggested that the minor fimbriae-DC-SIGN interaction was mediated by sugars. We therefore set out to identify carbohydrate moieties on the minor fimbriae that could account for its DC-SIGN-targeting function. Intact native minor fimbriae was purified and analyzed for glycosylation and for the presence of relevant monosaccharides. We show here by a combination of ProQ gel staining and gas chromatography-mass spectrometry (GC-MS) analysis that the minor fimbriae are glycosylated and express the DC-SIGN ligands fucose, mannose, GlcNAc and GalNAc. Use of classic N- and O-linked deglycosidases on the native minor fimbriae revealed a novel glycoprotein structure. Overall, these results indicate that the

minor fimbriae are glycosylated with DC-SIGN –binding motifs that likely account for the reported ability of *P. gingivalis* to bind to and invade DCs, resulting in an immunosuppressive DC response.

Results:

Purification of native minor fimbriae.

After growth of *P. gingivalis* DPG-3 under anaerobic conditions, the bacteria were disrupted by sonication, and minor fimbriae purified by ion exchange chromatography using a DEAE sepharose column. In Figure 11A we show a representative elution profile of the minor fimbriae on a DEAE-sepharose column. The minor fimbriae eluted at 0.3 M NaCl whereas other proteins were still bound until 0.5 M NaCl. An aliquot of the peak corresponding to the putative minor fimbriae was analyzed by SDS-PAGE, and rerun on the DEAE sepharose column multiple times, changing either the steepness of the elution gradient or the pH of the buffers. Protein purification was continued until minor fimbriae samples showed no contaminating bands (i.e. for LPS or other contaminants) by Coomassie staining and silver staining (Figure 11B) (93). Absence of endotoxin was further confirmed by LAL assay (Lonza). None of the dilutions tested generated a positive LAL reaction at assay sensitivity of 0.03 EU/ml (data not shown) (40, 153, 154). The native fimbriae were further analyzed by transmission electron microscopy (TEM), demonstrating the presence of oligomeric strands approximately 100-200 nm in length, which is similar to previous observations (151)

(Figure 11C). The single band corresponding to the correct 67 kDa size of the minor fimbriae protein was analyzed for protein purity and peptide sequence by MS/MS (Figure 12A). MS/MS confirmed the purity and correct peptide sequence (Figure 12A bold letters). Examination of the peptide sequence also revealed two conserved Asn-Xaa-Ser/Thr asparagine linked (N-linked) (putative) glycosylation motifs (grey boxes in Figure 12A) (41, 49). The Mfa1 amino acid sequence also contains numerous serines and threonines, which can function as putative O-linked glycosylation sites (41, 155). We further analyzed the purified native minor fimbriae for glycosylation by SDS-PAGE and ProQ staining (Figure 12B), revealing a positive staining reaction.

Native minor fimbriae are susceptible to some N- and O-linked enzymatic deglycosylation.

Based on the amino acid sequence, N-linked glycosylation was a distinct possibility. We therefore subjected the purified minor fimbriae to treatment with endoglycosidases F1, F2 and F3. These enzymes cleave N-linked glycoproteins, but differ significantly in their oligosaccharide specificity, as previously reported (156-159). Briefly, endoglycosidase F1 cleaves oligomannose and hybrid oligosaccharides but this activity is greatly reduced by core fucosylation. Endoglycosidase F1 will also not cleave any complex oligosaccharides. Endoglycosidase F2 does not cleave hybrid or triantennary complex oligosaccharide structures, but does cleave oligomannose and biantennary complex oligosaccharides. Core fucosylation has little-to-no affect on endoglycosidase F2 activity. Endoglycosidase F3 can cleave biantennary and triantennary complex oligosaccharides with a preference for those oligosaccharides with

core fucosylation. Endoglycosidase F3 will also cleave fucosylated trimannosyl core structures on oligosaccharides but has no activity on oligomannose or hybrid structures (156-159). The results under non-reducing (native) conditions (Figure 13A and 13B, lanes 3 and 4) show that endoglycosidase F2 and F3 had moderate effects on the native minor fimbriae, as revealed by either by ProQ staining or apparent molecular mass shift. This suggested one of several possibilities. First, that the minor fimbriae contain N-linked complex biantennary complex oligosaccharide glycosylation, but that the glycosylation site might be inaccessible to the endoglycosidases under its oligomeric native configuration (Figure 11C) resulting in the "step ladder" pattern in lanes 3 and 4 (Figure 13 A and B). Secondly, it is possible that the minor fimbriae are O-linked glycoproteins or contain both N- and O-linked motifs. Finally, the minor fimbriae may contain a novel glycosylation structure that is resistant to classic deglycosylation. To address the first two possibilities, we employed an additional N-linked endoglycosidase, PNGase F and denatured the minor fimbriae prior to enzymatic treatment (Figure 13 C-F). PNGase F is a more potent N-linked deglycosidase which optimally works on non-core-fucosylated denatured proteins, as reported (156). It works by specifically recognizing an Asp-GlcNAc-oligosaccharide complex. Under these conditions we observed that the protein retained its glycosylation even when denatured and treated with PNGase F (Figure 13 C and D). To address the possibility that fucose residues are interfering with PNGase F, as previously reported (156), we pre-treated the minor fimbriae with α-L-fucosidase. Again, pretreatment had no affect on PNGase F, ruling out classic Asp-GlcNAc-oligosaccharide linkages or the presence of other blocking carbohydrates.

To examine O-linked glycosylation, the purified minor fimbriae were treated with α-2(3,6,8,9) neuraminidase (removes sialic acids), O-glycosidase, which cleaves serine or threonine linked unsubstituted Gal-β(1-3)-GalNAc-α-, β-1,4 galactosidase, which releases the terminal β(1-4) galactose provided that it is non-reducing, and β-N-acetylglucosaminidase, which cleaves terminal non-reducing β-linked-N-acetylglucosamine residues (Figure 13 C-F) (156). Intriguingly, we did observe a reduction in ProQ staining of the 67 kDa band in response to treatment with β (1,4) galactosidase, and β-N-acetylglucosaminidase (Figure 13C and 13D, lanes 6 and 7), suggesting the presence of O-linked galactose and N-acetylglucosamine motifs in the minor fimbriae. Furthermore, the samples treated with β-1,4 galactosidase (Figure 13E and 13F, lanes 4 and 7) were partially deglycosylated, and contained a band with an approximate molecular weight of 55 kDa, suggesting a modest amount of β (1-4) galactose on the minor fimbriae. The 55 kDa band does not correlate to any of the known molecular weights of the enzymes we tested. It should be mentioned in this context that the predicted molecular mass of the minor fimbriae is 61 kDa (151, 160), based on the complete amino acid sequence as analyzed by ExPASy (Expert Protein Analysis System; Swiss Institute of Bioinformatics, Geneva, Switzerland) Protemics Server (http://au.expasy.org/cgi-bin/protparam). However, Mfa1 has two predicted signal peptidase cleavage sites. We propose that the 55 kDa band is a cleaved form of the Mfa1 that had been tethered by carbohydrates, as further discussed below. The 55 kDa bands were confirmed to be the minor fimbriae (lacking the first 50 amino acids) by tandem MS/MS analysis (data not shown). Overall, these results suggest a novel pattern of

glycosylation of the minor fimbriae that is resistant to common methods of enzymatic deglycosylation.

Monosaccharide Analysis of the minor fimbriae by GC-MS.

Samples of the purified native minor fimbriae were analyzed by GC-MS as described in Materials and Methods. A representative chromatograph is shown (Figure 14) and results are summarized (Table 3). We confirmed that monosaccharides fucose, mannose and N-acetylglucosamine were present on the purified minor fimbriae (1.35 nmol/mg, 2.68 nmol/mg and 2.27 nmol/mg respectively) (Table 3). These carbohydrates have been implicated in ligation of DC-SIGN on dendritic cells, which promotes an immunosuppressive response (20, 72, 74). Also present in large quantities was xylose, galactose, and glucose (3.76 nmol/mg, 5.71 nmol/mg, and 14.1 nmol/mg respectively) (Table 3). N-acetylgalactosamine was also present in low concentrations (0.65 nmol/mg) (Table 3).

Discussion:

Our results demonstrate that the purified minor fimbriae are present as strands 100-200 nm in length and are glycosylated (Figure 11). The glycosylation of the minor fimbriae, while susceptible to endoglycosidase F2 and F3 as well as β (1-4) galactosidase (Figure 13), was resistant to other classical N-linked and O-linked deglycosylation enzymes, suggesting a novel structural linkage. Finally, we showed using GC-MS that the monosaccharide composition of the minor fimbriae contains moderate amounts of

DC-SIGN ligands fucose, mannose, and N-acetylglucosamine, and large amounts of xylose, galactose and glucose (Figure 14 and Table 3).

Many mucosal pathogens exhibit glycosylation motifs on their flagella, pili, and fimbriae (41). Glycosylation reportedly plays a role in maintaining the protein structure, protection from proteolytic degradation, immune evasion, host cell adhesion and surface recognition (41). There is previous evidence suggesting a role for glycosylation of the major fimbriae in *P. gingivalis*. Knockouts of *gftA* (a *wcaE* glycotransferase homolog of *E. coli*) in *P. gingivalis* fail to make mature fimbriae (42). There is evidence that the gingipains are glycosylated and that the isoforms are differentially glycosylated (43, 161). The glycosylation activity is regulated by the *vimF, vimA* and *vimE* glycotransferase genes (44, 45). Knocking out these genes causes a failure to glycosylate these gingipains, leading to their inactivation (43-45). Recently, it was discovered that the OMP85 protein of *P. gingivalis* is glycosylated (46). All of these outer membrane proteins encode for a signal peptide that gets cleaved before they exit the periplasm (29, 47, 48). Given that all of the elements for glycosylation are present in *P. gingivalis*, and that the minor fimbriae apparently target DC-SIGN (20), this study confirms our suspicion that the minor fimbriae are glycosylated.

We have shown that the minor fimbriae do not contain LPS by LAL test and silver staining (Figure 11B). Although the LPS structures of different strains of *P. gingivalis* may not be conserved (43, 162-164), it is worth mentioning a study by Curtis et al. (1999), which characterized the LPS of *P. gingivalis* and determined that the LPS does not contain mannose or fucose (43), while our minor fimbriae do. Furthermore, the Curtis study determined that the core region of *P. gingivalis* LPS lacked N-

acetylglucosamine and N-acetylgalactosamine (43), while our minor fimbriae contain these sugars. The Curtis study was also the first to characterize the glycosylation of the gingipains, which contained arabinose, rhamnose, fucose, mannose, galactose, glucose, N-acetylglucosamine, N- acetylgalactosamine and N-acetylneuraminic acid (43). Again, our samples lacked the gingipains as determined by both silver staining (Figure 11B) and tandem MS (Figure 12A). However, the molar ratios of monosaccharides that we detected on the minor fimbriae (Table 3) differ from those previously published for the gingipains and LPS (43, 161, 162, 164, 165). Finally, the fimbriae were purified from a non-encapsulated *P. gingivalis* strain, ruling out the possibility that the monosaccharides originated from the capsule (40, 166).

The Mfa1 protein component of minor fimbriae has a predicted size of 61 kDa, but reported sizes vary starkly from 67-75 kDa (151, 167). These size discrepancies could be attributed to glycosylation, the extent of which may depend on purification protocols and growth conditions (24, 25, 27, 168, 169).

Although the predicted molecular weight for Mfa1 is approximately 61 kDa (151, 160), we showed that the purified native minor fimbriae migrated at 67 kDa. Shoji *et al.* (2004) identified that the minor fimbriae are processed by a lipoprotein signal peptidase (signal peptidase II), as evidenced by improper processing in the presence of globomycin (29). They also described that the precursor proteins of the minor fimbriae are lipidated (29). Moreover, they describe that the minor fimbriae get processed twice, first by the lipoprotein signal peptide and then again by the gingipains (29). This lead us to search for signal peptide cleavage sites on Mfa1 using the SignalP server (http://www.cbs.dtu.dk/services/SignalP) (170). Interestingly, this analysis revealed two

potential signal peptide cleavage sites, at amino acid (AA) positions 21-22 and 50-51 (170, 171). Removal of the first signal peptide (AA 21-22) by signal peptidase I would result in a protein of approximately 58 kDa (based on ExPASy prediction). However, removal of the second signal peptide (AA 50-51) by lipoprotein signal peptidase would result in a protein of approximately 55 kDa (based on ExPASy prediction). We demonstrated that treatment with β (1-4) galactosidase resulted in the minor fimbriae migrating at 55 kDa, corresponding to the second cleavage site. Therefore, it is possible that Mfa1 is processed at this site, but that the N-terminal piece is tethered to the mature protein by carbohydrates with a β (1-4) galactose linkage.

Additionally, the minor fimbriae are not the only fimbriae expressed by *P. gingivalis* that exhibit a range in expected sizes. The major fimbriae are also reported to vary in size (41-43 kDa) (167). Efforts are underway to determine if the major fimbriae are also glycosylated. Since both fimbriae and gingipains undergo similar mechanisms of translocation to the outer membrane, it is feasible that during this process they might become glycosylated.

While non-pathogenic *E. coli* normally do not express the glycosylation machinery necessary to modify proteins, recent studies have transferred the *pgl* gene cluster of *Campylobacter jejuni* enabling *E. coli* to perform N-linked glycosylation (155, 172). Also, Fleckenstein *et al.* (2006) reported that EptA from a naturally occurring strain of Enterotoxigenic *E. coli* (ETEC) is glycosylated. The report further went on to demonstrate that the entire *eptBAC* locus is necessary for production of glycosylated EptA, and that the loss of EptC results in non-glycosylated EptA (171). Moreover, they demonstrated that the *eptBAC* gene locus was restricted to some ETEC strains but was

absent in other pathogenic and non-pathogenic strains of *E. coli*, confirming that *E. coli* can glycosylate proteins when provided with the proper genes (171). Recently Sartain and Belisle (2009) showed that expression of recombinant SodC (of *M. tuberculosis*) resulted in a proteins that are not processed correctly nor are they glycosylated (173). These studies suggest that *E. coli* normally does not possess the necessary glycosylation machinery. Our finding that the native minor fimbriae are glycosylated suggests that caution should be used in interpretation of studies that use recombinant minor fimbriae expressed in *E. coli* (151).

Of important note is that bacterial O-glycosylation makes use of unusual sugars (155). Also, sugar carbohydrates are not always added in a sequential manner to the protein. There are reports that sugars are preassembled and added to a lipid carrier before being added to the protein acceptor (155). Understanding how these *P. gingivalis* minor fimbriae become glycosylated and translocated would expand our understanding of this organism and how it eludes host immunity.

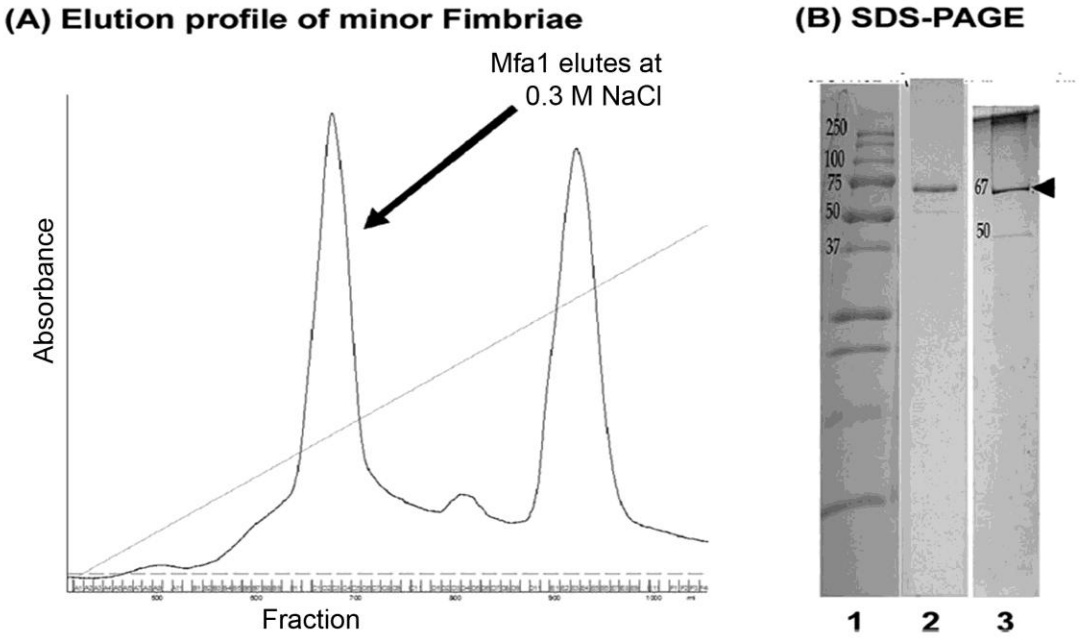
(A) Elution profile of minor Fimbriae
Mfa1 elutes at
0.3 M NaCl
Absorbance
Fraction
(B) SDS-PAGE
250
100
75
50
37
67
50
1
2
3

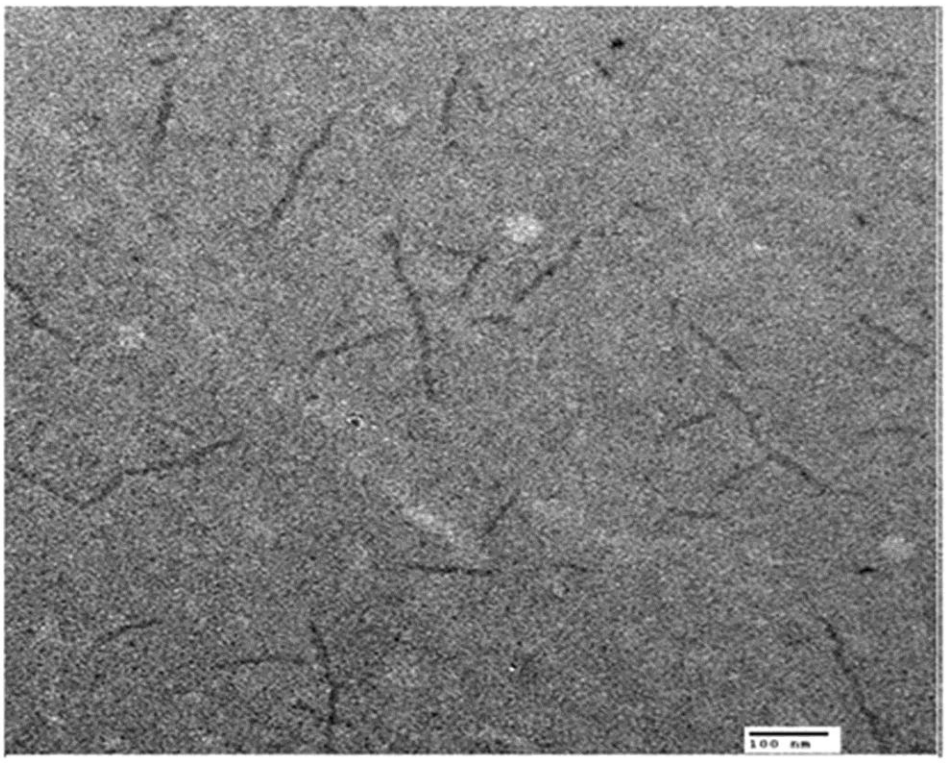
(C) TEM of minor fimbriae
100 nm

Figure 11. Purification and characterization of minor (Mfa1) fimbriae.

(A) Elution profile of 67 kDa fimbriae on DEAE-Sepharose CL-6B, showing a peak that eluted with 0.3M NaCl. **(B)** SDS-PAGE analysis of the minor fimbriae. Lane 1: MW standard; Lane 2: Coomassie blue stain showing 67 kDa minor fimbriae; Lane 3: Silver stain showing single band of minor fimbriae (arrow). **(C)** Transmission electron micrograph of purified minor fimbriae showing 100-200 nm fibers (scale bar = 100 nm)

(A) Peptide sequence of 67 kDa (minor) fimbrillin

```
1 MKLNKMFLVG ALLSLGFASC SKEGNGPDPD NAAKSYMSMT LSMPMGSARA
 51 GDGQDQANPD YHYVGEWAGK DKIEKVSIYM VPQGGPGLVE SAEDLDFGTY
101 YENPTIDPAT HNAILKPKKG IKVNSAVGKT VKVYVVLNDI AGKAKALLAN
151 VNAADFDAKF KKIIELSTQA QALGTVADGP NPATAAGKIA KKNGTTDETI
201 MMTCLQPSDA LTIEAAVSEA NAIAGIKNQA KVTVERSVAR AMVSTKAQSY
251 EIKATTQIGE IAAGSVLATI TDIRWVVAQG ERRQYLSKKR GTVPENTWVT
301 PGSGFVPTSS TFYTNATEYY DYAGLWEDHN TNEAVISGTQ VPTLADYQLQ
351 DVTGELANAL SGKFLLPNTH KSGANAASSD YKRGNTAYVL VRAKFTPKKE
401 AFIDRGKTYS DNTAVPEYVA GEDFFVGENG QFYVSMKSVT DPKVGGVAGM
451 KAHKYVKGKV LYYAWLNPST TSPDSWWNSP VVRNNIYHIH IKSIKKLGFN
501 WNPLVPDPDP SNPENPNNPD PNPDEPGTPV PTDPENPLPD QDTFMSVEVT
551 VLPWKVHSYE VDL
```

(B) ProQ staining of minor fimbriae

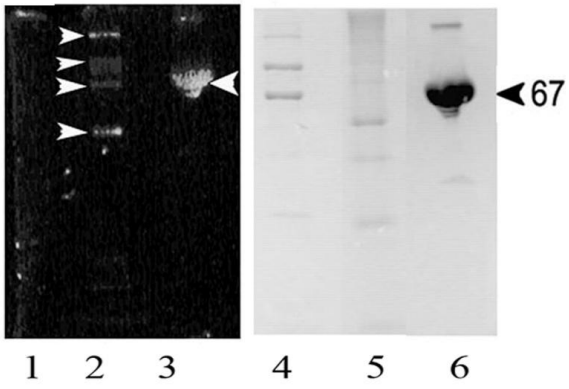

Figure 12 Glycosylation of the minor fimbriae.

(A) Peptide sequence obtained by MS/MS **(bold)** confirming the identity of the minor fimbriae. Boxed are putative N-X-S/T Asparagine-linkage motifs. **(B)** Confirmation of glycosylation on the minor fimbriae by ProQ (glycosylation stain).Minor fimbriae were run on SDS-PAGE and stained with ProQ (Lanes 1-3) and then the same gel was stained with Coomassie (Lanes 4-6). Lanes 1 and 4: non-glycosylated MW std; Lanes 2 and 5 "CandyCane" glycoprotein standard; Lanes 3 and 6: minor fimbriae. White arrow heads highlighting the CandyCane™ (Molecular Probes) glycoprotein standard

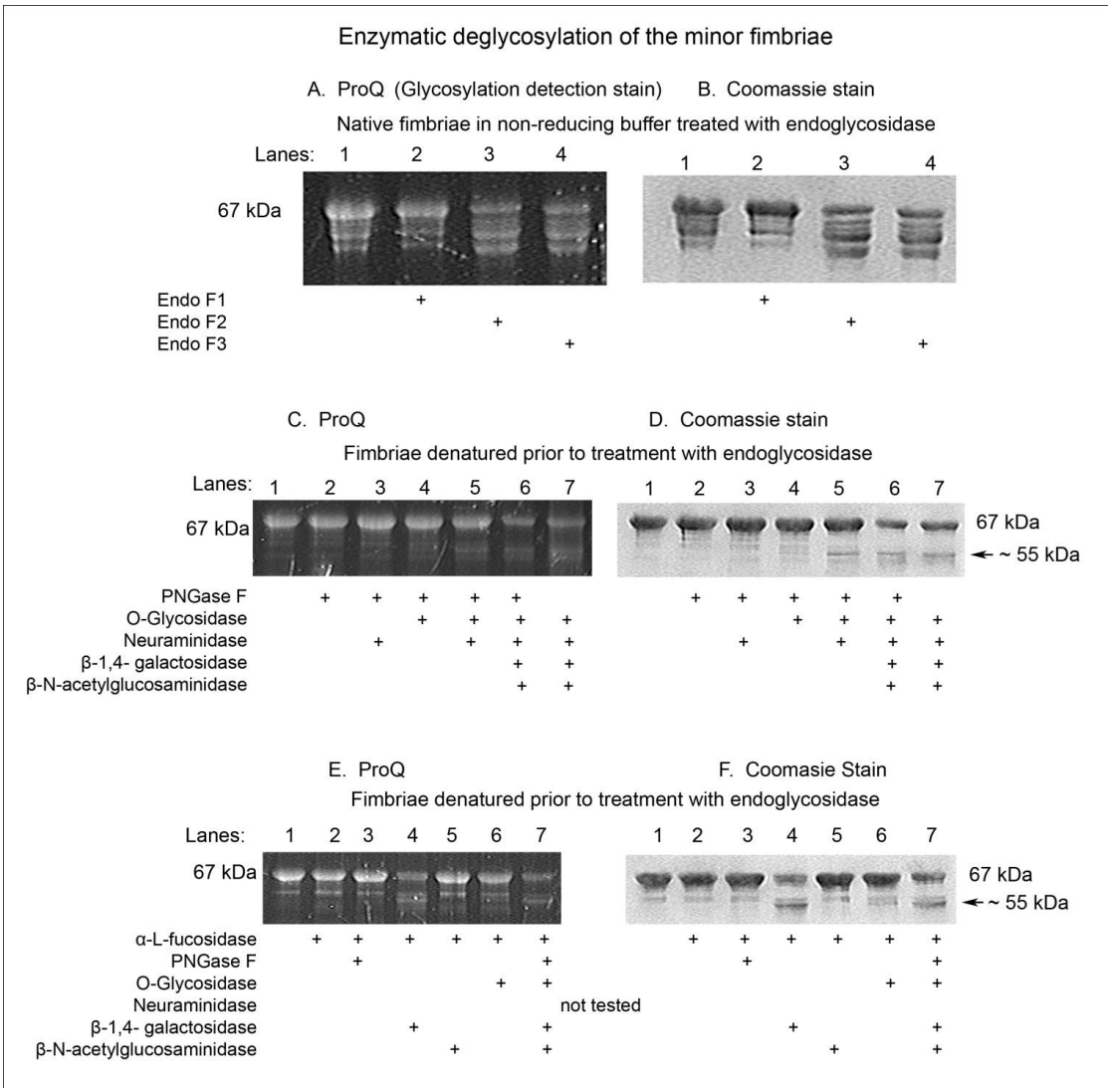
Enzymatic deglycosylation of the minor fimbriae
A. ProQ (Glycosylation detection stain)
B. Coomassie stain
Native fimbriae in non-reducing buffer treated with endoglycosidase
Lanes: 1 2 3 4
67 kDa
Endo F1
Endo F2
Endo F3
C. ProQ
D. Coomassie stain
Fimbriae denatured prior to treatment with endoglycosidase
Lanes: 1 2 3 4 5 6 7
67 kDa
~ 55 kDa
PNGase F
O-Glycosidase
Neuraminidase
β-1,4- galactosidase
β-N-acetylglucosaminidase
E. ProQ
F. Coomasie Stain
Fimbriae denatured prior to treatment with endoglycosidase
α-L-fucosidase
PNGase F
O-Glycosidase
Neuraminidase
not tested
β-1,4- galactosidase
β-N-acetylglucosaminidase

Figure 13 Enzymatic deglycosylation of minor fimbriae observed in the presence of Endoglycosidase F2, Endoglycosidase F3 and β-1,4- galactosidase.

Enzymatic deglycosylation treatment on purified minor fimbriae (Mfa1), as verified by lack of shift or the loss of ProQ (glycosylation detection) signal.

Figure 2A, C, E are ProQ gels, Figure 2B, D, F are the same gel after Coomassie blue staining.

Panels (A & B) non-reduced native fimbriae treated with endoglycosidase: all lanes loaded with 5μg of Mfa1 and digested with the indicated endoglycosidases.

Panels (C & D) fimbriae denatured prior to treatment with endoglycosidase: all lanes loaded with 7μg of Mfa1 and digested with the indicated endoglycosidases.

Panels (E & F) minor fimbriae pre-treated with α-L-fucosidase then denatured and treated with endoglycosidase: all lanes loaded with 7μg Mfa1 and digested with the indicated endoglycosidases.

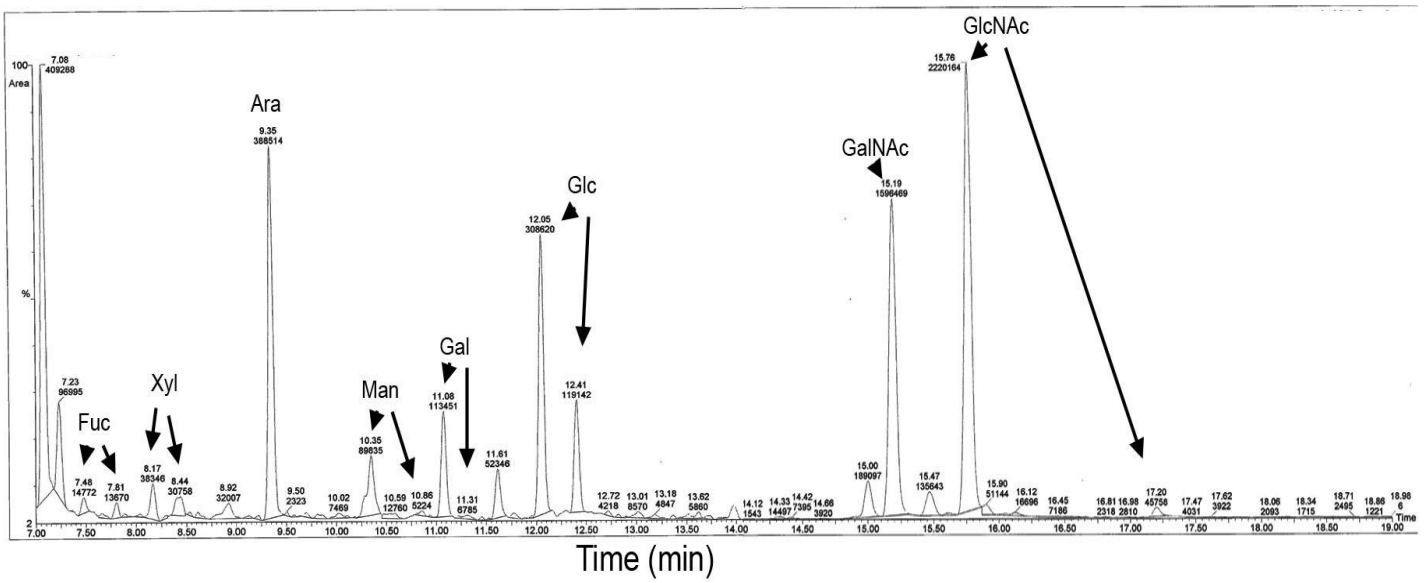
GlcNAc
Ara
GalNAc
Glc
Gal
Xyl
Man
Fuc
Time (min)

Figure 14 Representative chromatograph of Gas Chromatography-Mass Spectrometry (GC-MS) analysis of purified minor fimbriae.

Purified minor fimbriae was analyzed by GC-MS for monosaccharide content relative to monosaccharide standards for fucose (Fuc), xylose (Xyl), mannose (Man), galactose (Gal), glucose (Glc), N-acetylgalactosamine (GalNAc), and N-acetylglucosamine (GlcNAc)

TABLE 3. Summary of monosaccharide compositional analysis by GC-MS of purified minor fimbriae.

Summary of monosaccharide analysis by GC-MS		
Monosaccharide	nmol/mg of Mfa1	Ratio to GalNAc[a] = 1.0
Fuc	1.35	2.07
Xyl	3.76	5.77
Man	2.68	4.11
Gal	5.71	8.76
Glc	14.1	21.6
GalNAc	0.652	1.00
GlcNAc	2.27	3.48

[a] Shown here are the ratios of monosaccharides found on the minor fimbriae relative to N-acetylgalactosamine

Chapter Five: Conclusions/Significance/Future Directions.

Abstract:

An estimated 80 million U.S. adults have one or more types of cardiovascular diseases. Atherosclerosis is the single most important contributor to cardiovascular diseases; however, only 50% of atherosclerosis patients have currently identified risk factors. Chronic periodontitis, a common inflammatory disease, is linked to an increased cardiovascular risk. Dendritic cells (DCs) are potent antigen presenting cells that infiltrate arterial walls and may destabilize atherosclerotic plaques in cardiovascular disease. While the source of these DCs in atherosclerotic plaques is presently unclear, we propose that dermal DCs from peripheral inflamed sites, such as CP tissues are a potential source. This chapter will examine the role of the opportunistic oral pathogen *Porphyromonas gingivalis* in invading DCs and stimulating their mobilization and misdirection through the bloodstream. Based on our published observations, combined with some new data, as well as a focused review of the literature we will propose a model for how *P. gingivalis* may exploit dendritic cells to gain access to systemic circulation and contribute to coronary artery disease. Our published evidence supports a significant role for *P. gingivalis* in subverting normal DC function, promoting a semi-mature highly migratory and immunosuppressive DC phenotype that contributes to the inflammatory development of atherosclerosis and eventually, plaque rupture.

Introduction:

The pathological manifestations of chronic periodontitis (CP) have a high prevalence in the general adult population (174, 175). CP is characterized namely as the destruction of the soft and hard tissues that support the dentition, culminating in tooth loss (174, 175). Well documented is the specific role of the anaerobic Gram-negative species, *Porphyromonas gingivalis* (*P. gingivalis*) in infection of the tissues around the dentition in CP and in initiation of CP (176). *P. gingivalis*, along with two other species, *Tannerella forsythia* and *Treponema denticola*, comprise the so-called "red complex" of pathogens (177) that function cooperatively within the subgingival plaque of CP (1, 20, 50, 174, 175). *In situ* studies describe the cytokine response to *P. gingivalis* as eliciting increased IL-8, IL-6, IL-1β and TNF-α secretion (178). In response, the gingiva mucosa becomes infiltrated with neutrophils which are purportedly responsible for some the tissue destruction (179). *P. gingivalis* has been associated with several important systemic diseases such as cardiovascular disease, rheumatoid arthritis, preterm birth weight, and diabetes mellitus (180, 181). Our group is particularly interested in the influx and efflux of various dendritic cells (DCs) in response to *P. gingivalis* and their role in local and systemic inflammatory processes. DCs are very active antigen-capture cells when immature. When DCs mature, they become potent antigen-presenting cells and are very efficient at stimulating T cells to differentiate into T cell effectors (reviewed in (116, 182)). DCs have been implicated in a number of allergic and inflammatory diseases in the periphery (reviewed in (183)), including atherosclerosis (184, 185). DCs being central to the development of immunologic memory and tolerance (186), function

by patrolling the periphery, capturing infecting microbes and then migrate out to the secondary lymphoid organs. In the lymph nodes, DCs can initiate and regulate the adaptive immune response (187). DC functions are tightly regulated and depend on the activation signals that DCs receive in the periphery (reviewed in(187)). These signals include inflammatory cytokines, chemokines, as well as pathogen associated molecular patterns (PAMPS) of bacteria. The development of gingivitis and periodontitis involves the influx and efflux of different DC subsets at distinct stages of disease (Figure 15). Dendritic Langerhans cells (LC) infiltrate the gingival epithelium in gingivitis and then efflux into the lamina propria in CP, where they begin to undergo maturation (114). Dermal dendritic cells (DC-SIGN+) increase in the lamina propria in CP, and become localized towards the lymphatics and vasculature (54, 57, 103). LCs have been implicated in both the initiation and regulation of contact-hypersensitivity responses in mice (188), (reviewed in (189)). While dermal DCs have been implicated in many other inflammatory diseases, including rheumatoid arthritis and inflammatory bowel disease (78). This chapter will focus on *P. gingivalis* and DCs and their respective contributions to the development (and instability) of atherosclerotic plaques.

Atherosclerosis and Microbes

Atherosclerosis (ATH) is a progressive disease characterized by the accumulation of lipids, fibrous elements and inflammatory cells in the large arteries. ATH constitutes the single most important contributor to the growing worldwide burden of cardiovascular disease. Only about 50% of patients with ATH have currently identified risk factors

(190). This suggests how little we know about ATH risk. Inflammation in the arterial vessel wall is particularly important in the development of ATH. Four mechanisms have been proposed for how bacterial pathogens may induce or accelerate ATH (191). These include: (i) direct invasion of the vascular endothelium by pathogens in the blood, (ii) immunological sounding, (iii) molecular mimicry, (iv) pathogen trafficking of microbes within leukocytes in peripheral blood.

Of particular relevance to atherogenesis are bacterial species that infect and survive within endothelial cells and within migrating leukocytes (reviewed in (192)). A prevailing hypothesis is that, regardless of their viability status, bacteria release PAMPs that serve as agonists for TLRs, thus activating inflammatory leukocytes and endothelial cells, and can contribute to the development of ATH (193). Large population studies support the role of bacterial species in ATH (194, 195). However, the results of clinical trials using antibiotics to treat cardiovascular disease have been disappointing (196-199). Many atherogenic bacteria, including *P. gingivalis*, are intracellular pathogens (138, 200). An apparent consequence of this is that these pathogens are less susceptible to antibiotics when sequestered inside host cells. *P. gingivalis* is 100-fold more resistant to moxofloxocin, 10-fold more resistant to clindamycin and metronidazole when inside host epithelial cells (201). Clindamycin- and azithromycin-resistant *P. gingivalis* isolates have been identified in human subjects with CP (202).

P. gingivalis has also been identified in human ATH plaques (139), as have other atherogenic bacteria such as *Chlamydophila pneumoniae* (*C. pneumoniae*) and *Helicobacter pylori* (*H. pylori*) (193, 203, 204). Experimental infection with *P. gingivalis* accelerates ATH in animal models (138, 205). The FINRISK 1992 cohort

study of 6051 individuals implicates exposure to *P. gingivalis* or endotoxin in increased risk for cardiovascular diseases (206). A recent meta-analysis indicated that the level of systemic bacterial exposure in CP mediates ATH risk (207, 208). Another meta-analysis studied human cohort studies, case-control studies and cross-sectional studies and concluded that CP is a significant risk factor for developing coronary artery disease (CAD) (208). The degree of increased risk of CAD conferred by CP appears comparable to smoking (209), and elevated serum triglycerides (210). Viable and invasive *P. gingivalis,* though in a dormant state, have been cultured from human ATH plaques (139). This has not been shown with other atherogenic bacteria such as *C. pneumoniae* and *H. pylori,* which have only been identified by DNA based methods (193, 203, 204). Overall, several infectious agents have been shown to be disseminated by pathogen trafficking leukocytes, include *Streptococcus pyogenes* (211), *C. pneumoniae* (212), *Listeria monocytogenes* (213).

P. gingivalis virulence and targeting of DCs

P. gingivalis is a an amino acid fermentor with an absolute requirement for hemin (175). The bacteria utilizes its many virulence factors to fulfill its complex nutritional requirements, while still enabling it to evade and even modulate the host immune system (20, 174, 175). Several virulence factors including the polysaccharide capsule, fimbriae, proteases for opsonins C3, proteases for IgG, gingipains, bacterial lipopolysaccharides (LPS), toxins and hemagglutinins enable *P. gingivalis* to persist in the oral mucosa and help facilitate some of the physiopathology of CP (7, 8, 57, 59, 145-148).

There are two fimbriae that are essential adhesins for the invasion and colonization of the oral mucosa by *P. gingivalis*. These adhesins are termed the major and minor fimbriae. The fimbriae are distinct antigenically, by amino acid composition, and by size from one another (22, 23). The major fimbriae form long projections from the bacteria and have been shown in most reports to facilitate their adhesion to and invasion of the host cells. Major fimbriae are comprised of a 41 kDa protein, encoded by the *fimA* gene (21). Its cellular receptors have been identified as being either the β-1 integrins (CD29) (33, 34) or the β-2 integrins (CD18) (36, 37, 149). Minor fimbriae (though much shorter on TEM) are comprised of a 67 kDa protein encoded by the *mfa1* gene (22). We have recently shown that the minor fimbriae targets dendritic cell specific ICAM-3 grabbing non-integrin (DC-SIGN or CD209) on monocyte derived DCs for entry (20). DC-SIGN is a type II membrane protein in which the extracellular domain consists of a stalk that promotes tetramerization (71). It contains a C-terminal carbohydrate recognizing domain (CRD) that belongs to the C-type lectin superfamily (71). Early studies by Feinberg *et al.* (2001) showed that the DC-SIGN CRD preferentially binds to the high-mannose N-linked oligosaccharides GlcNAc (N-acetylglucosamine) and Manα1-3[Manα1-6] Man (mannose) (71). Furthermore, Appelmelk *et al.* (2003) showed that DC-SIGN also binds to fucose-containing Lewis blood antigens (72). Guo *et al.* (2004) utilized an extensive glycan array and showed that DC-SIGN will bind high mannose-containing glycans or glycans that contain terminal fucose residues (73). We have previously published that the minor fimbriae of *P. gingivalis* is glycosylated (50). Moreover many of the carbohydrates present on the minor fimbriae are known DC-SIGN agonists (50). Previous studies showed that DC-SIGN is used by microorganisms such as *N.*

gonorrhoeae (74), *M. tuberculosis* (72, 75, 76), *M. leprae*, HIV (77), *H. pylori* (72) and *P. gingivalis* (20) to target DCs for entry and immune suppression.

Pathological consequences of DC-SIGN targeting

The ability of minor fimbriae to specifically target DC-SIGN on DCs has significant pathological and immunological repercussions. Periodontitis lesions contain an intense infiltrate of DC-SIGN+ DCs (113, 214). DCs in the lesions become activated and appear to mobilize towards the capillary-rich lamina propria (214). Further, we have observed an intimate interaction of *P. gingivalis* with DC-SIGN+ DCs in human gingival tissue (Figure 16). We propose that, reverse transmigration of *P. gingivalis*-infected gingival DCs into circulation may contribute to the pathogenesis of ATH (Figure 15). Evidence exists for the presence of activated DC-SIGN+ myeloid DCs in rupture prone unstable plaques (102, 184). The sources of these DC-SIGN+ atherosclerotic plaque DCs are not clear, but presumably may include DCs from inflamed peripheral tissues. Other sources of DCs may include ‘CD14+ CD16− monocytes, CD14low CD16+ monocytes (215) that differentiate into DCs *in situ* (20).

DCs that infiltrate rupture-prone atherosclerotic plaques were reported to express atherogenic markers, including C1q, (a classical complement pathway component involved in apoptotic cell clearance), HSP60 and HSP70, (chaperone proteins involved in autoimmune responses), and chemokine receptors CCR2, CCR5, CX3CR1, and chemokines CXCL16, CCL19 and CCL21 (involved in DC transmigration and leukocyte homing) (215-217). Also expressed are DC maturation markers CD40, CD80 and CD86

(102, 218). Matrix-metalloproteinase-9 (MMP-9), which are highly expressed in vulnerable regions of the atherosclerotic plaques, and suggested to be causally involved in plaque rupture (219) is produced by leukocytes, including DCs. *P. gingivalis* LPS is a particularly potent inducer of MMP-9 by DCs, but not its inhibitor TIMP-1, suggesting that *P. gingivalis* induces an MMP-9/TIMP-1 imbalance in DCs (220). Our published data indicated that fimbriated strains of *P. gingivalis* infect DCs and induce atherogenic biomarkers in vitro, but the mechanisms are not presently clear (20).

Immunological consequence of targeting DC-SIGN on DCs

DC-SIGN targeting by minor fimbriae results in dampening the maturation status and the inflammatory cytokine profile of DCs. Conversely, removal of the minor fimbriae results in robust DC maturation coupled with a strong pro-inflammatory cytokine response (20). This regulation of DC immunogenic functions based on minor fimbriae expression extends to the T cell effector response elicited by DCs. In DC-CD4+ T cell co-culture experiments, *P. gingivalis* strains expressing solely the minor fimbriae induced DCs to prime T cells into a Th_2 effector phenotype, whereas, strains expressing solely the major fimbriae induced DCs to prime T cells into a Th_1 effector phenotype (20). Intriguingly, the wild type strain was able to stimulate a mixed or anergic T cell effector phenotype (20). Furthermore, *in vitro* studies in the presence of DC-SIGN targeting agonists (e.g. mannan from *S. cerevisiae* or glycosylated HIV gp120) resulted in a diminished association of minor fimbriated strains with cells (20). When the wild type strain of *P. gingivalis* was co-cultured with glycosylated HIV gp120, we observed a

dramatic uncoupling of DC maturation from dendritic cell inflammatory cytokine secretion (20). The presence of HIV or even *Candida albicans* (oral thrush) might act synergistically with *P. gingivalis* to further exasperate this uncoupling, and act to greatly diminish DC maturation.

Mechanisms of DC mobilization, access to peripheral blood

Experimental studies demonstrate the important role that chemokines and chemokine receptors play in trafficking of leukocytes to and invasion of the arterial wall in ATH (221-225). Immature DCs express inflammatory chemokine receptors (Table 4) that direct their migration into infected tissues. In response to capture of antigens or to TLR-mediated recognition of microbes, DCs undergo a process called functional maturation in which they down-regulate inflammatory chemokine receptors and up-regulate homeostatic chemokine receptors (Table 4). This directs DC migration out of the tissues towards lymph nodes. When the DC maturation process is disrupted, as occurs upon DC-SIGN ligation (20), activated DCs ostensibly undergo reverse transmigration into the blood (Figure 15), which can lead to systemic inflammation.

This process contributes to the initiation, progression and instability of arterial plaque in patients with coronary artery disease (CAD). Recent studies have investigated the presence of blood dendritic cells in patients with CAD, but the results are controversial (226, 227). Shi *et al*. (2007) found that the total peripheral blood CD11c+DCs were significantly higher in patients with CAD compared to healthy controls (226). Conversely, Yilmaz *et al*. found a decrease in circulating DCs in patients with CAD

(227). However, the patient population and markers used for DC isolation were different. None of the studies reported the presence of CP on these patients, which might have affected these conflicting findings. An attempt has been made to correlate the presence of blood DCs as a risk factor for CAD (228). Further, much speculation has been made about the source of these DCs that infiltrate the atheroma.

Fully matured DCs lose their ability to uptake and process antigens (51). Mature DCs stop migrating, express CD83 and other co-stimulatory molecules involved in antigen presentation to T-cells (51). Full maturation of DCs also results in loss of expression of many endocytic receptors, including DC-SIGN. Thus expression of DC-SIGN is an indicator that DC are not fully mature (229). There is evidence that a particular subset of blood DCs express DC-SIGN, and that this receptor may be involved in the uptake and dissemination of HIV (99). Engering *et al.* showed that DC-SIGN+ blood DCs are able to stimulate proliferation of allogeneic T cells, as well as infect these T cells in trans (99). Potentially, DC-SIGN+ blood DCs can disseminate pathogens, increase systemic inflammation, and contribute to plaque instability.

Environmental regulation of fimbriae: possible role in systemic immunosuppression/ dissemination

Wu *et al.* (2007) discovered that the major and minor fimbriae are regulated by a two component regulatory system termed FimS/FimR (27). It was determined that while FimR binds directly to *mfa1*, it will only bind to the first gene of the *fimA* gene cluster, *pg2130* (Figure 1) (27, 28). Moreover, this two component regulatory system responds to

environmental cues like heme and temperature (27). However, it is still not clear how these adhesive fimbriae are regulated *in vivo*. The possibility of major and minor fimbriae being differentially regulated in response to different environmental cues/ stimuli may allow this organism to modulate the immune system to expand its ecological niche. Moreover, our observations of intact bacteria inside DC-SIGN rich vesicles (Figure 7) might explain the dissemination of this organism to atherosclerotic plaques (20). We propose here that *P. gingivalis* interacts with DC-SIGN on dermal DCs from the gingiva mucosa (Figure 16). This interaction facilitates uptake of *P. gingivalis* and results in immuno-modulation of normal DC functions. Directed migration is disrupted and DCs then migrate through the endothelium instead of the lymphatic system (Figure 15). Once in the endothelium the DC undergoes partial maturation resulting in adherence to the endothelium and recruitment of other leukocytes. Soilleux *et al.* (2002) previously described the presence of immature (lacking CD83 but expressing HLA-DR and LAMP) DC-SIGN^{+} dendritic cells on atherosclerotic plaques (102). Strikingly, this maturation profile is very similar to our results with minor fimbriated strains (Pg381 and DPG-3) and DCs (20). Thus, *P. gingivalis* infected DCs may exit into the bloodstream and migrate to the site of developing atheroma, where they adhere to and invade the arterial endothelium. Recent reports suggest that *P. gingivalis* is able to spread from infected epithelial, endothelial and smooth muscle cells to new host cells, where it multiplies (230). These mechanisms might explain how an oral opportunistic pathogen is able to disseminate throughout its host and potentially facilitate the formation of atherosclerotic plaques.

Minor fimbriae secretion, assembly and modifications

The pili/fimbriae adhesins of Gram negative bacteria can be categorized into seven major classes based on export/secretion pathways involved to get them on the outer membrane (Figure 17) (231). Gram negative protein secretion can be subdivided into two major groups (i) Sec dependent and (ii) Sec independent secretion pathways (232, 233). Sec dependent pathways must first secrete proteins into the periplasm across the inner membrane via the Sec translocon. Pathways that utilize this machinery include: the type II secretion system, some type IV secretion systems, the type V secretion system (the autotransporter), and the two partner secretion systems (the chaperone/usher pathway) (232, 233). The Sec independent pathways tend to exclude the periplasm and proteins are translocated directly from the cytoplasm to the outer membrane with no periplasmic intermediates. Pathways that utilize this process include: type I secretion system (ATP-binding cassette), the type III secretion systems (injectisomes), and most type IV secretion systems (232-234). Recently a type VI pathway was identified and it appears to not use the Sec pathway (233).

The minor fimbriae are assembled and secreted while undergoing multiple post-translational modifications. We have shown that the minor fimbriae are post-translationally modified via glycosylation, and that the carbohydrates used are known DC-SIGN ligands (50). Both O-linked and N-linked bacterial glycosylation are thought to be assembled via two distinct methods. The first involves “direct addition of carbohydrates to nucleotide-activated sugars on the accepting protein” (235, 236). The second involves “preassembly of the oligosaccharide via the sequential addition of

nucleotide-activated monosaccharides onto a lipid carrier" before transfer (as a unit) from the cytoplasm to the periplasm and onto the accepting protein (155, 235, 236). For the second method to take place, the lipid carrier must then transfer its oligosaccharide cargo to an "O-OTAse" or and "N-OTAse" (oligosaccharyltransferases) (155, 235, 236). The OTAse then transfers the oligosaccharide to hydroxylated amino acids on proteins (155, 235, 236). The few OTAse's discovered to date have been described as integral inner membrane proteins, but there are no conserved or homologous domains between different bacteria (235). Furthermore, it appears that most bacterial N and O linked glycosylation utilizes the OTAse intermediates (155). We propose that since the minor fimbriae contain both O-linked and N-linked glycosylation, it too might use some yet uncharacterized N- or O- OTAses.

Shoji *et al.* (2004) describe that the minor fimbriae are lipidated and undergo cleavage by an N-terminal lipoprotein signal peptidase (29, 50). These findings were verified by the use of globomycin and the observation of an 80 kDa precursor protein on the inner membrane (29). There are three established signal peptidases that function to process the N-terminus of the protein being translocated into the periplasm (29, 234). We recently described that *P. gingivalis* minor fimbriae contain two distinct signal peptide cleavage sites, at amino acid positions 21-22 and 50-51 (50). These sites get recognized and are presumably processed by signal peptidase I (LepB) and signal peptidase II (LspA) (50, 170, 234). Further, upon deglycosylation of the minor fimbriae the protein runs at approximately 55 kDa (Figure 13) which is approximately the same predicted size of the minor fimbriae minus 50 amino acids. Presumably the minor fimbriae are processed by both of the signal peptidases. This suggests that *P. gingivalis* uses a Sec

translocase homologue for transfer of pre-minor fimbriae proteins across the inner membrane from the cytoplasm into the periplasm (29, 232-234, 237). Being Sec dependent and assembling a pili/fimbria structure allows us to rule out that the minor fimbriae belong to the type I secretion system, the type III secretion system, most type IV secretion system and the newly discovered type VI secretion systems (Figure 17) (232-234).

Once inside the periplasm, pre-minor fimbriae would get glycosylated by both O-OTAse and an N-OTAse. The promiscuity of the OTAse in terms of the oligosaccharide they carry enables different glycosylation motifs to be present on different proteins (235). This intriguing possibility might be revealed after a more thorough structure and linkage analysis is done on the glycoprotein to determine where and how the minor fimbriae are glycosylated. Further, Zeituni *et al.* (2010) proposed that there might be a carbohydrate linkage between the lipidated N-terminal of the minor fimbriae connecting it to the main body that is susceptible to β(1-4) galactosidase (50). We propose that all of these post translational modifications (lipidation, glycosylation, processing by gingipains and signal peptidases) are necessary for the assembly of mature minor fimbriae. To elucidate these possibilities, we propose to first purify the minor fimbriae using affinity chromatography with our newly made AEZαMFA1 mAb (Figure 16). Minor fimbriae will be treated with trypsin and with an endoglycosidase F3 to release N-linked glycan (50). The N-glycans, O-glycopeptides and peptides will be separated sequentially by passing the sample through a C18 Sep Pak (238). The O-glycans are then released from the peptide using "β-elimination followed by Michael addition with dithiothreitol" (BEMAD). Released

N- or O-glycans are permethylated and then can be analyzed by mass spectrometry (MALDI/TOF-MS) (238).

The glycosylated pre-minor fimbriae are processed into their mature form by the gingipains, and are then transported to the outer face of the outer membrane, by some unknown process (29, 32, 48, 50, 237). Further, we propose that this glycosylation facilitates the oligomerization and stability of the newly processed "mature" minor fimbriae (41, 50). As stated earlier, gingipains are essential for final fimbriae maturation, are important for the degradation of host proteins (presumably to facilitate short amino acid peptide uptake and fermentation), and for the degradation of cytokines (29, 50, 174, 175, 239). The involvement of a Sec dependant translocation pathway that utilizes intermediates such as the gingipains, as well as glycosylation, allows us to rule out the type V secretion (autotransporter) and the type II secretion pathways. Ruling out the type II and V secretion systems, and still following the Sec dependant pathway, we are left with a two partner (chaperone/ usher) pathway, a type IV secretion system or a new model (Figure 18) (232).

While the gingipains can serve as a chaperone since they are essential for proper minor fimbriae formation, they are also found on the outer membrane. As yet, no usher has been described for the minor fimbriae (237). Conversely, type IV pilus components are translocated across the inner membrane as pre-pilins (231, 232, 237). In some cases type IV pilin can be translocated via a Sec dependent manner (232, 237, 240, 241). Once the pre-pilin are in the inner-membrane, a peptidase recognizes and cleaves a conserved N-terminal leader sequence, releasing a pilin peptide. Most of these pre-pilin have an unusually long signal peptide (30-50 AA) that is cleaved by a dedicated signal peptidase

(242). We have recently published that the minor fimbriae contain two different signal peptides one of which is approximately 50 AA away from the N-terminus (50). The pilin peptide is sometimes further processed into a mature pilin where it is free to associate with the outer membrane and oligomerize (231, 232, 237, 240). This processing can be done by the signal peptidases or gingipains (50). So we are left with these three possibilities: (i) the minor fimbriae are secreted using a two partner pathway (ii) the minor fimbriae are secreted via a type IV secretion pathway or (iii) the minor fimbriae are secreted via a novel pathway (Figure 18). However, it is very likely that minor fimbriae secretion is done in a completely novel manner, since the genome of *P. gingivalis* has no sequence homology for any of the established pili/fimbriae secretion pathways (29, 50).

The questions to be addressed in future studies are (i) how are the fimbriae exported outside of the outer membrane (ii) at what step do the unidentified OTAse's glycosylate the minor fimbriae (iii) do the gingipains process the minor fimbriae in the periplasmic inner membrane or outer membrane leaflet (iv) are we dealing with a completely novel pili assembly pathway? Clearly more research needs to be done on how the minor fimbriae are glycosylated, secreted, and processed from the cytoplasm and assembled on the outer surface of *P. gingivalis*.

Table 4. Summary of Results of IHC, cDNA microarray and qRT-PCR			
Chemokine Receptors (their ligands)	**Class**	*P. gingivalis* pulsed MoDC (fold change)	Chronic Periodontitis tissue (fold change)
CCR2 (**CCL2** / MCP-1, CCL7 / MCP3, CCL8 / MCP2, CCL13 / MCP4	Inflammatory	5.7x ↑[4] 10x↑[1]	2000x↑[4]
CXCR6 (**CXCL16** or SR-PSOX)	Inflammatory	2x↑[4]	300x↑[4]
CCR5 (CCL3 or MIP-1α, CCL4 or MIP-1β, CCL5 or RANTES, CCL11, CXCL8 or IL-8	Inflammatory	12x↑[1]	20x↑[2]
CXCR3 (CXCL10)	Inflammatory	NT**	2.2x↑[3]
CX3CR1 (CX3CL1)	Inflammatory	NT**	NT**
CCR4 (CCL22)	Homeostatic	NT**	2.3x↑[3]
CCR6 (MIP-3α)	Homeostatic/ Inflammatory	NT**	10x↑[4]
CCR7 (**CCL19** or MIP-3β, **CCL20** or LARC	Homeostatic	3x↑[1]	25x↑[4]
NT** Not Tested. 1cDNA microarray (GEArray, Superarray) of *P. gingivalis* pulsed MoDC (3hr) or gingival tissues from diseased vs. control patients, normalized vs. β Actin; 2. # cells/ per field (IHC), 11 healthy vs. 11 control; 3. Affymetrix chip results, normalized against internal standard; 4. qRT-PCR results normalized against GAPDH			

A.

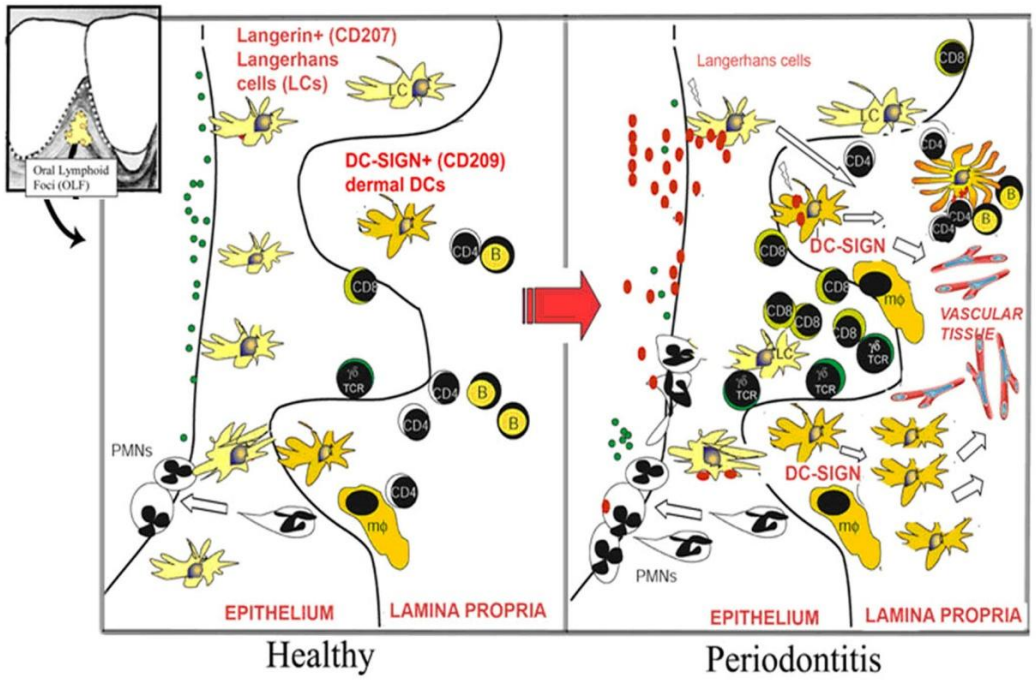
Oral Lymphoid Foci (OLF)
Langerin+ (CD207) Langerhans cells (LCs)
DC-SIGN+ (CD209) dermal DCs
PMNs
EPITHELIUM
LAMINA PROPRIA
Healthy
Langerhans cells
DC-SIGN
VASCULAR TISSUE
DC-SIGN
PMNs
EPITHELIUM
LAMINA PROPRIA
Periodontitis

B.

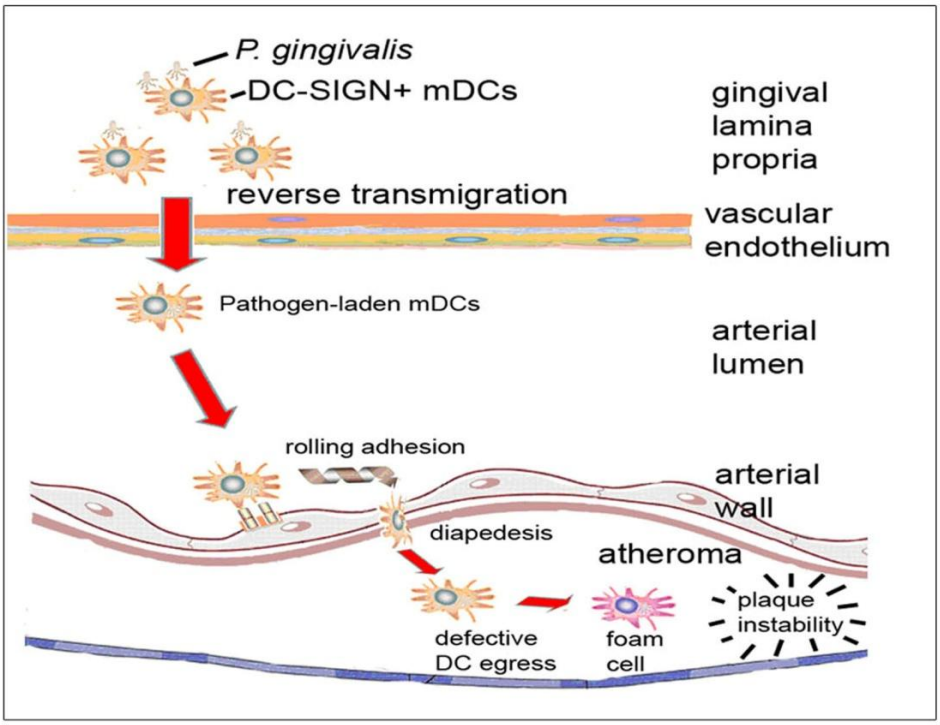
P. gingivalis
DC-SIGN+ mDCs
gingival lamina propria
reverse transmigration
vascular endothelium
Pathogen-laden mDCs
arterial lumen
rolling adhesion
arterial wall
diapedesis
atheroma
plaque instability
defective DC egress
foam cell

Figure 15. Schematic representation of how *P. gingivalis*-laden dendritic cells may promote atheroma formation and maturation.

A) Representation of the oral lymphoid foci, its organized inflammatory infiltrate. The left panel depicts the healthy oral biofilm in the gingival crevice, comprised predominantly of gram positive bacteria (green dots). Healthy gingival tissue is infiltrated with numerous Langerhans cells in the epithelium, with sparse dermal dendritic cells in the lamina propria. As disease progresses the oral biofilm changes to a predominantly gram negative subgingival flora (red dots). In response, a dramatic loss (efflux) of Langerhans cells occurs from the epithelium towards the lamina propria. Also observed is an influx of myeloid-derived DC-SIGN+ dermal dendritic cells (DCs) into the lamina propria. Present are neutrophils, macrophages (mϕ), B cells and CD4+ and CD8+ T cells. The DCs form immune conjugates with CD4+ T cells and also mobilize towards the vasculature; **B)** Hypothetical model in periodontitis, showing mobilization of *P. gingivalis*-laden DC-SIGN+ myeloid DCs (mDCs) in the gingival lamina propria. These mDCs undergo reverse transmigration through the vascular endothelium. Once in the circulation, mDCs carrying *P. gingivalis* attach to endothelial integrins via DC-SIGN and, after rolling adhesion, undergo diapedesis between endothelial cells. As the atheroma continues to mature and DCs contribute to the foam cells and release MMP-9, the atheroma becomes highly unstable and eventually, thrombus formation occurs.

.

A) Western blot characterization
of monoclonal antibody AEZαMfa1

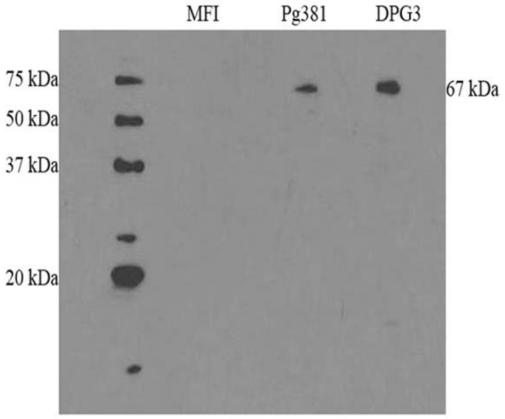

B) Immuno gold showing polarity and specificity
of monoclonal antibody AEZαMfa1

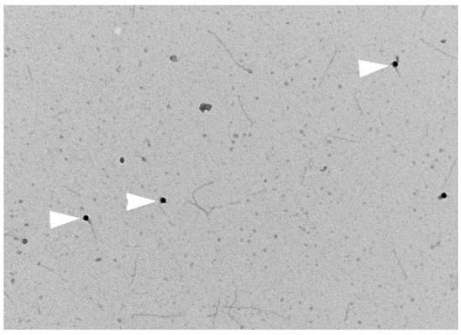

C) *In-situ* association of Pg minor fimbriae with DCs
in inflamed gingival tissues in CP

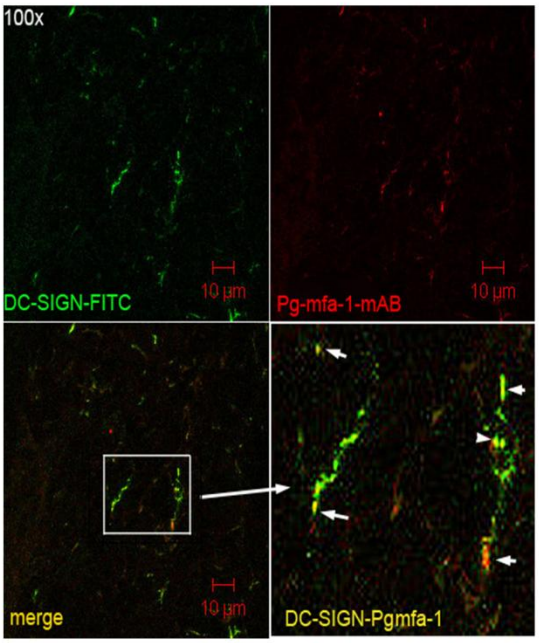

Figure 16. Characterization of AEZαMFA1 monoclonal antibody.

(A) Western blot characterization of monoclonal antibody AEZαMfa1. 12% SDS-PAGE lanes were loaded with MFI (lacks minor fimbriae), Pg381 (has both fimbriae) or DPG3 (lacks major fimbriae) and Laemmli sample buffer (Bio-Rad). Samples were boiled at 100°C for 10 min; the gel was run and transferred to PVDF membrane. Membranes were blocked and incubated with AEZαMfa1 overnight, washed and treated with secondary antibody conjugated with HRP. Detection was done on Kodak film with SuperSignal West Pico Chemiluminescent substrate (Thermo Scientific). **(B) TEM Immunogold Labeling.** AEZαMfa1 specificity was determined by TEM Immunogold labeling. White arrow heads highlight immunogold Mfa1 interactions. This interaction was not observed using isotype control antibody (not shown). **(C) *In situ* association of *P. gingivalis* minor fimbriae with DCs in inflamed gingival tissues from patients with CP**. 5-8μm serial sections were obtained from human patients with CP under IRB approval. Slides were probed with FITC labeled anti-human DC-SIGN-green, followed by mouse anti-minor fimbriae *P. gingivalis* (monoclonal) primary antibody. This was followed by secondary goat anti-mouse IgG Texas Red®. Co-localization of DC-SIGN-Pg is seen in merge channels (yellow). As negative control, slides were processed with pre-immune rabbit-serum and with isotype control FITC-Mouse IgG2b (not shown).

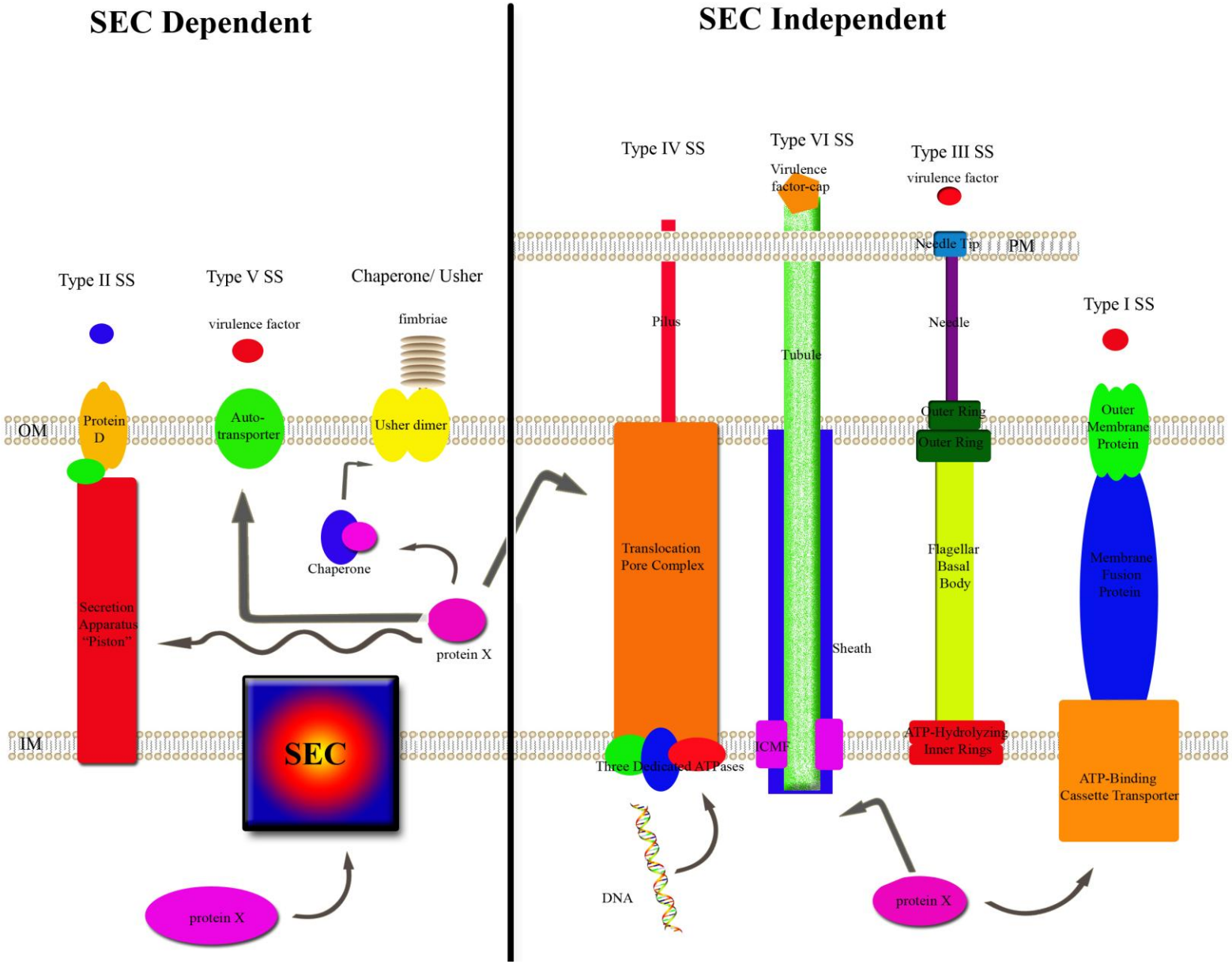
SEC Dependent
SEC Independent
Type II SS
Type V SS
Chaperone/ Usher
virulence factor
fimbriae
OM
Protein D
Auto-transporter
Usher dimer
Chaperone
Secretion Apparatus "Piston"
protein X
IM
SEC
protein X
Type IV SS
Type VI SS
Type III SS
Virulence factor-cap
virulence factor
Needle Tip
PM
Pilus
Tubule
Needle
Type I SS
Outer Ring
Outer Ring
Outer Membrane Protein
Translocation Pore Complex
Flagellar Basal Body
Membrane Fusion Protein
Sheath
ATP-Hydrolyzing Inner Rings
ICM
Three Dedicated ATPases
ATP-Binding Cassette Transporter
DNA
protein X

Figure 17. Multiple schematic representations for protein secretion in gram negative bacteria.

Bacterial protein secretion occurs via SEC dependent or SEC independent manner.

SEC dependant pathways include:

Type II secretion utilize a two step secretion process. The first step is translocation of the protein across the inner membrane (IM) via the SEC translocon. Once inside the periplasm proteins get translocated out via a multi-component secretion apparatus that spans both the inner and outer membranes. Finally the protein is secreted via a protein D homo-oligomer.

Type V secretion (Auto-transporter) translocate multidomain proteins across the inner membrane via the SEC translocon. Once inside the periplasmic space, the translocator domain of the protein inserts itself in the outer membrane (OM) to form a β-barrel. The β-barrel then facilitates surface localization/ secretion of the passenger domains by auto-proteolysis.

Chaperone/ Usher pathway translocate proteins across the inner membrane via the SEC translocon. Once inside the periplasm the fimbriae/ pili subunits interact with a chaperone protein that promotes proper protein folding while preventing premature subunit-subunit interactions. Chaperone-subunit complexes are then targeted to the outer membrane usher protein for fimbriae/ pili assembly and secretion across the outer membrane.

SEC independent pathways include:

Type I secretion involve simple tripartite systems that utilize an ATP-binding cassette transporter, an adaptor protein that spans the inner and outer membranes and a pore on

the outer membrane. They secrete proteins in a single step without any periplasmic intermediates.

Type III secretion (injectisomes) function to deliver effector proteins into eukaryotic host cells in a single step SEC independent manner. The injectisomes are genetically, structurally and functionally related to bacterial flagella, and are usually comprised of approximately 20 proteins. These proteins assemble into a supramolecular structure that spans the cytoplasm and inserts into the host cell plasma membrane.

Type VI secretion function to insert effector proteins into the cytoplasm of host cells. Not much is known about this newly discovered secretion system. Protein secretion is presumed to be done in a SEC independent manner. Protein secretion is thought to occur after a pilus like structure punctures the host cell plasma membrane in a mechanism that is similar to ones employed by bacteriophage. The intracellular multiplication proteins (ICM's) are thought to form the core of this structure.

Type IV secretion secretes proteins or DNA in either a SEC dependant or SEC independent manner. DNA is presumably translocated in a single step via a SEC independent manner that utilizes ATPases for energy. Proteins are first thought to get translocated across the inner membrane via a SEC dependant manner where they then interact with the translocon to cross the outer membrane and host plasma membrane. This process also utilizes ATPases for energy. The type IV pilus may serve as a secretion tube for proteins and DNA into the host cell.

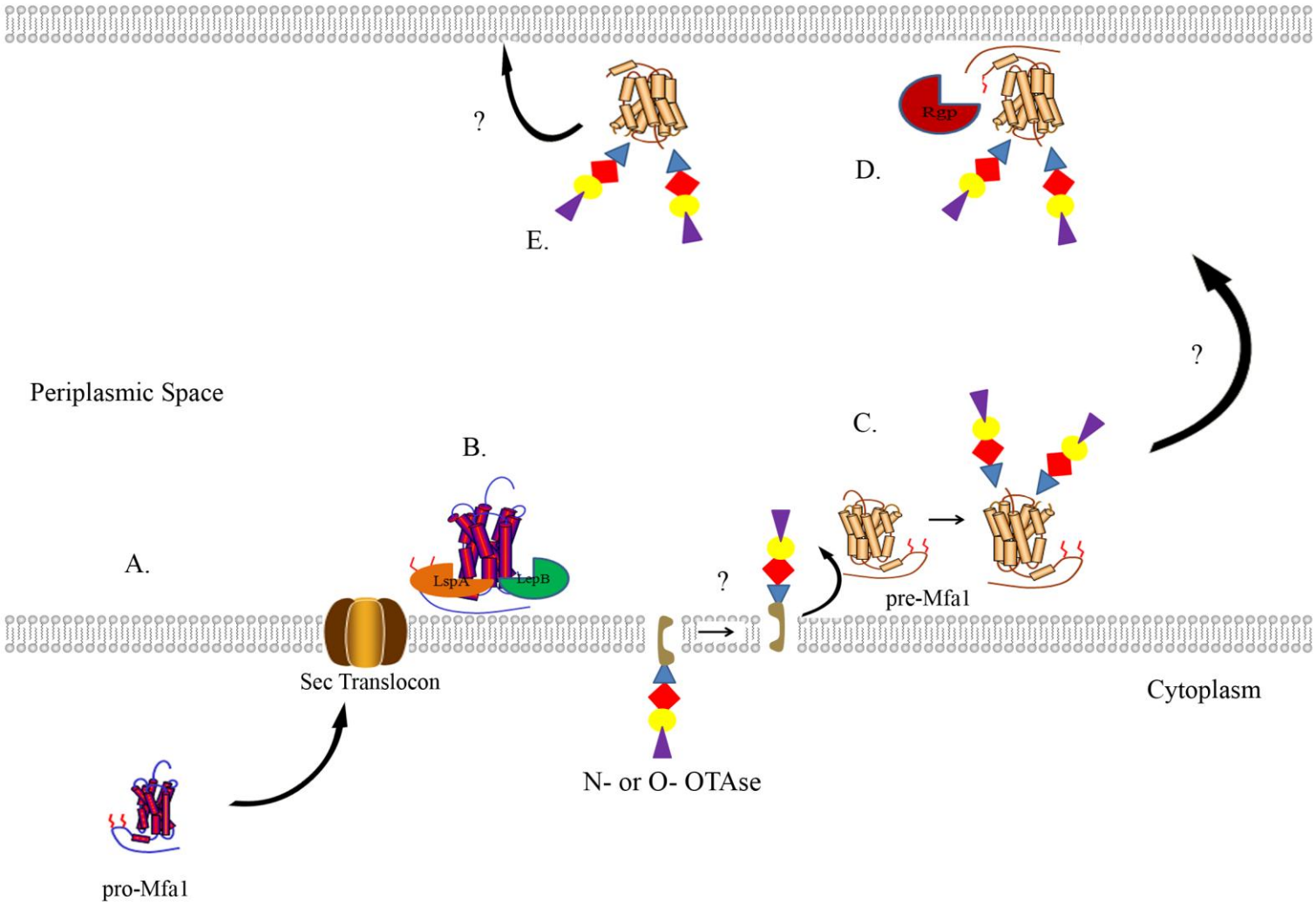
?
E.
Rgp
D.
?
Periplasmic Space
C.
B.
A.
LspA
LepB
?
pre-Mfa1
Sec Translocon
Cytoplasm
N- or O- OTAse
pro-Mfa1

Figure 18. Hypothetical model of minor fimbriae assembly.

A. Pro-Mfa1 crosses from the cytoplasm across the inner membrane using a Sec translocon homologue. **B.** While crossing via the Sec translocon homologue Pro-Mfa1 is processed at amino acid positions 21-22 and 50-51 by signal peptidase I (LepB in green) and signal peptidase II (LspA in orange). At the same time sugars preassemble on a lipid carrier present the cytoplasmic face of the inner membrane. **C.** The lipid carrier then transfers the oligosaccharide cargo to an OTAse. The OTAse then flips into the periplasmic space where it transfers the oligosaccharide to the minor fimbriae. **D.** The glycosylated minor fimbriae are then transferred to the outer membrane through a yet unknown mechanism where the pre-Mfa1 protein is further processed by gingipains (Rgp in red). **E.** Matured minor fimbriae are then exported across the outer membrane and assemble to short 100-200 nm fimbriae through an unknown manner.

References:

1. Burt, B. 2005. Position paper: epidemiology of periodontal diseases. *J Periodontol* 76:1406-1419.
2. Carranza, F. A., and M. G. Newman. 1996. *Clinical periodontology*. Saunders, Philadelphia.
3. Calkins, C. C., K. Platt, J. Potempa, and J. Travis. 1998. Inactivation of tumor necrosis factor-alpha by proteinases (gingipains) from the periodontal pathogen, Porphyromonas gingivalis. Implications of immune evasion. *J Biol Chem* 273:6611-6614.
4. Newman, M. G., and K. S. Kornman. 1990. *Antibiotic/antimicrobial use in dental practice*. Quintessence Pub. Co., Chicago.
5. Jotwani, R., M. Muthukuru, and C. W. Cutler. 2004. Increase in HIV receptors/co-receptors/alpha-defensins in inflamed human gingiva. *J Dent Res* 83:371-377.
6. Bodet, C., F. Chandad, and D. Grenier. 2005. Modulation of cytokine production by Porphyromonas gingivalis in a macrophage and epithelial cell co-culture model. *Microbes Infect* 7:448-456.
7. Cutler, C. W., J. R. Kalmar, and C. A. Genco. 1995. Pathogenic strategies of the oral anaerobe, Porphyromonas gingivalis. *Trends Microbiol* 3:45-51.
8. Lamont, R. J., and H. F. Jenkinson. 1998. Life below the gum line: pathogenic mechanisms of Porphyromonas gingivalis. *Microbiol Mol Biol Rev* 62:1244-1263.
9. Yonezawa, H., T. Kato, H. K. Kuramitsu, K. Okuda, and K. Ishihara. 2005. Immunization by Arg-gingipain A DNA vaccine protects mice against an invasive Porphyromonas gingivalis infection through regulation of interferon-gamma production. *Oral Microbiol Immunol* 20:259-266.
10. Yun, L. W., A. A. Decarlo, C. Collyer, and N. Hunter. 2003. Enhancement of Th2 pathways and direct activation of B cells by the gingipains of Porphyromonas gingivalis. *Clinical and experimental immunology* 134:295-302.
11. Yun, P. L., A. A. DeCarlo, C. Collyer, and N. Hunter. 2002. Modulation of an interleukin-12 and gamma interferon synergistic feedback regulatory cycle of T-cell and monocyte cocultures by Porphyromonas gingivalis lipopolysaccharide in the absence or presence of cysteine proteinases. *Infect Immun* 70:5695-5705.
12. Yun, P. L., A. A. DeCarlo, and N. Hunter. 1999. Modulation of major histocompatibility complex protein expression by human gamma interferon mediated by cysteine proteinase-adhesin polyproteins of Porphyromonas gingivalis. *Infect Immun* 67:2986-2995.
13. Fletcher, J., K. Reddi, S. Poole, S. Nair, B. Henderson, P. Tabona, and M. Wilson. 1997. Interactions between periodontopathogenic bacteria and cytokines. *J Periodontal Res* 32:200-205.
14. Potempa, J., A. Banbula, and J. Travis. 2000. Role of bacterial proteinases in matrix destruction and modulation of host responses. *Periodontol 2000* 24:153-192.

15. Jagels, M. A., J. Travis, J. Potempa, R. Pike, and T. E. Hugli. 1996. Proteolytic inactivation of the leukocyte C5a receptor by proteinases derived from Porphyromonas gingivalis. *Infect Immun* 64:1984-1991.
16. Teng, Y. T. 2006. Protective and destructive immunity in the periodontium: Part 1--innate and humoral immunity and the periodontium. *J Dent Res* 85:198-208.
17. Harbrecht, B. G., T. R. Billiar, R. D. Curran, J. Stadler, and R. L. Simmons. 1993. Hepatocyte injury by activated neutrophils in vitro is mediated by proteases. *Annals of surgery* 218:120-128.
18. Van Dyke, T. E., E. Bartholomew, R. J. Genco, J. Slots, and M. J. Levine. 1982. Inhibition of neutrophil chemotaxis by soluble bacterial products. *J Periodontol* 53:502-508.
19. Yun, P. L., A. A. Decarlo, C. Collyer, and N. Hunter. 2001. Hydrolysis of interleukin-12 by Porphyromonas gingivalis major cysteine proteinases may affect local gamma interferon accumulation and the Th1 or Th2 T-cell phenotype in periodontitis. *Infect Immun* 69:5650-5660.
20. Zeituni, A. E., R. Jotwani, J. Carrion, and C. W. Cutler. 2009. Targeting of DC-SIGN on human dendritic cells by minor fimbriated Porphyromonas gingivalis strains elicits a distinct effector T cell response. *J Immunol* 183:5694-5704.
21. Xie, H., and R. J. Lamont. 1999. Promoter architecture of the Porphyromonas gingivalis fimbrillin gene. *Infect Immun* 67:3227-3235.
22. Hamada, N., H. T. Sojar, M. I. Cho, and R. J. Genco. 1996. Isolation and characterization of a minor fimbria from Porphyromonas gingivalis. *Infect Immun* 64:4788-4794.
23. Arai, M., N. Hamada, and T. Umemoto. 2000. Purification and characterization of a novel secondary fimbrial protein from Porphyromonas gingivalis strain 381. *FEMS Microbiol Lett* 193:75-81.
24. Amano, A., A. Sharma, H. T. Sojar, H. K. Kuramitsu, and R. J. Genco. 1994. Effects of temperature stress on expression of fimbriae and superoxide dismutase by Porphyromonas gingivalis. *Infect Immun* 62:4682-4685.
25. Xie, H., S. Cai, and R. J. Lamont. 1997. Environmental regulation of fimbrial gene expression in Porphyromonas gingivalis. *Infect Immun* 65:2265-2271.
26. Xie, H., W. O. Chung, Y. Park, and R. J. Lamont. 2000. Regulation of the Porphyromonas gingivalis fimA (Fimbrillin) gene. *Infect Immun* 68:6574-6579.
27. Wu, J., X. Lin, and H. Xie. 2007. Porphyromonas gingivalis short fimbriae are regulated by a FimS/FimR two-component system. *FEMS Microbiol Lett* 271:214-221.
28. Wu, J., X. Lin, and H. Xie. 2008. OxyR is involved in coordinate regulation of expression of fimA and sod genes in Porphyromonas gingivalis. *FEMS Microbiol Lett* 282:188-195.
29. Shoji, M., M. Naito, H. Yukitake, K. Sato, E. Sakai, N. Ohara, and K. Nakayama. 2004. The major structural components of two cell surface filaments of Porphyromonas gingivalis are matured through lipoprotein precursors. *Mol Microbiol* 52:1513-1525.
30. Kato, T., T. Tsuda, H. Omori, T. Yoshimori, and A. Amano. 2007. Maturation of fimbria precursor protein by exogenous gingipains in Porphyromonas gingivalis gingipain-null mutant. *FEMS Microbiol Lett* 273:96-102.

31. Nakayama, K., F. Yoshimura, T. Kadowaki, and K. Yamamoto. 1996. Involvement of arginine-specific cysteine proteinase (Arg-gingipain) in fimbriation of Porphyromonas gingivalis. *J Bacteriol* 178:2818-2824.
32. Kadowaki, T., K. Nakayama, F. Yoshimura, K. Okamoto, N. Abe, and K. Yamamoto. 1998. Arg-gingipain acts as a major processing enzyme for various cell surface proteins in Porphyromonas gingivalis. *J Biol Chem* 273:29072-29076.
33. Yilmaz, O., K. Watanabe, and R. J. Lamont. 2002. Involvement of integrins in fimbriae-mediated binding and invasion by Porphyromonas gingivalis. *Cell Microbiol* 4:305-314.
34. Nakagawa, I., A. Amano, M. Kuboniwa, T. Nakamura, S. Kawabata, and S. Hamada. 2002. Functional differences among FimA variants of Porphyromonas gingivalis and their effects on adhesion to and invasion of human epithelial cells. *Infect Immun* 70:277-285.
35. Hajishengallis, G., M. Wang, E. Harokopakis, M. Triantafilou, and K. Triantafilou. 2006. Porphyromonas gingivalis fimbriae proactively modulate beta2 integrin adhesive activity and promote binding to and internalization by macrophages. *Infect Immun* 74:5658-5666.
36. Hajishengallis, G., and E. Harokopakis. 2007. Porphyromonas gingivalis interactions with complement receptor 3 (CR3): innate immunity or immune evasion? *Front Biosci* 12:4547-4557.
37. Takeshita, A., Y. Murakami, Y. Yamashita, M. Ishida, S. Fujisawa, S. Kitano, and S. Hanazawa. 1998. Porphyromonas gingivalis fimbriae use beta2 integrin (CD11/CD18) on mouse peritoneal macrophages as a cellular receptor, and the CD18 beta chain plays a functional role in fimbrial signaling. *Infect Immun* 66:4056-4060.
38. Wang, M., M. A. Shakhatreh, D. James, S. Liang, S. Nishiyama, F. Yoshimura, D. R. Demuth, and G. Hajishengallis. 2007. Fimbrial proteins of porphyromonas gingivalis mediate in vivo virulence and exploit TLR2 and complement receptor 3 to persist in macrophages. *J Immunol* 179:2349-2358.
39. Ogawa, T., Y. Asai, M. Hashimoto, and H. Uchida. 2002. Bacterial fimbriae activate human peripheral blood monocytes utilizing TLR2, CD14 and CD11a/CD18 as cellular receptors. *Eur J Immunol* 32:2543-2550.
40. Davey, M., X. Liu, T. Ukai, V. Jain, C. Gudino, F. C. Gibson, 3rd, D. Golenbock, A. Visintin, and C. A. Genco. 2008. Bacterial fimbriae stimulate proinflammatory activation in the endothelium through distinct TLRs. *J Immunol* 180:2187-2195.
41. Szymanski, C. M., and B. W. Wren. 2005. Protein glycosylation in bacterial mucosal pathogens. *Nat Rev Microbiol* 3:225-237.
42. Narimatsu, M., Y. Noiri, S. Itoh, N. Noguchi, T. Kawahara, and S. Ebisu. 2004. Essential role for the gtfA gene encoding a putative glycosyltransferase in the adherence of Porphyromonas gingivalis. *Infect Immun* 72:2698-2702.
43. Curtis, M. A., A. Thickett, J. M. Slaney, M. Rangarajan, J. Aduse-Opoku, P. Shepherd, N. Paramonov, and E. F. Hounsell. 1999. Variable carbohydrate modifications to the catalytic chains of the RgpA and RgpB proteases of Porphyromonas gingivalis W50. *Infect Immun* 67:3816-3823.

44. Vanterpool, E., F. Roy, and H. M. Fletcher. 2005. Inactivation of vimF, a putative glycosyltransferase gene downstream of vimE, alters glycosylation and activation of the gingipains in Porphyromonas gingivalis W83. *Infect Immun* 73:3971-3982.
45. Vanterpool, E., F. Roy, L. Sandberg, and H. M. Fletcher. 2005. Altered gingipain maturation in vimA- and vimE-defective isogenic mutants of Porphyromonas gingivalis. *Infect Immun* 73:1357-1366.
46. Nakao, R., Y. Tashiro, N. Nomura, S. Kosono, K. Ochiai, H. Yonezawa, H. Watanabe, and H. Senpuku. 2008. Glycosylation of the OMP85 homolog of Porphyromonas gingivalis and its involvement in biofilm formation. *Biochem Biophys Res Commun* 365:784-789.
47. Okamoto, K., Y. Misumi, T. Kadowaki, M. Yoneda, K. Yamamoto, and Y. Ikehara. 1995. Structural characterization of argingipain, a novel arginine-specific cysteine proteinase as a major periodontal pathogenic factor from Porphyromonas gingivalis. *Arch Biochem Biophys* 316:917-925.
48. Nagano, K., Y. Murakami, K. Nishikawa, J. Sakakibara, K. Shimozato, and F. Yoshimura. 2007. Characterization of RagA and RagB in Porphyromonas gingivalis: study using gene-deletion mutants. *J Med Microbiol* 56:1536-1548.
49. Medzihradszky, K. F. 2008. Characterization of site-specific N-glycosylation. *Methods Mol Biol* 446:293-316.
50. Zeituni, A. E., W. McCaig, E. Scisci, D. G. Thanassi, and C. W. Cutler. 2010. Native 67 kDa minor fimbriae of Porphyromonas gingivalis: a novel glycoprotein with DC-SIGN -targeting motifs. *J Bacteriol*.
51. Banchereau, J., and R. M. Steinman. 1998. Dendritic cells and the control of immunity. *Nature* 392:245-252.
52. Nakahara, T., Y. Moroi, H. Uchi, and M. Furue. 2006. Differential role of MAPK signaling in human dendritic cell maturation and Th1/Th2 engagement. *Journal of dermatological science* 42:1-11.
53. Shortman, K., and S. H. Naik. 2007. Steady-state and inflammatory dendritic-cell development. *Nat Rev Immunol* 7:19-30.
54. Jotwani, R., and C. W. Cutler. 2004. Fimbriated Porphyromonas gingivalis is more efficient than fimbria-deficient P. gingivalis in entering human dendritic cells in vitro and induces an inflammatory Th1 effector response. *Infect Immun* 72:1725-1732.
55. Nakajima, T., R. Amanuma, K. Ueki-Maruyama, T. Oda, T. Honda, H. Ito, and K. Yamazaki. 2008. CXCL13 expression and follicular dendritic cells in relation to B-cell infiltration in periodontal disease tissues. *J Periodontal Res* 43:635-641.
56. Schaumann, F., M. Muller, A. Braun, B. Luettig, D. B. Peden, J. M. Hohlfeld, and N. Krug. 2008. Endotoxin augments myeloid dendritic cell influx into the airways in patients with allergic asthma. *Am J Respir Crit Care Med* 177:1307-1313.
57. Jotwani, R., B. Pulendran, S. Agrawal, and C. W. Cutler. 2003. Human dendritic cells respond to Porphyromonas gingivalis LPS by promoting a Th2 effector response in vitro. *Eur J Immunol* 33:2980-2986.
58. Puig-Kroger, A., M. Relloso, O. Fernandez-Capetillo, A. Zubiaga, A. Silva, C. Bernabeu, and A. L. Corbi. 2001. Extracellular signal-regulated protein kinase signaling pathway negatively regulates the phenotypic and functional maturation of monocyte-derived human dendritic cells. *Blood* 98:2175-2182.

59. Pulendran, B., P. Kumar, C. W. Cutler, M. Mohamadzadeh, T. Van Dyke, and J. Banchereau. 2001. Lipopolysaccharides from distinct pathogens induce different classes of immune responses in vivo. *J Immunol* 167:5067-5076.
60. Kadowaki, N. 2007. Dendritic Cells -A Conductor of T Cell Differentiation. *Allergol Int* 56:193-199.
61. Lanzavecchia, A., and F. Sallusto. 2001. Regulation of T cell immunity by dendritic cells. *Cell* 106:263-266.
62. Arrighi, J. F., M. Rebsamen, F. Rousset, V. Kindler, and C. Hauser. 2001. A critical role for p38 mitogen-activated protein kinase in the maturation of human blood-derived dendritic cells induced by lipopolysaccharide, TNF-alpha, and contact sensitizers. *J Immunol* 166:3837-3845.
63. Pan, H., J. Xie, F. Ye, and S. J. Gao. 2006. Modulation of Kaposi's sarcoma-associated herpesvirus infection and replication by MEK/ERK, JNK, and p38 multiple mitogen-activated protein kinase pathways during primary infection. *J Virol* 80:5371-5382.
64. Agrawal, S., A. Agrawal, B. Doughty, A. Gerwitz, J. Blenis, T. Van Dyke, and B. Pulendran. 2003. Cutting edge: different Toll-like receptor agonists instruct dendritic cells to induce distinct Th responses via differential modulation of extracellular signal-regulated kinase-mitogen-activated protein kinase and c-Fos. *J Immunol* 171:4984-4989.
65. Steinman, R. M. 2007. Dendritic cells: understanding immunogenicity. *Eur J Immunol* 37 Suppl 1:S53-60.
66. Blander, J. M., and R. Medzhitov. 2006. On regulation of phagosome maturation and antigen presentation. *Nat Immunol* 7:1029-1035.
67. Blander, J. M., and R. Medzhitov. 2006. Toll-dependent selection of microbial antigens for presentation by dendritic cells. *Nature* 440:808-812.
68. Medzhitov, R. 2007. Recognition of microorganisms and activation of the immune response. *Nature* 449:819-826.
69. Muthukuru, M., and C. W. Cutler. 2008. Antigen capture of Porphyromonas gingivalis by human macrophages is enhanced but killing and antigen presentation are reduced by endotoxin tolerance. *Infect Immun* 76:477-485.
70. Gringhuis, S. I., J. den Dunnen, M. Litjens, B. van Het Hof, Y. van Kooyk, and T. B. Geijtenbeek. 2007. C-type lectin DC-SIGN modulates Toll-like receptor signaling via Raf-1 kinase-dependent acetylation of transcription factor NF-kappaB. *Immunity* 26:605-616.
71. Feinberg, H., D. A. Mitchell, K. Drickamer, and W. I. Weis. 2001. Structural basis for selective recognition of oligosaccharides by DC-SIGN and DC-SIGNR. *Science* 294:2163-2166.
72. Appelmelk, B. J., I. van Die, S. J. van Vliet, C. M. Vandenbroucke-Grauls, T. B. Geijtenbeek, and Y. van Kooyk. 2003. Cutting edge: carbohydrate profiling identifies new pathogens that interact with dendritic cell-specific ICAM-3-grabbing nonintegrin on dendritic cells. *J Immunol* 170:1635-1639.
73. Guo, Y., H. Feinberg, E. Conroy, D. A. Mitchell, R. Alvarez, O. Blixt, M. E. Taylor, W. I. Weis, and K. Drickamer. 2004. Structural basis for distinct ligand-binding and targeting properties of the receptors DC-SIGN and DC-SIGNR. *Nat Struct Mol Biol* 11:591-598.

74. Zhang, P., O. Schwartz, M. Pantelic, G. Li, Q. Knazze, C. Nobile, M. Radovich, J. He, S. C. Hong, J. Klena, and T. Chen. 2006. DC-SIGN (CD209) recognition of Neisseria gonorrhoeae is circumvented by lipooligosaccharide variation. *J Leukoc Biol* 79:731-738.
75. Maeda, N., J. Nigou, J. L. Herrmann, M. Jackson, A. Amara, P. H. Lagrange, G. Puzo, B. Gicquel, and O. Neyrolles. 2003. The cell surface receptor DC-SIGN discriminates between Mycobacterium species through selective recognition of the mannose caps on lipoarabinomannan. *J Biol Chem* 278:5513-5516.
76. Soilleux, E. J., E. N. Sarno, M. O. Hernandez, E. Moseley, J. Horsley, U. G. Lopes, M. J. Goddard, S. L. Vowler, N. Coleman, R. J. Shattock, and E. P. Sampaio. 2006. DC-SIGN association with the Th2 environment of lepromatous lesions: cause or effect? *J Pathol* 209:182-189.
77. Pohlmann, S., F. Baribaud, B. Lee, G. J. Leslie, M. D. Sanchez, K. Hiebenthal-Millow, J. Munch, F. Kirchhoff, and R. W. Doms. 2001. DC-SIGN interactions with human immunodeficiency virus type 1 and 2 and simian immunodeficiency virus. *J Virol* 75:4664-4672.
78. Kwon, D. S., G. Gregorio, N. Bitton, W. A. Hendrickson, and D. R. Littman. 2002. DC-SIGN-mediated internalization of HIV is required for trans-enhancement of T cell infection. *Immunity* 16:135-144.
79. Neumann, A. K., N. L. Thompson, and K. Jacobson. 2008. Distribution and lateral mobility of DC-SIGN on immature dendritic cells--implications for pathogen uptake. *J Cell Sci* 121:634-643.
80. Engering, A., T. B. Geijtenbeek, S. J. van Vliet, M. Wijers, E. van Liempt, N. Demaurex, A. Lanzavecchia, J. Fransen, C. G. Figdor, V. Piguet, and Y. van Kooyk. 2002. The dendritic cell-specific adhesion receptor DC-SIGN internalizes antigen for presentation to T cells. *J Immunol* 168:2118-2126.
81. Bergman, M. P., A. Engering, H. H. Smits, S. J. van Vliet, A. A. van Bodegraven, H. P. Wirth, M. L. Kapsenberg, C. M. Vandenbroucke-Grauls, Y. van Kooyk, and B. J. Appelmelk. 2004. Helicobacter pylori modulates the T helper cell 1/T helper cell 2 balance through phase-variable interaction between lipopolysaccharide and DC-SIGN. *J Exp Med* 200:979-990.
82. Darveau, R. P., C. M. Belton, R. A. Reife, and R. J. Lamont. 1998. Local chemokine paralysis, a novel pathogenic mechanism for Porphyromonas gingivalis. *Infect Immun* 66:1660-1665.
83. Tam, V., N. M. O'Brien-Simpson, Y. Y. Chen, C. J. Sanderson, B. Kinnear, and E. C. Reynolds. 2009. The RgpA-Kgp proteinase-adhesin complexes of Porphyromonas gingivalis Inactivate the Th2 cytokines interleukin-4 and interleukin-5. *Infect Immun* 77:1451-1458.
84. Zhou, Q., T. Desta, M. Fenton, D. T. Graves, and S. Amar. 2005. Cytokine profiling of macrophages exposed to Porphyromonas gingivalis, its lipopolysaccharide, or its FimA protein. *Infect Immun* 73:935-943.
85. Wilson, M., R. Seymour, and B. Henderson. 1998. Bacterial perturbation of cytokine networks. *Infect Immun* 66:2401-2409.
86. Sundqvist, G., J. Carlsson, B. Herrmann, and A. Tarnvik. 1985. Degradation of human immunoglobulins G and M and complement factors C3 and C5 by black-pigmented Bacteroides. *J Med Microbiol* 19:85-94.

87. Takahashi, Y., M. Davey, H. Yumoto, F. C. Gibson, 3rd, and C. A. Genco. 2006. Fimbria-dependent activation of pro-inflammatory molecules in Porphyromonas gingivalis infected human aortic endothelial cells. *Cell Microbiol* 8:738-757.
88. Tuominen-Gustafsson H, P. M., Hytönen J, Viljanen MK. 2006. Use of CFSE staining of borreliae in studies on the interaction between borreliae and human neutrophils. *BMC Microbiol.* 6:92.
89. Cutler, C. W., J. R. Kalmar, and R. R. Arnold. 1991. Phagocytosis of virulent Porphyromonas gingivalis by human polymorphonuclear leukocytes requires specific immunoglobulin G. *Infect Immun* 59:2097-2104.
90. Boggiano, C., N. Manel, and D. R. Littman. 2007. Dendritic cell-mediated trans-enhancement of human immunodeficiency virus type 1 infectivity is independent of DC-SIGN. *J Virol* 81:2519-2523.
91. Vander Top, E. A., G. A. Perry, and M. J. Gentry-Nielsen. 2006. A novel flow cytometric assay for measurement of in vivo pulmonary neutrophil phagocytosis. *BMC Microbiol* 6:61.
92. Pils, S., T. Schmitter, F. Neske, and C. R. Hauck. 2006. Quantification of bacterial invasion into adherent cells by flow cytometry. *J Microbiol Methods* 65:301-310.
93. Hamada, N., K. Watanabe, M. Arai, H. Hiramine, and T. Umemoto. 2002. Cytokine production induced by a 67-kDa fimbrial protein from Porphyromonas gingivalis. *Oral Microbiol Immunol* 17:197-200.
94. Shevchenko, A., O. N. Jensen, A. V. Podtelejnikov, F. Sagliocco, M. Wilm, O. Vorm, P. Mortensen, H. Boucherie, and M. Mann. 1996. Linking genome and proteome by mass spectrometry: large-scale identification of yeast proteins from two dimensional gels. *Proc Natl Acad Sci U S A* 93:14440-14445.
95. Tanner, S., H. Shu, A. Frank, L. C. Wang, E. Zandi, M. Mumby, P. A. Pevzner, and V. Bafna. 2005. InsPecT: identification of posttranslationally modified peptides from tandem mass spectra. *Anal Chem* 77:4626-4639.
96. Savitt, A. G., P. Mena-Taboada, G. Monsalve, and J. L. Benach. 2009. Francisella tularensis infection-derived monoclonal antibodies provide detection, protection, and therapy. *Clin Vaccine Immunol* 16:414-422.
97. Garcia-Vallejo, J. J., E. van Liempt, P. da Costa Martins, C. Beckers, B. van het Hof, S. I. Gringhuis, J. J. Zwaginga, W. van Dijk, T. B. Geijtenbeek, Y. van Kooyk, and I. van Die. 2008. DC-SIGN mediates adhesion and rolling of dendritic cells on primary human umbilical vein endothelial cells through LewisY antigen expressed on ICAM-2. *Mol Immunol* 45:2359-2369.
98. Cambi, A., M. Koopman, and C. G. Figdor. 2005. How C-type lectins detect pathogens. *Cell Microbiol* 7:481-488.
99. Engering, A., S. J. Van Vliet, T. B. Geijtenbeek, and Y. Van Kooyk. 2002. Subset of DC-SIGN(+) dendritic cells in human blood transmits HIV-1 to T lymphocytes. *Blood* 100:1780-1786.
100. van Lent PL, F. C., Barrera P, van Ginkel K, Slöetjes A, van den Berg WB, Torensma R. 2003. Expression of the dendritic cell-associated C-type lectin DC-SIGN by inflammatory matrix metalloproteinase-producing macrophages in rheumatoid arthritis synovium and interaction with intercellular adhesion molecule 3-positive T cells.

. *Arthritis Rheum.* 48:360-369.
101. Bobryshev, Y. V. 2005. Intracellular localization of oxidized low-density lipoproteins in atherosclerotic plaque cells revealed by electron microscopy combined with laser capture microdissection. *J Histochem Cytochem* 53:793-797.
102. Soilleux, E. J., L. S. Morris, J. Trowsdale, N. Coleman, and J. J. Boyle. 2002. Human atherosclerotic plaques express DC-SIGN, a novel protein found on dendritic cells and macrophages. *J Pathol* 198:511-516.
103. Bodineau, A., B. Coulomb, A. C. Tedesco, and S. Seguier. 2009. Increase of gingival matured dendritic cells number in elderly patients with chronic periodontitis. *Arch Oral Biol* 54:12-16.
104. den Dunnen, J., S. I. Gringhuis, and T. B. Geijtenbeek. 2008. Innate signaling by the C-type lectin DC-SIGN dictates immune responses. *Cancer Immunol Immunother*.
105. Caparros, E., P. Munoz, E. Sierra-Filardi, D. Serrano-Gomez, A. Puig-Kroger, J. L. Rodriguez-Fernandez, M. Mellado, J. Sancho, M. Zubiaur, and A. L. Corbi. 2006. DC-SIGN ligation on dendritic cells results in ERK and PI3K activation and modulates cytokine production. *Blood* 107:3950-3958.
106. Zhou, Z., M. C. Connell, and D. J. MacEwan. 2007. TNFR1-induced NF-kappaB, but not ERK, p38MAPK or JNK activation, mediates TNF-induced ICAM-1 and VCAM-1 expression on endothelial cells. *Cell Signal* 19:1238-1248.
107. Geijtenbeek, T. B., S. J. Van Vliet, E. A. Koppel, M. Sanchez-Hernandez, C. M. Vandenbroucke-Grauls, B. Appelmelk, and Y. Van Kooyk. 2003. Mycobacteria target DC-SIGN to suppress dendritic cell function. *J Exp Med* 197:7-17.
108. Steeghs, L., S. J. van Vliet, H. Uronen-Hansson, A. van Mourik, A. Engering, M. Sanchez-Hernandez, N. Klein, R. Callard, J. P. van Putten, P. van der Ley, Y. van Kooyk, and J. G. van de Winkel. 2006. Neisseria meningitidis expressing lgtB lipopolysaccharide targets DC-SIGN and modulates dendritic cell function. *Cell Microbiol* 8:316-325.
109. Smits, H. H., A. Engering, D. van der Kleij, E. C. de Jong, K. Schipper, T. M. van Capel, B. A. Zaat, M. Yazdanbakhsh, E. A. Wierenga, Y. van Kooyk, and M. L. Kapsenberg. 2005. Selective probiotic bacteria induce IL-10-producing regulatory T cells in vitro by modulating dendritic cell function through dendritic cell-specific intercellular adhesion molecule 3-grabbing nonintegrin. *The Journal of allergy and clinical immunology* 115:1260-1267.
110. Muthukuru, M., and C. W. Cutler. 2006. Upregulation of immunoregulatory Src homology 2 molecule containing inositol phosphatase and mononuclear cell hyporesponsiveness in oral mucosa during chronic periodontitis. *Infect Immun* 74:1431-1435.
111. Muthukuru, M., R. Jotwani, and C. W. Cutler. 2005. Oral mucosal endotoxin tolerance induction in chronic periodontitis. *Infect Immun* 73:687-694.
112. Gaffen, S. L., and G. Hajishengallis. 2008. A new inflammatory cytokine on the block: re-thinking periodontal disease and the Th1/Th2 paradigm in the context of Th17 cells and IL-17. *J Dent Res* 87:817-828.
113. Jotwani, R., A. K. Palucka, M. Al-Quotub, M. Nouri-Shirazi, J. Kim, D. Bell, J. Banchereau, and C. W. Cutler. 2001. Mature dendritic cells infiltrate the T cell-

rich region of oral mucosa in chronic periodontitis: in situ, in vivo, and in vitro studies. *J Immunol* 167:4693-4700.
114. Jotwani, R., and C. W. Cutler. 2003. Multiple dendritic cell (DC) subpopulations in human gingiva and association of mature DCs with CD4+ T-cells in situ. *J Dent Res* 82:736-741.
115. Ivanov, I. I., R. d. L. Frutos, N. Manel, K. Yoshinaga, D. B. Rifkin, R. B. Sartor, B. B. Finlay, and D. R. Littman. 2008. Specific Microbiota Direct the Differentiation of IL-17-Producing T-Helper Cells in the Mucosa of the Small Intestine. *Cell Host & Microbe* 4:337-349.
116. Cutler CW, J. R. 2006. Dendritic cells at the oral mucosal interface. *J Dent Res.* 85:678-689.
117. Socransky SS, H. A. 2002. Dental biofilms: difficult therapeutic targets. *Periodontol 2000* 28.
118. Ezzo, P. J., and C. W. Cutler. 2003. Microorganisms as risk indicators for periodontal disease. *Periodontol 2000* 32:24-35.
119. Hajishengallis, G., R. I. Tapping, E. Harokopakis, S. Nishiyama, P. Ratti, R. E. Schifferle, E. A. Lyle, M. Triantafilou, K. Triantafilou, and F. Yoshimura. 2006. Differential interactions of fimbriae and lipopolysaccharide from Porphyromonas gingivalis with the Toll-like receptor 2-centred pattern recognition apparatus. *Cell Microbiol* 8:1557-1570.
120. Umemoto, T., and N. Hamada. 2003. Characterization of biologically active cell surface components of a periodontal pathogen. The roles of major and minor fimbriae of Porphyromonas gingivalis. *J Periodontol* 74:119-122.
121. Cutler, C. W., R. Jotwani, K. A. Palucka, J. Davoust, D. Bell, and J. Banchereau. 1999. Evidence and a novel hypothesis for the role of dendritic cells and Porphyromonas gingivalis in adult periodontitis. *J Periodontal Res* 34:406-412.
122. Cutler, C. W., and R. Jotwani. 2004. Antigen-presentation and the role of dendritic cells in periodontitis. *Periodontol 2000* 35:135-157.
123. Timpano, G., G. Tabarani, M. Anderluh, D. Invernizzi, F. Vasile, D. Potenza, P. M. Nieto, J. Rojo, F. Fieschi, and A. Bernardi. 2008. Synthesis of novel DC-SIGN ligands with an alpha-fucosylamide anchor. *Chembiochem* 9:1921-1930.
124. Zhang, J., J. M. Qu, and L. X. He. 2009. IL-12 suppression, enhanced endocytosis and up-regulation of MHC-II and CD80 in dendritic cells during experimental endotoxin tolerance. *Acta Pharmacol Sin* 30:582-588.
125. Koga, T., T. Nishihara, T. Fujiwara, T. Nisizawa, N. Okahashi, T. Noguchi, and S. Hamada. 1985. Biochemical and immunobiological properties of lipopolysaccharide (LPS) from Bacteroides gingivalis and comparison with LPS from Escherichia coli. *Infect Immun* 47:638-647.
126. Bramanti, T. E., G. G. Wong, S. T. Weintraub, and S. C. Holt. 1989. Chemical characterization and biologic properties of lipopolysaccharide from Bacteroides gingivalis strains W50, W83, and ATCC 33277. *Oral Microbiol Immunol* 4:183-192.
127. Shan, M., P. J. Klasse, K. Banerjee, A. K. Dey, S. P. Iyer, R. Dionisio, D. Charles, L. Campbell-Gardener, W. C. Olson, R. W. Sanders, and J. P. Moore. 2007. HIV-1 gp120 mannoses induce immunosuppressive responses from dendritic cells. *PLoS Pathog* 3:e169.

128. Amano, A., H. T. Sojar, J. Y. Lee, A. Sharma, M. J. Levine, and R. J. Genco. 1994. Salivary receptors for recombinant fimbrillin of Porphyromonas gingivalis. *Infect Immun* 62:3372-3380.
129. Heroven, A. K., K. Bohme, H. Tran-Winkler, and P. Dersch. 2007. Regulatory elements implicated in the environmental control of invasin expression in enteropathogenic Yersinia. *Adv Exp Med Biol* 603:156-166.
130. Aguirre, A., M. L. Cabeza, S. V. Spinelli, M. McClelland, E. Garcia Vescovi, and F. C. Soncini. 2006. PhoP-induced genes within Salmonella pathogenicity island 1. *J Bacteriol* 188:6889-6898.
131. Hautefort, I., A. Thompson, S. Eriksson-Ygberg, M. L. Parker, S. Lucchini, V. Danino, R. J. Bongaerts, N. Ahmad, M. Rhen, and J. C. Hinton. 2008. During infection of epithelial cells Salmonella enterica serovar Typhimurium undergoes a time-dependent transcriptional adaptation that results in simultaneous expression of three type 3 secretion systems. *Cell Microbiol* 10:958-984.
132. Amano, A., T. Fujiwara, H. Nagata, M. Kuboniwa, A. Sharma, H. T. Sojar, R. J. Genco, S. Hamada, and S. Shizukuishi. 1997. Prophyromonas gingivalis fimbriae mediate coaggregation with Streptococcus oralis through specific domains. *J Dent Res* 76:852-857.
133. Amano, A., T. Nakamura, S. Kimura, I. Morisaki, I. Nakagawa, S. Kawabata, and S. Hamada. 1999. Molecular interactions of Porphyromonas gingivalis fimbriae with host proteins: kinetic analyses based on surface plasmon resonance. *Infect Immun* 67:2399-2405.
134. Tsuda, K., N. Furuta, H. Inaba, S. Kawai, K. Hanada, T. Yoshimori, and A. Amano. 2008. Functional analysis of alpha5beta1 integrin and lipid rafts in invasion of epithelial cells by Porphyromonas gingivalis using fluorescent beads coated with bacterial membrane vesicles. *Cell Struct Funct* 33:123-132.
135. Njoroge, T., R. J. Genco, H. T. Sojar, N. Hamada, and C. A. Genco. 1997. A role for fimbriae in Porphyromonas gingivalis invasion of oral epithelial cells. *Infect Immun* 65:1980-1984.
136. Lamont, R. J., S. Gil, D. R. Demuth, D. Malamud, and B. Rosan. 1994. Molecules of Streptococcus gordonii that bind to Porphyromonas gingivalis. *Microbiology* 140 (Pt 4):867-872.
137. Lamont, R. J., G. W. Hsiao, and S. Gil. 1994. Identification of a molecule of Porphyromonas gingivalis that binds to Streptococcus gordonii. *Microb Pathog* 17:355-360.
138. Gibson, F. C., 3rd, and C. A. Genco. 2007. Porphyromonas gingivalis mediated periodontal disease and atherosclerosis: disparate diseases with commonalities in pathogenesis through TLRs. *Curr Pharm Des* 13:3665-3675.
139. Kozarov, E. V., B. R. Dorn, C. E. Shelburne, W. A. Dunn, Jr., and A. Progulske-Fox. 2005. Human atherosclerotic plaque contains viable invasive Actinobacillus actinomycetemcomitans and Porphyromonas gingivalis. *Arterioscler Thromb Vasc Biol* 25:e17-18.
140. Hajishengallis, G., M. A. Shakhatreh, M. Wang, and S. Liang. 2007. Complement receptor 3 blockade promotes IL-12-Mediated Clearance of Porphyromonas gingivalis and Negates Its Virulence In Vivo. *J Immunol* 179:2359-2367.

141. Cario, E. 2008. Barrier-protective function of intestinal epithelial Toll-like receptor 2. *Mucosal Immunol* 1 Suppl 1:S62-66.
142. Sanjuan, M. A., S. Milasta, and D. R. Green. 2009. Toll-like receptor signaling in the lysosomal pathways. *Immunol Rev* 227:203-220.
143. Swanson, J. A. 2008. Shaping cups into phagosomes and macropinosomes. *Nat Rev Mol Cell Biol* 9:639-649.
144. Shreffler, W. G., R. R. Castro, Z. Y. Kucuk, Z. Charlop-Powers, G. Grishina, S. Yoo, A. W. Burks, and H. A. Sampson. 2006. The major glycoprotein allergen from Arachis hypogaea, Ara h 1, is a ligand of dendritic cell-specific ICAM-grabbing nonintegrin and acts as a Th2 adjuvant in vitro. *J Immunol* 177:3677-3685.
145. Imamura, T., J. Travis, and J. Potempa. 2003. The biphasic virulence activities of gingipains: activation and inactivation of host proteins. *Curr Protein Pept Sci* 4:443-450.
146. Mezyk-Kopec, R., M. Bzowska, J. Potempa, N. Jura, A. Sroka, R. A. Black, and J. Bereta. 2005. Inactivation of membrane tumor necrosis factor alpha by gingipains from Porphyromonas gingivalis. *Infect Immun* 73:1506-1514.
147. Potempa, J., J. Mikolajczyk-Pawlinska, D. Brassell, D. Nelson, I. B. Thogersen, J. J. Enghild, and J. Travis. 1998. Comparative properties of two cysteine proteinases (gingipains R), the products of two related but individual genes of Porphyromonas gingivalis. *J Biol Chem* 273:21648-21657.
148. Sroka, A., M. Sztukowska, J. Potempa, J. Travis, and C. A. Genco. 2001. Degradation of host heme proteins by lysine- and arginine-specific cysteine proteinases (gingipains) of Porphyromonas gingivalis. *J Bacteriol* 183:5609-5616.
149. Harokopakis, E., M. H. Albzreh, E. M. Haase, F. A. Scannapieco, and G. Hajishengallis. 2006. Inhibition of proinflammatory activities of major periodontal pathogens by aqueous extracts from elder flower (Sambucus nigra). *J Periodontol* 77:271-279.
150. Lamont, R. J., A. El-Sabaeny, Y. Park, G. S. Cook, J. W. Costerton, and D. R. Demuth. 2002. Role of the Streptococcus gordonii SspB protein in the development of Porphyromonas gingivalis biofilms on streptococcal substrates. *Microbiology* 148:1627-1636.
151. Park, Y., M. R. Simionato, K. Sekiya, Y. Murakami, D. James, W. Chen, M. Hackett, F. Yoshimura, D. R. Demuth, and R. J. Lamont. 2005. Short fimbriae of Porphyromonas gingivalis and their role in coadhesion with Streptococcus gordonii. *Infect Immun* 73:3983-3989.
152. Zhang, P., S. Snyder, P. Feng, P. Azadi, S. Zhang, S. Bulgheresi, K. E. Sanderson, J. He, J. Klena, and T. Chen. 2006. Role of N-acetylglucosamine within core lipopolysaccharide of several species of gram-negative bacteria in targeting the DC-SIGN (CD209). *J Immunol* 177:4002-4011.
153. Asai, Y., M. Hashimoto, H. M. Fletcher, K. Miyake, S. Akira, and T. Ogawa. 2005. Lipopolysaccharide preparation extracted from Porphyromonas gingivalis lipoprotein-deficient mutant shows a marked decrease in toll-like receptor 2-mediated signaling. *Infect Immun* 73:2157-2163.
154. Seydel, U., A. B. Schromm, L. Brade, S. Gronow, J. Andra, M. Muller, M. H. Koch, K. Fukase, M. Kataoka, M. Hashimoto, S. Kusumoto, and K. Brandenburg.

2005. Physicochemical characterization of carboxymethyl lipid A derivatives in relation to biological activity. *FEBS J* 272:327-340.
155. Abu-Qarn, M., J. Eichler, and N. Sharon. 2008. Not just for Eukarya anymore: protein glycosylation in Bacteria and Archaea. *Curr Opin Struct Biol* 18:544-550.
156. O'Neill, R. A. 1996. Enzymatic release of oligosaccharides from glycoproteins for chromatographic and electrophoretic analysis. *J Chromatogr A* 720:201-215.
157. Tarentino, A. L., G. Quinones, W. P. Schrader, L. M. Changchien, and T. H. Plummer, Jr. 1992. Multiple endoglycosidase (Endo) F activities expressed by Flavobacterium meningosepticum. Endo F1: molecular cloning, primary sequence, and structural relationship to Endo H. *J Biol Chem* 267:3868-3872.
158. Tarentino, A. L., and T. H. Plummer, Jr. 1994. Substrate specificity of Flavobacterium meningosepticum Endo F2 and endo F3: purity is the name of the game. *Glycobiology* 4:771-773.
159. Tarentino, A. L., G. Quinones, L. M. Changchien, and T. H. Plummer, Jr. 1993. Multiple endoglycosidase F activities expressed by Flavobacterium meningosepticum endoglycosidases F2 and F3. Molecular cloning, primary sequence, and enzyme expression. *J Biol Chem* 268:9702-9708.
160. Chung, W. O., D. R. Demuth, and R. J. Lamont. 2000. Identification of a Porphyromonas gingivalis receptor for the Streptococcus gordonii SspB protein. *Infect Immun* 68:6758-6762.
161. Gallagher, A., J. Aduse-Opoku, M. Rangarajan, J. M. Slaney, and M. A. Curtis. 2003. Glycosylation of the Arg-gingipains of Porphyromonas gingivalis and comparison with glycoconjugate structure and synthesis in other bacteria. *Curr Protein Pept Sci* 4:427-441.
162. Paramonov, N., D. Bailey, M. Rangarajan, A. Hashim, G. Kelly, M. A. Curtis, and E. F. Hounsell. 2001. Structural analysis of the polysaccharide from the lipopolysaccharide of Porphyromonas gingivalis strain W50. *European journal of biochemistry / FEBS* 268:4698-4707.
163. Paramonov, N. A., J. Aduse-Opoku, A. Hashim, M. Rangarajan, and M. A. Curtis. 2009. Structural analysis of the core region of O-lipopolysaccharide of Porphyromonas gingivalis from mutants defective in O-antigen ligase and O-antigen polymerase. *J Bacteriol* 191:5272-5282.
164. Schifferle, R. E., M. S. Reddy, J. J. Zambon, R. J. Genco, and M. J. Levine. 1989. Characterization of a polysaccharide antigen from Bacteroides gingivalis. *J Immunol* 143:3035-3042.
165. Rangarajan, M., A. Hashim, J. Aduse-Opoku, N. Paramonov, E. F. Hounsell, and M. A. Curtis. 2005. Expression of Arg-Gingipain RgpB is required for correct glycosylation and stability of monomeric Arg-gingipain RgpA from Porphyromonas gingivalis W50. *Infect Immun* 73:4864-4878.
166. Aduse-Opoku, J., J. M. Slaney, A. Hashim, A. Gallagher, R. P. Gallagher, M. Rangarajan, K. Boutaga, M. L. Laine, A. J. Van Winkelhoff, and M. A. Curtis. 2006. Identification and characterization of the capsular polysaccharide (K-antigen) locus of Porphyromonas gingivalis. *Infect Immun* 74:449-460.
167. Yoshimura, F., Y. Murakami, K. Nishikawa, Y. Hasegawa, and S. Kawaminami. 2009. Surface components of Porphyromonas gingivalis. *J Periodontal Res* 44:1-12.

168. Park, Y., C. E. James, F. Yoshimura, and R. J. Lamont. 2006. Expression of the short fimbriae of Porphyromonas gingivalis is regulated in oral bacterial consortia. *FEMS Microbiol Lett* 262:65-71.
169. Masuda, T., Y. Murakami, T. Noguchi, and F. Yoshimura. 2006. Effects of various growth conditions in a chemostat on expression of virulence factors in Porphyromonas gingivalis. *Appl Environ Microbiol* 72:3458-3467.
170. Emanuelsson, O., S. Brunak, G. von Heijne, and H. Nielsen. 2007. Locating proteins in the cell using TargetP, SignalP and related tools. *Nat Protoc* 2:953-971.
171. Fleckenstein, J. M., K. Roy, J. F. Fischer, and M. Burkitt. 2006. Identification of a two-partner secretion locus of enterotoxigenic Escherichia coli. *Infect Immun* 74:2245-2258.
172. Wacker, M., D. Linton, P. G. Hitchen, M. Nita-Lazar, S. M. Haslam, S. J. North, M. Panico, H. R. Morris, A. Dell, B. W. Wren, and M. Aebi. 2002. N-linked glycosylation in Campylobacter jejuni and its functional transfer into E. coli. *Science* 298:1790-1793.
173. Sartain, M. J., and J. T. Belisle. 2009. N-Terminal clustering of the O-glycosylation sites in the Mycobacterium tuberculosis lipoprotein SodC. *Glycobiology* 19:38-51.
174. Darveau, R. P. 2010. Periodontitis: a polymicrobial disruption of host homeostasis. *Nat Rev Microbiol* 8:481-490.
175. Pathirana, R. D., N. M. O'Brien-Simpson, and E. C. Reynolds. 2010. Host immune responses to Porphyromonas gingivalis antigens. *Periodontol 2000* 52:218-237.
176. Rylev, M., and M. Kilian. 2008. Prevalence and distribution of principal periodontal pathogens worldwide. *J Clin Periodontol* 35:346-361.
177. Ximenez-Fyvie, L. A., A. D. Haffajee, and S. S. Socransky. 2000. Comparison of the microbiota of supra- and subgingival plaque in health and periodontitis. *J Clin Periodontol* 27:648-657.
178. Sandros, J., C. Karlsson, D. F. Lappin, P. N. Madianos, D. F. Kinane, and P. N. Papapanou. 2000. Cytokine responses of oral epithelial cells to Porphyromonas gingivalis infection. *J Dent Res* 79:1808-1814.
179. Delima, A. J., and T. E. Van Dyke. 2003. Origin and function of the cellular components in gingival crevice fluid. *Periodontol 2000* 31:55-76.
180. Gibson, F. C., 3rd, C. Hong, H. H. Chou, H. Yumoto, J. Chen, E. Lien, J. Wong, and C. A. Genco. 2004. Innate immune recognition of invasive bacteria accelerates atherosclerosis in apolipoprotein E-deficient mice. *Circulation* 109:2801-2806.
181. Reddy, M. S. 2007. Reaching a better understanding of non-oral disease and the implication of periodontal infections. *Periodontol 2000* 44:9-14.
182. Steinman, R. M. 2001. Dendritic cells and the control of immunity: enhancing the efficiency of antigen presentation. *Mt Sinai J Med* 68:160-166.
183. Velazquez, J. R., and L. M. Teran. 2010. Chemokines and Their Receptors in the Allergic Airway Inflammatory Process. *Clin Rev Allergy Immunol*.
184. Bobryshev, Y. V. 2005. Dendritic cells in atherosclerosis: current status of the problem and clinical relevance. *Eur Heart J* 26:1700-1704.

185. Niessner, A., and C. M. Weyand. 2010. Dendritic cells in atherosclerotic disease. *Clin Immunol* 134:25-32.
186. Geissmann, F., M. G. Manz, S. Jung, M. H. Sieweke, M. Merad, and K. Ley. 2010. Development of monocytes, macrophages, and dendritic cells. *Science* 327:656-661.
187. Cutler, C. W., and R. Jotwani. 2006. Dendritic cells at the oral mucosal interface. *J Dent Res* 85:678-689.
188. Igyarto, B. Z., M. C. Jenison, J. C. Dudda, A. Roers, W. Muller, P. A. Koni, D. J. Campbell, M. J. Shlomchik, and D. H. Kaplan. 2009. Langerhans cells suppress contact hypersensitivity responses via cognate CD4 interaction and langerhans cell-derived IL-10. *J Immunol* 183:5085-5093.
189. Igyarto, B. Z., and D. H. Kaplan. 2010. The evolving function of Langerhans cells in adaptive skin immunity. *Immunol Cell Biol* 88:361-365.
190. Vita, J. A., and J. Loscalzo. 2002. Shouldering the risk factor burden: infection, atherosclerosis, and the vascular endothelium. *Circulation* 106:164-166.
191. Gibson, F. C., 3rd, H. Yumoto, Y. Takahashi, H. H. Chou, and C. A. Genco. 2006. Innate immune signaling and Porphyromonas gingivalis-accelerated atherosclerosis. *J Dent Res* 85:106-121.
192. Rackley, C. E. 2005. Vascular abnormalities in the metabolic syndrome: mechanisms and therapy. *Curr Atheroscler Rep* 7:403-404.
193. Erridge, C. 2008. The roles of pathogen-associated molecular patterns in atherosclerosis. *Trends Cardiovasc Med* 18:52-56.
194. Kiechl, S., G. Egger, M. Mayr, C. J. Wiedermann, E. Bonora, F. Oberhollenzer, M. Muggeo, Q. Xu, G. Wick, W. Poewe, and J. Willeit. 2001. Chronic infections and the risk of carotid atherosclerosis: prospective results from a large population study. *Circulation* 103:1064-1070.
195. Espinola-Klein, C., H. J. Rupprecht, S. Blankenberg, C. Bickel, H. Kopp, A. Victor, G. Hafner, W. Prellwitz, W. Schlumberger, and J. Meyer. 2002. Impact of infectious burden on progression of carotid atherosclerosis. *Stroke* 33:2581-2586.
196. Celik, T., A. Iyisoy, M. Celik, and E. Isik. 2007. The ongoing debate over the association between Chlamydia pneumoniae infection and coronary artery disease: Antibiotic dilemma. *Int J Cardiol*.
197. Aghajanian, A., E. S. Wittchen, M. J. Allingham, T. A. Garrett, and K. Burridge. 2008. Endothelial cell junctions and the regulation of vascular permeability and leukocyte transmigration. *J Thromb Haemost*.
198. O'Connor, C. M., M. W. Dunne, M. A. Pfeffer, J. B. Muhlestein, L. Yao, S. Gupta, R. J. Benner, M. R. Fisher, and T. D. Cook. 2003. Azithromycin for the secondary prevention of coronary heart disease events: the WIZARD study: a randomized controlled trial. *JAMA* 290:1459-1466.
199. Cannon, C. P., E. Braunwald, C. H. McCabe, J. T. Grayston, B. Muhlestein, R. P. Giugliano, R. Cairns, and A. M. Skene. 2005. Antibiotic treatment of Chlamydia pneumoniae after acute coronary syndrome. *N Engl J Med* 352:1646-1654.
200. Capestany, C. A., G. D. Tribble, K. Maeda, D. R. Demuth, and R. J. Lamont. 2008. Role of the Clp system in stress tolerance, biofilm formation, and intracellular invasion in Porphyromonas gingivalis. *J Bacteriol* 190:1436-1446.

201. Eick, S., and W. Pfister. 2004. Efficacy of antibiotics against periodontopathogenic bacteria within epithelial cells: an in vitro study. *J Periodontol* 75:1327-1334.
202. RAMS TM, F. D. 2003. Occurrence of Clindamycin-resistant Porphyromonas gingivalis in Human Periodontitis. In *International Association for Dental Research*, San Antonio.
203. Kaplan, M., S. S. Yavuz, B. Cinar, V. Koksal, M. S. Kut, F. Yapici, H. Gercekoglu, and M. M. Demirtas. 2006. Detection of Chlamydia pneumoniae and Helicobacter pylori in atherosclerotic plaques of carotid artery by polymerase chain reaction. *Int J Infect Dis* 10:116-123.
204. Watson, C., and N. J. Alp. 2008. Role of Chlamydia pneumoniae in atherosclerosis. *Clin Sci (Lond)* 114:509-531.
205. Lalla, E., I. B. Lamster, M. A. Hofmann, L. Bucciarelli, A. P. Jerud, S. Tucker, Y. Lu, P. N. Papapanou, and A. M. Schmidt. 2003. Oral infection with a periodontal pathogen accelerates early atherosclerosis in apolipoprotein E-null mice. *Arterioscler Thromb Vasc Biol* 23:1405-1411.
206. Pussinen, P. J., K. Tuomisto, P. Jousilahti, A. S. Havulinna, J. Sundvall, and V. Salomaa. 2007. Endotoxemia, immune response to periodontal pathogens, and systemic inflammation associate with incident cardiovascular disease events. *Arterioscler Thromb Vasc Biol* 27:1433-1439.
207. Mustapha, I. Z., S. Debrey, M. Oladubu, and R. Ugarte. 2007. Markers of systemic bacterial exposure in periodontal disease and cardiovascular disease risk: a systematic review and meta-analysis. *J Periodontol* 78:2289-2302.
208. Bahekar, A. A., S. Singh, S. Saha, J. Molnar, and R. Arora. 2007. The prevalence and incidence of coronary heart disease is significantly increased in periodontitis: a meta-analysis. *Am Heart J* 154:830-837.
209. Trichopoulou, A., N. Yiannakouris, C. Bamia, V. Benetou, D. Trichopoulos, and J. M. Ordovas. 2008. Genetic predisposition, nongenetic risk factors, and coronary infarct. *Arch Intern Med* 168:891-896.
210. Austin, M. A., B. L. Rodriguez, B. McKnight, M. J. McNeely, K. L. Edwards, J. D. Curb, and D. S. Sharp. 2000. Low-density lipoprotein particle size, triglycerides, and high-density lipoprotein cholesterol as risk factors for coronary heart disease in older Japanese-American men. *Am J Cardiol* 86:412-416.
211. Loof, T. G., M. Rohde, G. S. Chhatwal, S. Jung, and E. Medina. 2007. The contribution of dendritic cells to host defenses against Streptococcus pyogenes. *J Infect Dis* 196:1794-1803.
212. MacIntyre, A., R. Abramov, C. J. Hammond, A. P. Hudson, E. J. Arking, C. S. Little, D. M. Appelt, and B. J. Balin. 2003. Chlamydia pneumoniae infection promotes the transmigration of monocytes through human brain endothelial cells. *J Neurosci Res* 71:740-750.
213. Greiffenberg, L., W. Goebel, K. S. Kim, I. Weiglein, A. Bubert, F. Engelbrecht, M. Stins, and M. Kuhn. 1998. Interaction of Listeria monocytogenes with human brain microvascular endothelial cells: InlB-dependent invasion, long-term intracellular growth, and spread from macrophages to endothelial cells. *Infect Immun* 66:5260-5267.

214. Jotwani, R. C., C. W. 2003. Multiple dendritic cell (DC) subpopulations in human gingiva and association of mature DCs with CD4+ T-cells in situ. *J Dent Res* 82:736-741.
215. Tacke, F., D. Alvarez, T. J. Kaplan, C. Jakubzick, R. Spanbroek, J. Llodra, A. Garin, J. Liu, M. Mack, N. van Rooijen, S. A. Lira, A. J. Habenicht, and G. J. Randolph. 2007. Monocyte subsets differentially employ CCR2, CCR5, and CX3CR1 to accumulate within atherosclerotic plaques. *J Clin Invest* 117:185-194.
216. Bobryshev, Y. V., and R. S. Lord. 2002. Expression of heat shock protein-70 by dendritic cells in the arterial intima and its potential significance in atherogenesis. *J Vasc Surg* 35:368-375.
217. Cao, W., Y. V. Bobryshev, R. S. Lord, R. E. Oakley, S. H. Lee, and J. Lu. 2003. Dendritic cells in the arterial wall express C1q: potential significance in atherogenesis. *Cardiovasc Res* 60:175-186.
218. Erbel, C., K. Sato, F. B. Meyer, S. L. Kopecky, R. L. Frye, J. J. Goronzy, and C. M. Weyand. 2007. Functional profile of activated dendritic cells in unstable atherosclerotic plaque. *Basic Res Cardiol* 102:123-132.
219. Muzzio, M. L., V. Miksztowicz, F. Brites, D. Aguilar, E. M. Repetto, R. Wikinski, M. Tavella, L. Schreier, and G. A. Berg. 2009. Metalloproteases 2 and 9, Lp-PLA(2) and lipoprotein profile in coronary patients. *Arch Med Res* 40:48-53.
220. Jotwani, R., S. V. Eswaran, S. Moonga, and C. W. Cutler. 2010. MMP-9/TIMP-1 imbalance induced in human dendritic cells by Porphyromonas gingivalis. *FEMS Immunol Med Microbiol* 58:314-321.
221. Price, D. T., and J. Loscalzo. 1999. Cellular adhesion molecules and atherogenesis. *Am J Med* 107:85-97.
222. Reape, T. J., and P. H. Groot. 1999. Chemokines and atherosclerosis. *Atherosclerosis* 147:213-225.
223. Reape, T. J., K. Rayner, C. D. Manning, A. N. Gee, M. S. Barnette, K. G. Burnand, and P. H. Groot. 1999. Expression and cellular localization of the CC chemokines PARC and ELC in human atherosclerotic plaques. *Am J Pathol* 154:365-374.
224. Weber, C., A. Schober, and A. Zernecke. 2004. Chemokines: key regulators of mononuclear cell recruitment in atherosclerotic vascular disease. *Arterioscler Thromb Vasc Biol* 24:1997-2008.
225. Pan, S., L. S. Kleppe, T. A. Witt, C. S. Mueske, and R. D. Simari. 2004. The effect of vascular smooth muscle cell-targeted expression of tissue factor pathway inhibitor in a murine model of arterial thrombosis. *Thromb Haemost* 92:495-502.
226. Shi, H., J. Ge, W. Fang, K. Yao, A. Sun, R. Huang, Q. Jia, K. Wang, Y. Zou, and X. Cao. 2007. Peripheral-blood dendritic cells in men with coronary heart disease. *Am J Cardiol* 100:593-597.
227. Yilmaz, A., J. Weber, I. Cicha, C. Stumpf, M. Klein, D. Raithel, W. G. Daniel, and C. D. Garlichs. 2006. Decrease in circulating myeloid dendritic cell precursors in coronary artery disease. *J Am Coll Cardiol* 48:70-80.
228. Yilmaz, A., T. Schaller, I. Cicha, R. Altendorf, C. Stumpf, L. Klinghammer, J. Ludwig, W. G. Daniel, and C. D. Garlichs. 2009. Predictive value of the decrease

in circulating dendritic cell precursors in stable coronary artery disease. *Clin Sci (Lond)* 116:353-363.
229. Figdor, C. G., Y. van Kooyk, and G. J. Adema. 2002. C-type lectin receptors on dendritic cells and Langerhans cells. *Nat Rev Immunol* 2:77-84.
230. Li, L., R. Michel, J. Cohen, A. Decarlo, and E. Kozarov. 2008. Intracellular survival and vascular cell-to-cell transmission of Porphyromonas gingivalis. *BMC Microbiol* 8:26.
231. Rego, A. T., V. Chandran, and G. Waksman. 2010. Two-step and one-step secretion mechanisms in Gram-negative bacteria: contrasting the type IV secretion system and the chaperone-usher pathway of pilus biogenesis. *Biochem J* 425:475-488.
232. Kostakioti, M., C. L. Newman, D. G. Thanassi, and C. Stathopoulos. 2005. Mechanisms of protein export across the bacterial outer membrane. *J Bacteriol* 187:4306-4314.
233. Bonemann, G., A. Pietrosiuk, and A. Mogk. 2010. Tubules and donuts: a type VI secretion story. *Mol Microbiol* 76:815-821.
234. Stathopoulos, C., D. R. Hendrixson, D. G. Thanassi, S. J. Hultgren, J. W. St Geme, 3rd, and R. Curtiss, 3rd. 2000. Secretion of virulence determinants by the general secretory pathway in gram-negative pathogens: an evolving story. *Microbes Infect* 2:1061-1072.
235. Faridmoayer, A., M. A. Fentabil, M. F. Haurat, W. Yi, R. Woodward, P. G. Wang, and M. F. Feldman. 2008. Extreme substrate promiscuity of the Neisseria oligosaccharyl transferase involved in protein O-glycosylation. *J Biol Chem* 283:34596-34604.
236. Faridmoayer, A., M. A. Fentabil, D. C. Mills, J. S. Klassen, and M. F. Feldman. 2007. Functional characterization of bacterial oligosaccharyltransferases involved in O-linked protein glycosylation. *J Bacteriol* 189:8088-8098.
237. Kline, K. A., S. Falker, S. Dahlberg, S. Normark, and B. Henriques-Normark. 2009. Bacterial adhesins in host-microbe interactions. *Cell Host Microbe* 5:580-592.
238. Morelle, W., V. Faid, F. Chirat, and J. C. Michalski. 2009. Analysis of N- and O-linked glycans from glycoproteins using MALDI-TOF mass spectrometry. *Methods Mol Biol* 534:5-21.
239. Dashper, S. G., K. J. Cross, N. Slakeski, P. Lissel, P. Aulakh, C. Moore, and E. C. Reynolds. 2004. Hemoglobin hydrolysis and heme acquisition by Porphyromonas gingivalis. *Oral Microbiol Immunol* 19:50-56.
240. Burns, D. L. 2003. Type IV transporters of pathogenic bacteria. *Curr Opin Microbiol* 6:29-34.
241. Ding, Z., K. Atmakuri, and P. J. Christie. 2003. The outs and ins of bacterial type IV secretion substrates. *Trends Microbiol* 11:527-535.
242. Fronzes, R., P. J. Christie, and G. Waksman. 2009. The structural biology of type IV secretion systems. *Nat Rev Microbiol* 7:703-714.

Appendix:

Protein Purification: Fimbriae major and minor purification with slight modifications of

Dr. Mike Davey's protocol.

1) Grow up 3 Liters of to maximum OD_{660}. Dr. Caroline Genco Suggested as high as 2.0.
-This will ensure as much starting material as possible since this is a native protein
- Dr. Davey's thesis stated that he grew up 10 Liters. This would yield a final concentration of 1 mg/mL of pure Fimbriae.

2) Centrifuge in Large oak-ridge screw top sorval tubes to pellet the bacteria 7500 RPM at 4°C for 30 minutes.
-You can keep on adding more media to these tubes until all of the media is used. Be sure to warn lab mates since this part stinks!

3) Discard supernatant.

4) Suspend the pellet in 20mM Tris-HCl (pH 8.0), 0.15M NaCl, 10mM MgCl. Do not wash the pellet so as to not lose fimbriae.

5) Ultrasonic Treatment.
-Pulse the homogenate at 50% power for 5 min at least 4-5 times. Do this step on ice and let the homogenate recover between pulses.

6) Centrifuge to remove the cell debris, again in an oak ridge tube at 11000 RPM.
-This will ensure that as much unwanted cell particles are removed as possible.

7) Slowly, add saturated ammonium sulfate into the saved supernatant with a stirring until the total concentration of ammonium sulfate becomes 40%.
-Do not add all the ammonium sulfate at the same time doing this will result in unwanted proteins precipitating out.

8) For best results leave sample stirring over night at 4°C or for 2 hours at Room Temperature.

9) Centrifuge to pellet out Fimbriae.

10) Dissolve the pellet in a small amount (less than 10mL) of 20mM Tris-HCl (pH 8.0).

11) Dialyze the sample in 5-20mM Tris-HCl (pH 8.0) for a day or more. Change the dialysis buffer at least 4 times.

-It is essential to remove all of the salts especially ammonium sulfate since they can interfere with the ion exchange columns

12) At this stage it is a good idea to check the sample by SDS-PAGE the minor fimbriae is 67 KDa and the major fimbriae is 41 KDa.

13) Load a column with DEAE-Sepharose CL-6B.

14) The column should then be washed with 20% alcohol at least 3 column volumes

15) After the 20% alcohol 3 column volumes of dH_2O should be used to wash the column

16) The column should then be washed with buffer A and buffer B (3 volumes again) Buffer A is 20 mM Tris-HCl pH 8.0, buffer B is 1 M NaCl

17) Equilibrate the column with 20mM Tris-HCl (pH 7.5-8.0)

18) Apply the dialyzed and re-concentrated fimbriae to the column and wash out with a 20 mM Tris-HCl for at least 1-2 hour.

19) Elute Fimbriae with a 0-1M NaCl Gradient.

20) Analyze the fractions by SDS-PAGE and or Silver stain.

21) Dialyze against 5mM Tris-HCl or if SDS-PAGE shows contaminants pool and concentrate fractions and re-run on column. This step will be needed to be done numerous times before pure fimbriae are available.

22) If I still see multiple proteins getting eluted at the same fraction I will have to do gel filtration to clean up the fractions. For gel filtration the longer the column the better the resolution. Keep the flow rate as low as possible. Fimbriae binds best at pH 7.8.

Troubleshooting and general tips:

23) For SDS PAGE samples. Put at least 10 µl of loading dye with 20 µl of sample. Boil at 100°C for 5-10 min then immediately add to ice. Spin down and then load to gel.

24) For minute samples or dilute samples do silver stain as per directions.

25) Some samples may need to be concentrated. Add 1 volume of protein solution to 9 volumes of cold ethanol 100%. Mix and keep at least 10 min at -20°C (some see better results overnight). Spin 15 min at 4°C in a micro-centrifuge at maximum speed (15000g). Carefully discard the supernatant and retain the pellet. Dry the tube by inversion on tissue paper. Wash pellet with 90% cold ethanol and keep at -20°C. Vortex and re-pellet samples.